THE JOURNAL
OF
CHEMICAL PHYSICS

VOLUME 10 JANUARY, 1942 NUMBER 1

# Infra-Red Spectra of Axially Symmetric $XY_3Z$ Molecules

## I. Vibration-Rotation Energies

WAVE HENRY SHAFFER
*Mendenhall Laboratory of Physics, Ohio State University, Columbus, Ohio*

(Received October 3, 1941)

The vibration-rotation energies of the axially symmetric $XY_3Z$ molecular model are investigated to second order of approximation, including cubic and quartic anharmonic terms in the potential energy, all Coriolis interactions between rotation and vibration, centrifugal stretching and dependence of the rotational constants on the vibrational state. The energies are expressed in term value form, $E=hc(G_V+F_R-F_C)$, where $G_V$, $F_R$ and $F_C$ are, respectively, the vibrational, rotational, and Coriolis terms which are given explicitly as functions of the molecular constants appearing in the Hamiltonian.

### I. INTRODUCTION

THE axially symmetric $XY_3Z$ molecular model, of which examples are the methyl halides, is of considerable interest to chemists and physicists and the infra-red and Raman spectra of many molecules of this type have been subjects for much experimental study. Various aspects of the theory underlying the interpretation of these spectra have been considered by many workers. The normal vibrations have been studied by several workers[1–3] using different types of potential functions and other writers[4, 5] have studied the symmetry properties of the normal vibrations from the standpoint of group theory. Several authors[6, 7] have attempted to set up simplified quadratic potential functions to fit the observed vibrational frequencies. Dennison[1] has given the rudimentary theory of the rotational fine structure of the infra-red spectra of $XY_3Z$ molecules. Other writers have treated certain aspects of Coriolis interactions,[8–10] centrifugal stretching[11] and accidental degeneracies.[12]

In view of the fact that the theory of the rotation-vibration spectra of $XY_3Z$ molecules exists in the literature in fragmentary form and it has not been carried to the high order of approximation necessary for the interpretation of certain features of experimental data obtainable with improved

[1] D. M. Dennison, Rev. Mod. Phys. **3**, 280 (1931).
[2] G. B. B. M. Sutherland and D. M. Dennison, Proc. Roy. Soc. **A148**, 250 (1935).
[3] J. E. Rosenthal and H. H. Voge, J. Chem. Phys. **4**, 134 (1936).
[4] E. B. Wilson, Jr., J. Chem. Phys. **2**, 432 (1934).
[5] J. E. Rosenthal and G. M. Murphy, Rev. Mod. Phys. **8**, 317 (1936).
[6] H. H. Voge and J. E. Rosenthal, J. Chem. Phys. **4**, 137 (1936).
[7] Z. I. Slawsky and D. M. Dennison, J. Chem. Phys. **7**, 522 (1939); J. W. Linnett, J. Chem. Phys. **8**, 91 (1940).
[8] E. Teller and L. Tisza, Zeits. f. Physik **73**, 791 (1932).
[9] E. Teller, *Hand- und Jahrbuch der Chem. Physik* (1934), Vol. 9.
[10] M. Johnston and D. M. Dennison, Phys. Rev. **48**, 868 (1935).
[11] Z. I. Slawsky and D. M. Dennison, J. Chem. Phys. **7**, 509 (1939).
[12] A. Adel and E. F. Barker, J. Chem. Phys. **2**, 627 (1934).

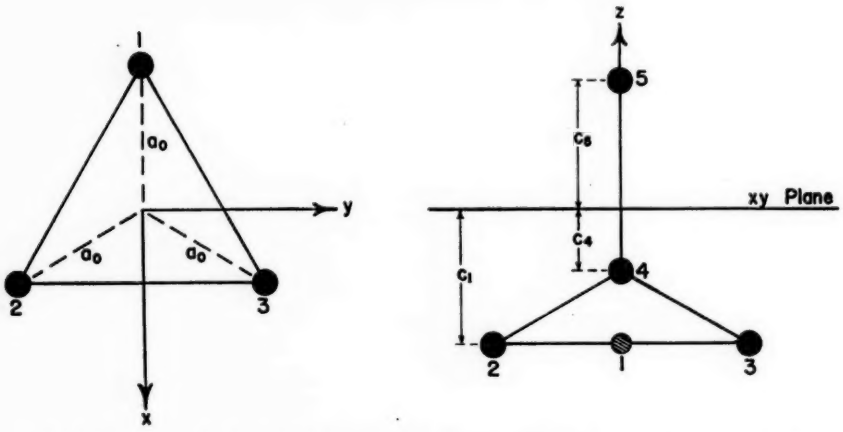


FIG. 1. Equilibrium configuration.

techniques, it has seemed desirable to carry out a unified treatment of the rotation-vibration energies of such molecules and to extend the calculations to second order of approximation in such a manner as to include, in addition to the energies associated with the harmonic oscillator and rigid top approximations, contributions arising from cubic and quartic anharmonic terms in the potential energy, all types of Coriolis interactions between rotation and vibration, centrifugal stretching and changes in the rotational constants arising from vibration. In subsequent papers the expressions developed in this paper will be applied to the interpretation of some new experimental observations on the infra-red spectra of the methyl halides.

## II. THE NORMAL COORDINATES

The model adopted for the axially symmetric $XY_3Z$ molecule consists, in its equilibrium configuration, of a symmetrical $XY_3$ pyramid, similar to that assumed by the writer[13] for the pyramidal $XY_3$ model, with a Z particle situated outside the pyramid on its symmetry axis and adjacent to the X particle. For describing the positions of the particles a body-fixed rectangular coordinate system, *xyz*, is adopted whose origin lies at the center of gravity of the model, whose positive *z* axis coincides with the symmetry axis of the model and points from the X particle toward the Z particle, and whose *xy* plane is parallel to the $X_3$ base of the pyramid. The particles, which are assigned indices $i$ ($i=1, \cdots 5$), for reference, have the masses $m_i$ and equilibrium coordinates $(x_i^0, y_i^0, z_i^0)$ shown in Table I. The equilibrium coordinates are illustrated in Fig. 1.

The instantaneous position of the $i$th particle during oscillation is given relative to the body-fixed coordinate system by $(x_i, y_i, z_i)=(x_i^0+x_i', y_i^0+y_i', z_i^0+z_i')$ where the primed quantities denote components of displacement from the equilibrium position. From a consideration of the six equations satisfying the Eckart conditions[14,15] and the expressions for the relative displacements of the particles during small oscillations it is evident that the following is a suitable choice of intermediate generalized coordinates† for discussing the rotating and vibrating model:

$$x=x_4'-[(x_1'+x_2'+x_3')/3]; \quad \xi=\{3^{-\frac{1}{2}}(2x_1'-x_2'-x_3')+(y_3'-y_2')\}/2$$
$$y=y_4'-[(y_1'+y_2'+y_3')/3]; \quad \eta=\{-3^{-\frac{1}{2}}(2y_1'-y_2'-y_3')+(x_3'-x_2')\}/2$$
$$z=z_4'-[(z_1'+z_2'+z_3')/3]; \quad \zeta=\{-3^{-\frac{1}{2}}(2x_1'-x_2'-x_3')+(y_3'-y_2')\}/2$$
$$p=x_5'-x_4'; \quad q=y_5'-y_4'; \quad r=z_5'-z_4'.$$

[13] W. H. Shaffer, J. Chem. Phys. **9**, 607 (1941).
[14] C. Eckart, Phys. Rev. **47**, 552 (1932).
[15] E. B. Wilson and J. B. Howard, J. Chem. Phys. **4**, 260 (1936).

† These intermediate coordinates and the similar ones of Slawsky and Dennison, reference 11, satisfy all the Eckart conditions and are therefore suitable for discussion of the rotating and vibrating model. The coordinates of Rosenthal and Voge, reference 3, do not satisfy the Eckart condition requiring conservation of internal angular momentum in zero approximation and could not readily be used for study of interactions between rotation and vibration.

TABLE I. Masses $m_i$ and equilibrium coordinates $x_i^0, y_i^0, z_i^0$.

| | $i$ | $m_i$ | $x_i^0$ | $y_i^0$ | $z_i^0$ |
|---|---|---|---|---|---|
| Y | 1 | $m_1$ | $-a_0$ | 0 | $-c_1$ |
| Y | 2 | $m_1$ | $+a_0/2$ | $-3^{\frac{1}{2}}a_0/2$ | $-c_1$ |
| Y | 3 | $m_1$ | $+a_0/2$ | $+3^{\frac{1}{2}}a_0/2$ | $-c_1$ |
| X | 4 | $m_4$ | 0 | 0 | $-c_4$ |
| Z | 5 | $m_5$ | 0 | 0 | $+c_5$ |

The kinetic energy of vibration, $T_V$, is given in terms of the above intermediate coordinates by the expression,

$$T_V=(1/2)\{\mu_1(\dot{p}^2+\dot{q}^2)+\mu_2(\dot{x}^2+\dot{y}^2)+2\mu_3(\dot{p}\dot{x}+\dot{q}\dot{y})+m_1(\dot{\xi}^2+\dot{\eta}^2+\dot{\zeta}^2)+\mu_4\dot{r}^2+\mu_5\dot{z}^2+2\mu_6\dot{r}\dot{z}\}, \quad (1)$$

where

$$\mu_4=[m_5(3m_1+m_4)/M]; \quad \mu_1=\mu_4+6m_1\alpha^2$$
$$\mu_5=[3m_1(m_4+m_5)/M]; \quad \mu_2=\mu_5+6m_1\beta^2$$
$$\mu_6=[3m_1m_5/M]; \quad \mu_3=\mu_6+6m_1\alpha\beta$$

in which $M=(3m_1+m_4+m_5)$; $\alpha=-(m_5c_5/3m_1a_0)$; $\beta=-(c_1/a_0)$. It can readily be shown that the generalized quadratic potential energy function, $U_0$, is

$$U_0=(1/2)\{k_1(\xi^2+\eta^2)+k_2(x^2+y^2)+k_3(p^2+q^2)+2k_4(px+qy)$$
$$+2k_5(\xi x+\eta y)+2k_6(\xi p+\eta q)+n_1\zeta^2+n_2z^2+n_3r^2+2n_4rz+2n_5\zeta z+2n_6\zeta r\}, \quad (2)$$

where the constants $k_1$, $k_2$, etc., are generalized force constants which may be expressed as functions of the constants occurring in any special type of potential function such as valence or central force types.*

The axial model $XY_3Z$ belongs to the symmetry point group $C_{3v}$ and has three non-degenerate parallel normal modes of class $A_1$ and three degenerate perpendicular modes of class $E$ as can be shown by the group theory treatment of Wilson[4] or Rosenthal and Murphy.[5] Approximate pictures of the normal modes are given by Sutherland[16] and Wu[17] where the single modes are arbitrarily called $\omega_1$, $\omega_3$, $\omega_5$, and the double modes $\omega_2$, $\omega_4$, $\omega_6$, following the notation of Sutherland and Dennison.[2]

From an inspection of the Lagrange's secular determinant for this case, which breaks up into three threefold steps, it is obvious that the intermediate coordinates $\zeta$, $r$, and $z$ are associated with the single modes and the sets ($\xi$, $p$, $x$) and ($\eta$, $q$, $y$) are each associated with one set of the double modes. The transformations to normal coordinates can be somewhat simplified by the following intermediate transformations:

$$m_1^{\frac{1}{2}}\xi=Q_1'; \qquad m_1^{\frac{1}{2}}\eta=R_1', \qquad m_1^{\frac{1}{2}}\zeta=S_1',$$
$$\mu_2^{\frac{1}{2}}x=2^{-\frac{1}{2}}(\sigma_1Q_2'+\sigma_2Q_3'), \quad \mu_2^{\frac{1}{2}}y=2^{-\frac{1}{2}}(\sigma_1R_2'+\sigma_2R_3'), \quad \mu_5^{\frac{1}{2}}z=2^{-\frac{1}{2}}(\sigma_3S_2'+\sigma_4S_3'),$$
$$\mu_1^{\frac{1}{2}}p=2^{-\frac{1}{2}}(\sigma_1Q_2'-\sigma_2Q_3'), \quad \mu_1^{\frac{1}{2}}q=2^{-\frac{1}{2}}(\sigma_1R_2'+\sigma_2R_3'), \quad \mu_4^{\frac{1}{2}}r=2^{-\frac{1}{2}}(\sigma_3S_2'-\sigma_4S_3'),$$

where

$$\sigma_1=\{1+[\mu_3/(\mu_1\mu_2)^{\frac{1}{2}}]\}^{\frac{1}{2}}; \quad \sigma_3=\{1+[\mu_6/(\mu_4\mu_5)^{\frac{1}{2}}]\}^{\frac{1}{2}};$$
$$\sigma_2=\{1-[\mu_3/(\mu_1\mu_2)^{\frac{1}{2}}]\}^{\frac{1}{2}}; \quad \sigma_4=\{1-[\mu_6/(\mu_4\mu_5)^{\frac{1}{2}}]\}^{\frac{1}{2}}.$$

* Computations of the constants in simplified potential functions for the methyl halides have been made by Voge and Rosenthal, reference 6, and by Slawsky and Dennison, reference 7, (SD), all basing their work on the generalized potential functions given by Rosenthal and Voge, reference 3; they obtained complex values for some of the force constants. The writer has made computations, basing his work on the generalized expression (2) above, on the constants in a potential function similar to that of SD; in the results, which will be published later, the difficulty involving complex roots does not seem to arise.

[16] G. B. B. M. Sutherland, *Infrared and Raman Spectra* (Methuen, London, 1935).

[17] Ta-You Wu, *Vibrational Spectra and Structure of Polyatomic Molecules* (Prentice-Hall, New York, 1940).

As a result of this transformation $T_V$ becomes

$$T_V=(1/2)\sum_{i=1}^{3}(\dot{Q}_i'^2+\dot{R}_i'^2+\dot{S}_i'^2) \tag{3}$$

and $U_0$ becomes

$$U_0=(1/2)\{\sum_{i=1}^{3}[K_i(Q_i'^2+R_i'^2)+N_iS_i'^2+2\sum_{i'>i}(K_{ii'}(Q_i'Q_{i'}'+R_i'R_{i'}')+N_{ii'}S_i'S_{i'}')]\}, \tag{4}$$

where

$$K_1=(k_1/m_1), \qquad N_1=(n_1/m_1),$$

$$K_2=(\sigma_1^2/2)[(k_2/\mu_2)+(k_3/\mu_1)+(2k_4/(\mu_1\mu_2)^{\frac{1}{2}})], \qquad N_2=(\sigma_3^2/2)[(n_2/\mu_5)+(n_3/\mu_4)+(2n_4/(\mu_4\mu_5)^{\frac{1}{2}})],$$

$$K_3=(\sigma_2^2/2)[(k_2/\mu_2)+(k_3/\mu_1)-(2k_4/(\mu_1\mu_2)^{\frac{1}{2}})], \qquad N_3=(\sigma_4^2/2)[(n_2/\mu_5)+(n_3/\mu_4)-(2n_4/(\mu_4\mu_5)^{\frac{1}{2}})],$$

$$K_{12}=\sigma_1(2m_1)^{-\frac{1}{2}}(\mu_2^{-\frac{1}{2}}k_5+\mu_1^{-\frac{1}{2}}k_6), \qquad N_{12}=\sigma_3(2m_1)^{-\frac{1}{2}}(\mu_5^{-\frac{1}{2}}n_5+\mu_4^{-\frac{1}{2}}n_6),$$

$$K_{13}=\sigma_2(2m_1)^{-\frac{1}{2}}(\mu_2^{-\frac{1}{2}}k_5-\mu_1^{-\frac{1}{2}}k_6), \qquad N_{13}=\sigma_4(2m_1)^{-\frac{1}{2}}(\mu_5^{-\frac{1}{2}}n_5-\mu_4^{-\frac{1}{2}}n_6),$$

$$K_{23}=(\sigma_1\sigma_2/2)[(k_2/\mu_2)-(k_3/\mu_1)], \qquad N_{23}=(\sigma_3\sigma_4/2)[(n_2/\mu_5)-(n_3/\mu_4)].$$

The generalized coordinates $Q_i'$ and $R_i'$ $(i=1, 2, 3)$ are associated with the twofold degenerate modes $(\omega_2, \omega_4, \omega_6)$ and the $S_i'$ with the single modes $(\omega_1, \omega_3, \omega_5)$. The normal frequencies of oscillation $\omega_j$ (in $\mathrm{cm}^{-1}$) are related to the roots $\lambda_j$ of Lagrange's determinantal equation by the expression, $\omega_j=(2\pi c)^{-1}\lambda_j^{\frac{1}{2}}$, in which $c$ denotes the velocity of light, and where the $\lambda_j$ satisfy the following relations:

$$\lambda_2+\lambda_4+\lambda_6=K_1+K_2+K_3,$$

$$\lambda_2\lambda_4+\lambda_4\lambda_6+\lambda_6\lambda_2=K_1K_2+K_2K_3+K_3K_1-K_{12}^2-K_{23}^2-K_{13}^2,$$

$$\lambda_2\lambda_4\lambda_6=K_1K_2K_3-K_{12}^2K_3-K_{13}^2K_2-K_{23}^2K_1,$$

$$\lambda_1+\lambda_3+\lambda_5=N_1+N_2+N_3,$$

$$\lambda_1\lambda_3+\lambda_3\lambda_5+\lambda_5\lambda_1=N_1N_2+N_2N_3+N_3N_1-N_{12}^2-N_{13}^2-N_{23}^2,$$

$$\lambda_1\lambda_3\lambda_5=N_1N_2N_3-N_{12}^2N_3-N_{13}^2N_2-N_{23}^2N_1.$$

The transformation to normal coordinates, $Q_j$, $R_j$, $S_k$, is accomplished by means of the following substitutions:

$$Q_i'=\textstyle\sum_j \alpha_{ij}Q_j; \quad R_i'=\sum_j \alpha_{ij}R_j \ (i=1, 2, 3; j=2, 4, 6)$$

and

$$S_i'=\textstyle\sum_k \beta_{ik}S_k \ (i=1, 2, 3; k=1, 3, 5)$$

where $\alpha_{ij}=A_jA_{ij}$ and $\beta_{ik}=B_kB_{ik}$ if

$$A_{1j}=(K_2-\lambda_j)(K_3-\lambda_j)-K_4^2, \qquad B_{1k}=(N_2-\lambda_k)(N_3-\lambda_k)-N_4^2,$$

$$A_{2j}=K_4K_5-K_6(K_3-\lambda_j), \qquad B_{2k}=N_4N_5-N_6(N_3-\lambda_k),$$

$$A_{3j}=K_4K_6-K_5(K_2-\lambda_j), \qquad B_{3k}=N_4N_6-N_5(N_2-\lambda_k),$$

$$A_j=(A_{1j}^2+A_{2j}^2+A_{3j}^2)^{-\frac{1}{2}}, \qquad B_k=(B_{1k}^2+B_{2k}^2+B_{3k}^2)^{-\frac{1}{2}}.$$

The transformation coefficients, $\alpha_{ij}$ and $\beta_{ik}$, satisfy the relations

$$\sum_i \alpha_{ij}^2=\sum_j \alpha_{ij}^2=1; \quad \sum_i \alpha_{ij}\alpha_{ij'}=\sum_j \alpha_{ij}\alpha_{i'j}=0,$$

$$\sum_i \beta_{ik}^2=\sum_k \beta_{ik}^2=1; \quad \sum_i \beta_{ik}\beta_{ik'}=\sum_k \beta_{ik}\beta_{i'k}=0.$$

If dimensionless coordinates $q_j$, $r_j$, $s_k$, are introduced by the relations, $Q_j=(\hbar^{\frac{1}{2}}/\lambda_j^{\frac{1}{4}})q_j$, etc., where $\hbar=(h/2\pi)$ and $h$ is Planck's constant, the vibrational energy of the system can be written, to zero approximation, in the Hamiltonian form as

$$H_{0v}=hc\{\sum_j \omega_j[((p_{q_j}^2+p_{r_j}^2)/\hbar^2)+(q_j^2+r_j^2)]+\sum_k \omega_k[(p_{s_k}^2/\hbar^2)+s_k^2]\}, \tag{5}$$

where $p_{s_k}=(\partial T_V/\partial \dot{s}_k)$ and is the momentum conjugate to $s_k$, etc. The pairs of coordinates, $q_j$ and $r_j$, associated with the doubly degenerate modes can be conveniently replaced by polar coordinates according to the substitution

$$q_j=\rho_j \cos\phi_j; \quad r_j=\rho_j \sin\phi_j.$$

It can be shown from consideration of the symmetry properties of the normal modes that the cubic and quartic parts of the anharmonic potential energy function contain the following terms:

$$U_1=hc\sum_k s_k[\beta_{kkk}s_k^2+\sum_j \beta_{kjj}\rho_j^2+\sum_{k'>k} \beta_{kk'k'}s_{k'}^2], \tag{6}$$

$$U_2=hc\{\sum_k s_k^2[\gamma_{kkkk}s_k^2+\sum_{k'>k} (\gamma_{kkk'k'}s_{k'}^2+\gamma_{kkkk'}s_ks_{k'})]$$

$$+\sum_j \rho_j^2[\gamma_{jjjj}\rho_j^2+\sum_{j'>j} \gamma_{jjj'j'}\rho_{j'}^2+\sum_k \gamma_{kkjj}s_k^2+\sum_k \sum_{k'>k} \gamma_{jjkk'}s_ks_{k'}]\}, \tag{7}$$

where the constants $\beta_{kkk}$, $\gamma_{kkkk}$, etc., are expressed in $cm^{-1}$.

## III. THE INTERNAL ANGULAR MOMENTUM

The Coriolis interaction between rotation and vibration gives rise to the term, $-[(p_xP_x/I_{0x})+(p_yP_y/I_{0y})+(p_zP_z/I_{0z})]$, in the quantum-mechanical Hamiltonian, where $\mathbf{p}=(p_x, p_y, p_z)$ = angular momentum associated with vibration, $\mathbf{P}=(P_x, P_y, P_z)$ = total angular momentum of the molecular system, and the equilibrium moments of inertia are

$$I_{0x}=I_{0y}=3m_1[c_1^2+(a_0^2/2)]+m_4c_4^2+m_5c_5^2, \tag{8}$$

$$I_{0z}=3m_1a_0^2. \tag{9}$$

The components of the internal angular momentum $\mathbf{p}$ have the following forms:

$$p_x=\sum_j \{\sum_k \xi_{jk}[(\omega_k/\omega_j)^{\frac{1}{2}}r_jp_{s_k}-(\omega_j/\omega_k)^{\frac{1}{2}}s_kp_{r_j}]$$

$$+\sum_{j'} \xi_{jj'}[(\omega_{j'}/\omega_j)^{\frac{1}{2}}(q_jp_{r_{j'}}+r_jp_{q_{j'}})-(\omega_j/\omega_{j'})^{\frac{1}{2}}(r_{j'}p_{q_j}+q_{j'}p_{r_j})]\},$$

$$p_y=-\sum_j \{\sum_k \xi_{jk}[(\omega_k/\omega_j)^{\frac{1}{2}}q_jp_{s_k}-(\omega_j/\omega_k)^{\frac{1}{2}}s_kp_{q_j}]$$

$$-\sum_{j'} \xi_{jj'}[(\omega_{j'}/\omega_j)^{\frac{1}{2}}(r_jp_{r_{j'}}-q_jp_{q_{j'}})-(\omega_j/\omega_{j'})^{\frac{1}{2}}(r_{j'}p_{r_j}-q_{j'}p_{q_j})]\},$$

$$p_z=\sum_j \{\zeta_j(q_jp_{r_j}-r_jp_{q_j})+\sum_{j'} \zeta_{jj'}[(\omega_{j'}/\omega_j)^{\frac{1}{2}}(q_jp_{r_{j'}}-r_jp_{q_{j'}})-(\omega_j/\omega_{j'})^{\frac{1}{2}}(r_{j'}p_{q_j}-q_{j'}p_{r_j})]\},$$

where the indices $j$ and $j'$ assume values 2, 4 and 6; the index $k$ runs over 1, 3, and 5; and the double subscripts on $\xi_{jj'}$ and $\zeta_{jj'}$ occur cyclically as 24, 46 and 62. The constants $\xi_{jk}$, $\xi_{jj'}$, $\zeta_j$ and $\zeta_{jj'}$ which occur in the above expressions are defined in the following manner:

$$\xi_{jk}=\alpha_{2j}\beta_{2k}a_{22}+\alpha_{3j}\beta_{3k}a_{33}+\alpha_{2j}\beta_{3k}a_{23}+\alpha_{3j}\beta_{2k}a_{32}+(\alpha_{2j}a_{12}+\alpha_{3j}a_{13})\beta_{1k},$$

$$\xi_{jj'}=(\alpha_{1j'}\alpha_{2j}-\alpha_{1j}\alpha_{2j'})a_{12}+(\alpha_{1j'}\alpha_{3j}-\alpha_{1j}\alpha_{3j'})a_{13},$$

$$\zeta_j=\alpha_{2j}^2 b_{22}+\alpha_{3j}^2 b_{33}+2\alpha_{2j}\alpha_{3j}b_{23}-\alpha_{1j}^2,$$

$$\zeta_{jj'}=\alpha_{2j}\alpha_{2j'}b_{22}+\alpha_{3j}\alpha_{3j'}b_{33}+(\alpha_{2j}\alpha_{3j'}+\alpha_{2j'}\alpha_{3j})b_{23}-\alpha_{1j}\alpha_{1j'},$$

where

$$a_{22}=(\sigma_1\sigma_3/2)(\sigma_{52}+\sigma_{41}+\sigma_{42}+\sigma_{51}),\quad a_{23}=(\sigma_1\sigma_4/2)(\sigma_{52}-\sigma_{41}-\sigma_{42}+\sigma_{51}),$$

$$a_{33}=(\sigma_2\sigma_4/2)(\sigma_{52}+\sigma_{41}-\sigma_{42}-\sigma_{51}),\quad a_{32}=(\sigma_2\sigma_3/2)(\sigma_{52}-\sigma_{41}+\sigma_{42}-\sigma_{51}),$$

$$b_{22}=(\sigma_1^2/2)(\sigma_{52}^2+\sigma_{41}^2+2\sigma_{42}\sigma_{41}),\qquad b_{23}=b_{32}=(\sigma_1\sigma_2/2)(\sigma_{52}^2-\sigma_{41}^2),$$

$$b_{33}=(\sigma_2^2/2)(\sigma_{52}^2+\sigma_{41}^2-2\sigma_{42}\sigma_{41}),$$

if $\sigma_{52}=(\mu_5/\mu_2)^{\frac{1}{2}}$; $\sigma_{41}=(\mu_4/\mu_1)^{\frac{1}{2}}$; $\sigma_{42}=\mu_6(\mu_4\mu_2)^{-\frac{1}{2}}$; $\sigma_{51}=\mu_6(\mu_5\mu_1)^{-\frac{1}{2}}$.

The parameters $\zeta_j$ satisfy the relation,

$$\zeta_2+\zeta_4+\zeta_6=(\mu_4\mu_5-\mu_6^2)/(\mu_1\mu_2-\mu_3^2)=(I_{0z}/2I_{0x}),$$

which has been pointed out by Johnston and Dennison.[10] Other identities involving the $\xi_{jj'}$, $\xi_{jk}$, $\zeta_{jj'}$ and $\zeta_j$ may be derived with the aid of the definitions given above.

Certain constants are defined below which occur in the rotational part of the Hamiltonian and are used in Section V in connection with the eigenvalues of the Hamiltonian operator:

$$e_j=-2(\alpha_{2j}\sigma_5+\alpha_{3j}\sigma_6),\qquad f_{kk}=[1-(1/2)\beta_{1k}^2-\textstyle\sum_j \xi_{jk}^2],$$

$$f_k=(\beta_{1k}-2\beta_{2k}\sigma_7-2\beta_{3k}\sigma_8),\qquad g_{jj}=[1-(3/2)\alpha_{1j}^2-\zeta_j-\textstyle\sum_{j'} \xi_{jj'}^2],$$

$$f_{jj}=[1-(1/2)\alpha_{1j}^2-\textstyle\sum_k \xi_{jk}^2-\sum_{j'} \xi_{jj'}^2],\qquad h_{jj}=[\zeta_j+2\alpha_{1j}^2-\zeta_j^2-\textstyle\sum_{j'} \zeta_{jj'}^2],$$

where

$$\sigma_5=\sigma_1(3m_1/2)^{\frac{1}{2}}(\alpha\mu_1^{-\frac{1}{2}}+\beta\mu_2^{-\frac{1}{2}}),\quad \sigma_7=\sigma_3(3m_1/2)^{\frac{1}{2}}(\beta\mu_5^{-\frac{1}{2}}+\alpha\mu_4^{-\frac{1}{2}}),$$

$$\sigma_6=\sigma_2(3m_1/2)^{\frac{1}{2}}(\beta\mu_2^{-\frac{1}{2}}-\alpha\mu_1^{-\frac{1}{2}}),\quad \sigma_8=\sigma_4(3m_1/2)^{\frac{1}{2}}(\beta\mu_5^{-\frac{1}{2}}-\alpha\mu_4^{-\frac{1}{2}}).$$

## IV. THE QUANTUM-MECHANICAL HAMILTONIAN

The quantum-mechanical Hamiltonian operator appropriate for studying the rotation-vibration energy states of a polyatomic molecule can be set up according to the method outlined by Wilson and Howard[15] in the form

$$H=(1/2)\sum_{\alpha,\beta}\mu^{\frac{1}{4}}(P_\alpha-p_\alpha)\mu_{\alpha\beta}\mu^{-\frac{1}{2}}(P_\beta-p_\beta)+(1/2)\mu^{\frac{1}{4}}\textstyle\sum_k p_k\mu^{-\frac{1}{2}}p_k+U_0+U_1+U_2+\cdots, \qquad (10)$$

where the quantities $P_\alpha$ and $p_\alpha$ are the operators associated with the $x$, $y$, and $z$ components of total and internal angular momentum, respectively; the quantities $\mu$ and $\mu_{\alpha\beta}$ are functions of the normal coordinates and are related to the instantaneous moments and products of inertia; the $p_k$ are operators associated with the momenta conjugate to the vibrational coordinates; and the quantities $U_0$, $U_1$ and $U_2$ are the zero-, first- and second-order parts of the potential function. For the purpose of computing the energies to second order of approximation the expansions of the quantities $\mu$ and $\mu_{\alpha\beta}$ are broken off with terms quadratic in the vibrational coordinates. The details of the procedure for

setting up the Hamiltonian operator $H$ for the $XY_3Z$ model are similar to those in papers on the $XY_4$ model by Shaffer, Nielsen and Thomas[18] (SNT) and the bent $XY_2$ model by Shaffer and Nielsen.[19]

A contact transformation of the type suggested by SNT may be applied to the Hamiltonian operator $H$ to yield a transformed operator $H'$ given by the expression, $H'=THT^{-1}$, where $T=\exp[(-1)^{\frac{1}{2}}\epsilon S]$ and $S$ is a function of the operators occurring in $H$. The transformed Hamiltonian, $H'$, has the form

$$H'=H_0'+\epsilon H_1'+\epsilon^2 H_2'+\cdots, \tag{11}$$

where $\epsilon$ is the parameter of smallness according to which the Hamiltonian is separated into its various orders of magnitude,

$$H_0'=H_0, \quad H_1'=H_1-(-1)^{\frac{1}{2}}(H_0S-SH_0), \quad H_2'=H_2+[(-1)^{\frac{1}{2}}/2][S(H_1+H_1')-(H_1+H_1')S].$$

By means of such a contact transformation it is possible to reduce very much the number of terms in $H_1'$ by transferring them to $H_2'$; this procedure simplifies the derivation of the second-order contributions to the energy expression. It can be shown that all terms can thus be eliminated from $H_1'$ except the Coriolis interaction terms arising from degenerate oscillations and certain terms in $U_1$ in the case of accidental degeneracies. Details of the application of the contact transformation have been given by SNT and by Silver and Shaffer.[20]

The basic wave functions for the perturbation calculation of the energies are similar to those given by Silver and Shaffer.[20] The quantum numbers defining the rotational states are denoted by $J$, $K$ and $M$ following the notation of Dennison;[1] the vibrational quantum number associated with normal mode $\omega_n$ is denoted by $v_n$ and, in the case of the twofold degenerate frequencies, the quantum number associated with the internal angular momentum is denoted by $l_n$.

## V. THE ENERGY EXPRESSION

The zero-order Hamiltonian contains the terms,

$$H_0=H_{0v}+(1/2)[(P_x^2/I_{0x})+(P_y^2/I_{0y})+(P_z^2/I_{0z})] \tag{12}$$

and has eigenvalues,

$$E_0=hc\{\sum_{n=1}^{6}\omega_n[v_n+(g_n/2)]+B_eJ(J+1)+(C_e-B_e)K^2\}, \tag{13}$$

where $B_e=(h/8\pi^2cI_{0x})$, $C_e=(h/8\pi^2cI_{0z})$ and $g_n$ is the degree of degeneracy of normal frequency $\omega_n$ ($g_1=g_3=g_5=1$; $g_2=g_4=g_6=2$).

The first-order Hamiltonian, $H_1'$, can be written, for the case of no accidental degeneracies, in the form

$$H_1'=-\textstyle\sum_j(\zeta_j/I_{0z})p_{\phi j}P_z, \tag{14}$$

where $p_{\phi j}=(q_jp_{r_j}-r_jp_{q_j})$; the first-order contribution to the energy is

$$E_1'=-hcF_C, \tag{15}$$

where $F_C=2C_e\sum_j\zeta_jl_jK$.

The second-order Hamiltonian, $H_2'$, for the $XY_3Z$ model is a very complicated expression and will not be given here since it is similar to the corresponding expression given by the writer[13] for the

[18] W. H. Shaffer, H. H. Nielsen, and L. H. Thomas, Phys. Rev. **56**, 895 (1939).
[19] W. H. Shaffer and H. H. Nielsen, Phys. Rev. **56**, 188 (1939).
[20] S. Silver and W. H. Shaffer, J. Chem. Phys. **9**, 599 (1941).

pyramidal $XY_3$ model. The second-order energy, $E_2'$, can be obtained by the usual perturbation calculation in a manner similar to that employed earlier by the writer.[13]

When the contributions $E_0'$, $E_1'$ and $E_2'$ are added together the total rotation-vibration energy $E$ can be written, to second-order of approximation, in the simple form

$$E=hc\{G_V+F_R-F_C\}, \tag{16}$$

where $F_C$ is the quantity defined in (15), $G_V$ and $F_R$ are, respectively, the vibrational and rotational term values. The quantities $G_V$ and $F_R$ are given by the following expressions:

$$G_V=G_0+\sum_{n=1}^{6}\{\omega_n[v_n+(g_n/2)]+x_{nn}[v_n+(g_n/2)]^2+\sum_{n'<n}x_{n'n}[v_{n'}+(g_{n'}/2)][v_n+(g_n/2)]\}$$
$$+\sum_i\{G_{ii}(l_i^2-1)+\sum_{i'<i}G_{i'i}l_{i'}l_i\}, \tag{17}$$

$$F_R=B_VJ(J+1)+(C_V-B_V)K^2-D_JJ^2(J+1)^2-D_{JK}J(J+1)K^2-D_KK^4, \tag{18}$$

in which the rotational constants $B_V$ and $C_V$ effective in the various vibrational states have the forms,

$$B_V=B_e\{1-\alpha_0+\sum_{n=1}^{6}\alpha_n[v_n+(g_n/2)]\}, \tag{19}$$

$$C_V=C_e\{1-\beta_0+\sum_{n=1}^{6}\beta_n[v_n+(g_n/2)]\}. \tag{20}$$

The constants occurring in (17) are

$$G_0=(1/16)\sum_k\{6\gamma_{kkkk}-7(\beta_{kkk}^2/\omega_k)+3\sum_{k'}[\omega_{k'}\beta_{k'kk}^2/(4\omega_k^2-\omega_{k'}^2)]\}$$
$$+\sum_i\{\zeta_i^2C_e-\sum_{j'}[\zeta_{ij'}^2C_e+2\xi_{ij'}^2B_e]-\sum_k\xi_{jk}^2\},$$

$$x_{kk}=(1/4)\{6\gamma_{kkkk}-15(\beta_{kkk}^2/\omega_k)+3\sum_{k'}[(8\omega_k^2-3\omega_{k'}^2)\beta_{k'kk}^2/\omega_{k'}(4\omega_k^2-\omega_{k'}^2)]\},$$

$$x_{jj}=(1/4)\{6\gamma_{jjjj}-\sum_k[(8\omega_j^2-3\omega_k^2)\beta_{kjj}^2/\omega_k(4\omega_j^2-\omega_k^2)]\},$$

$$x_{k'k}=\gamma_{k'k'kk}-3[(\beta_{kkk}\beta_{k'kk}/\omega_k)+(\beta_{k'k'k'}\beta_{kk'k'}/\omega_{k'})]-2\{[\omega_k\beta_{k'kk}^2/(4\omega_k^2-\omega_{k'}^2)]+[\omega_{k'}\beta_{kk'k'}^2/(4\omega_{k'}^2-\omega_k^2)]\},$$

$$x_{j'j}=\gamma_{j'j'jj}+(\xi_{jj'}^2B_e+\zeta_{jj'}^2C_e)[(\omega_j/\omega_{j'})+(\omega_{j'}/\omega_j)]-\sum_k(\beta_{kjj}\beta_{kj'j'}/\omega_k),$$

$$x_{jk}=-3(\beta_{kkk}\beta_{kjj}/\omega_k)-\sum_{k'}(\beta_{kjj}\beta_{k'kk}/\omega_{k'})-2[\omega_j\beta_{kjj}^2/(4\omega_j^2-\omega_k^2)]+\gamma_{kkjj}+\xi_{jk}^2B_e[(\omega_j/\omega_k)+(\omega_k/\omega_j)],$$

$$G_{jj}=-(1/2)\gamma_{jjjj}-\sum_k[\omega_k\beta_{kjj}^2/4(4\omega_j^2-\omega_k^2)]+\zeta_j^2C_e,$$

$$G_{jj'}=2\zeta_j\zeta_{j'}C_e.$$

The centrifugal expansion constants $D_J$, $D_{JK}$ and $D_K$, of (18) are defined as

$$D_J=(1/4)(3\tau_{xxxx}+2\tau_{xyxy}+\tau_{xxyy}),$$
$$D_{JK}=(1/2)(-3\tau_{xxxx}-2\tau_{xyxy}-\tau_{xxyy}+8\tau_{xzzz}+4\tau_{xzxz}),$$
$$D_K=-D_J-D_{JK}+\tau_{zzzz},$$

where

$$\tau_{xxxx}=(B_e^4/C_e)\{\sum_j(\alpha_{1j}^2/\omega_j^2)+\sum_k(f_k^2/\omega_k^2)\},$$

$$\tau_{zzzz}=C_e^3\sum_k(4\beta_{1k}^2/\omega_k^2),$$

$$\tau_{xyxy}=(B_e^4/C_e)\sum_j(\alpha_{1j}^2/\omega_j^2),$$

$$\tau_{xxyy}=\tau_{xxxx}-2\tau_{xyxy},$$

$$\tau_{xzxz}=B_e^2C_e\sum_j(e_j^2/\omega_j^2),$$

$$\tau_{xzzz}=B_e^2C_e\sum_k(2\beta_{1k}f_k/\omega_k^2).$$

The constants $\alpha_0$, $\beta_0$, $\alpha_n$ and $\beta_n$, occurring in (19) are

$$\alpha_0=(1/2)(-\tau_{xxxx}-2\tau_{xyxy}+\tau_{xxyy}+2\tau_{xzxz}),$$

$$\beta_0=(1/4)(3\tau_{xxxx}+6\tau_{xyxy}-3\tau_{xxyy}-16\tau_{xzxz}),$$

$$\alpha_k=(h/2\pi c\omega_kI_{0z})\{[(I_{0z}/I_{0x})f_k^2-f_{kk}]+\sum_j[\xi_{jk}^2(3\omega_k^2+\omega_j^2)/(\omega_k^2-\omega_j^2)]\}$$
$$+(h/2\pi c)^{\frac{1}{2}}\{(3f_k\beta_{kkk}/\omega_k^{\frac{1}{2}})+\sum_{k'}(f_{k'}\beta_{k'kk}/\omega_{k'}^{\frac{1}{2}})\},$$

$$\beta_k=(h/2\pi c\omega_kI_{0z})(3\beta_{1k}^2)+(h/2\pi c)^{\frac{1}{2}}\{(3h_k\beta_{kkk}/\omega_k^{\frac{1}{2}})+\sum_{k'}(h_{k'}\beta_{k'kk}/\omega_{k'}^{\frac{1}{2}})\},$$

$$\alpha_j=(h/2\pi c\omega_jI_{0x})\{f_j^2(I_{0z}/I_{0x})+(1/2)(e_j^2-f_{jj}-g_{jj})+\sum\xi_{jj'}^2[(3\omega_j^2+\omega_{j'}^2)/(\omega_j^2-\omega_{j'}^2)]$$
$$+(1/2)\sum_k\xi_{jk}^2[(3\omega_j^2+\omega_k^2)/(\omega_j^2-\omega_k^2)]\}+(h/2\pi c)^{\frac{1}{2}}\sum_k(f_k\beta_{kii}/\omega_k^{\frac{1}{2}}),$$

$$\beta_j=(h/2\pi c\omega_jI_{0z})\{e_j^2(I_{0z}/I_{0x})-h_{jj}+\sum_{j'}\zeta_{jj'}^2[(3\omega_j^2+\omega_{j'}^2)/(\omega_j^2-\omega_{j'}^2)]\}+(h/2\pi c)^{\frac{1}{2}}\sum_k(h_k\beta_{kii}/\omega_k^{\frac{1}{2}}).$$

Discussions of the selection rules governing transitions between the energy states have been given by Dennison,[1] Wilson,[4] Sutherland,[16] Teller,[9] and others.

## ACKNOWLEDGMENTS

The author takes pleasure in expressing his appreciation to the Fellowship Board of the National Research Council for the fellowship under which this work was carried out and to Professor R. S. Mulliken of Ryerson Laboratory for many helpful discussions during the course of the work.

# Infra-Red Spectra of Hydrocarbons

## I. Some Investigations of the Temperature Dependence of Absorption Bands

W. H. AVERY AND C. F. ELLIS
*Houston Refinery Research Laboratory of Shell Oil Company, Incorporated, Houston, Texas*
(Received October 14, 1941)

Theory indicates that the separation of the maxima of the *P* and *R* branches of an infra-red band should be proportional to the square root of the absolute temperature. This relation has been tested by experiments with ethane, propylene and 2, 2-dimethyl butane in which the temperature was varied between −195°C and room temperature. It has been found that the relation is approximately valid, the band widths being somewhat less than theory predicts in the liquid and considerably less in the solid. The positions of the bands are independent of the temperature in 2, 2-dimethyl butane and only slightly affected in the other compounds. Some bands of propylene display a pronounced variation in relative intensity with temperature. The usefulness of spectra obtained at low temperatures in the theoretical assignment of fundamentals, as a tool for the study of the liquid state and for analytical purposes, is pointed out.

### INTRODUCTION

BJERRUM first showed in 1912 that the infra-red absorption bands of diatomic molecules possess *P* and *R* branches symmetrically disposed with respect to the center of the band and that the separation in wave numbers of the maxima of the two branches is given by the relation,

$$\Delta\nu=\frac{1}{\pi c}\left(\frac{KT}{I}\right)^{\frac{1}{2}},^{*}$$

*K* being the Boltzmann constant, *T* the absolute temperature, *I* the moment of inertia and *c*, the velocity of light. Von Bahr and others have demonstrated that increasing the temperature causes a separation of the two maxima, in accord with the theory. She also pointed out the significance of variation of the temperature as a means of distinguishing double maxima produced by two bands and those due to *P* and *R* branches of a single band. However, because of the extreme temperatures required to produce a significant change in band width and the experimental difficulties involved, these studies at high temperatures do not appear to have been used in the interpretation of molecular spectra. Serious experimental obstacles are not encountered in the use of low temperatures, and in view of the problems presented by the theoretical interpretation of spectra where the fundamental bands overlap, it is surprising that low temperature studies have not heretofore been attempted as a means of obviating the difficulty.†

The use of infra-red spectra for analytical purposes is limited by the amount of overlapping

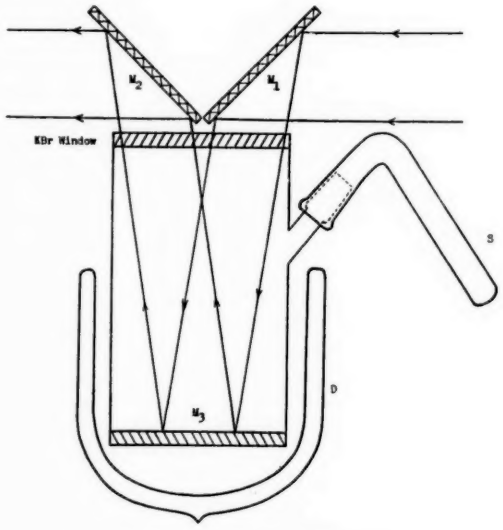


FIG. 1. Low temperature cell.

* See footnote on page 14.

† A few investigations of infra-red spectra of gases and liquids have been carried out at low temperatures. However, these studies were undertaken in investigations of rotation in the solid state. See Ruheman, *Low Temperature Physics* (Cambridge University Press, 1937). G. B. B. M. Sutherland and C. K. Wu in an article published after this work was begun (Proc. Roy. Soc. **176**, 485, 1940) mention the possibility of using low temperatures in the interpretation of molecular spectra.

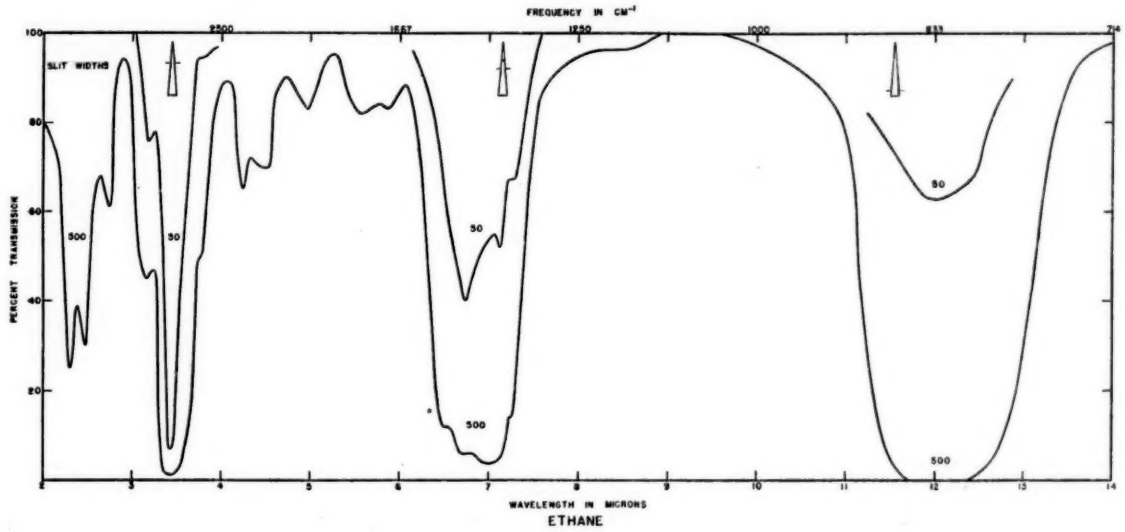


FIG. 2. Spectrum of ethane at room temperature.

of the bands in the various components of the mixture to be analyzed. Since this overlapping would be only half as great at −195°C as at room temperature, use of low temperatures might also be of value in this field.

## EXPERIMENTAL

The spectrometer has been described.[1] The absorption cell and optical arrangement used for the low temperature experiments are shown in Fig. 1. Parallel light was reflected by the front-surface aluminized mirror $M_1$ to the silvered bottom of the cell $M_3$ then to $M_2$ which returned the beam to its original direction. The cell was constructed by the American Instrument Company, and the surface $M_3$ was flat to 6 wavelengths of sodium light. To facilitate filling, the cell was mounted on a tripod set in V-ways which permitted the cell to be moved and returned accurately to its original position. A similar arrangement allowed the mirrors $M_1$ and $M_2$ to be removed and replaced without change of the focus. Leveling screws were provided for both tripod and mirror mounting, and the angle of the two mirrors with respect to each other or to the mirror $M_3$ could be adjusted. The cell was 7 cm in diameter and 15 cm in depth.

Absorption spectra were obtained as follows: After the cell had been filled to a known gas pressure, the gas was condensed in the side arm $S$ with liquid nitrogen and a given region of the spectrum, usually about 2 mu, recorded on the chart. The side arm was then warmed, the gas condensed on the cooled plane surface $M_3$ and the same spectral region was again recorded. Percentage transmissions were computed in the usual manner. This procedure, in addition to being convenient and rapid, eliminated errors which inevitably arise in regions of small absorption from the use of null cells.

The fraction of light reflected at a liquid surface depends indirectly on the absorption spectrum of the compound being investigated and could become appreciable (~10 percent) in regions of strong absorption.[2] A correction for this reflection would be desirable but this is not possible in the absence of dispersion data.

In many of the experiments at the lowest temperatures a polycrystalline layer was formed which scattered an appreciable fraction of the incident radiation. This fraction varied from experiment to experiment, the nature of the solid formed evidently being sensitive to small differences in the rate of cooling. Therefore, in preparing the absorption curves, it was assumed that regions showing no absorption in the gas

[1] W. H. Avery, J. Opt. Soc. Am. **31**, 633 (1941).

[2] See, for example, the dispersion data for three methyl halides given by A. I. Mahan, J. Opt. Soc. Am. **31**, 248 (1941) and dispersion data on water by M. Centeno, J. Opt. Soc. Am. **31**, 244 (1941).

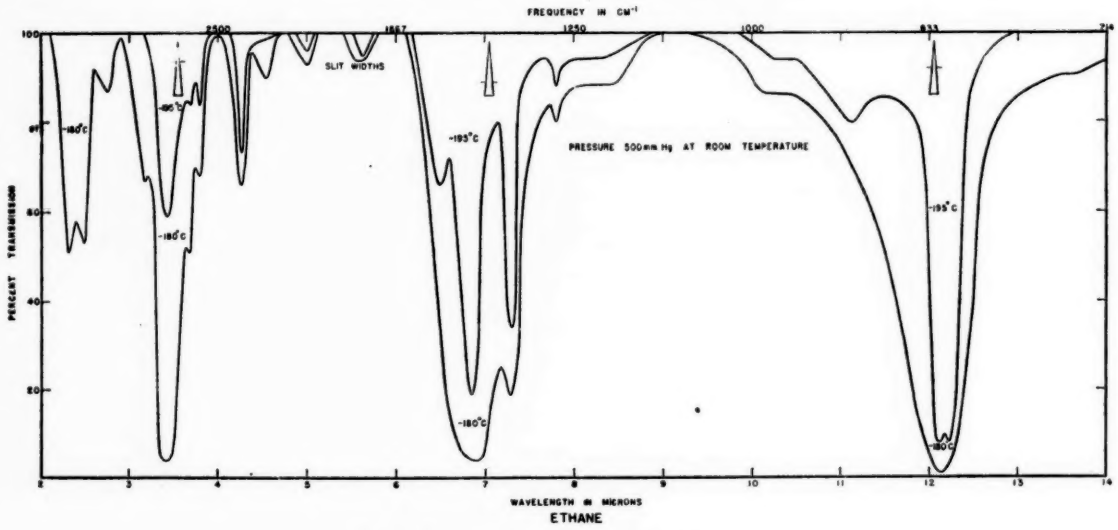


FIG. 3. Low temperature spectra of ethane.

represented 100 percent transmission in the solid; the assumption seemed justified by the fact that the solid displayed wide regions in which the transmission remained at a high (60–70 percent) constant value. Since the correction is large, numerical values of the transmission listed for the lowest temperature may be somewhat in error, but the positions of the absorption bands and the relative intensities of the bands are presumably not seriously altered by the correction.

A temperature of −195°C was obtained by immersing the lower part of the cell in liquid nitrogen contained in the Dewar flask, *D*, Fig. 1. Other temperatures could be obtained by proper adjustment of the distance between the bottom surface of the cell and the upper surface of the liquid nitrogen. The KBr window remained at room temperature. Temperatures were estimated by measurement of the difference in potential of two opposed iron constantan thermocouples, one immersed in liquid nitrogen and the other attached to the *outside* bottom surface of the cell. The temperatures are uncertain by ±10° with the exception of −195°C. To assure a uniform layer the gases were condensed on the surface $M_3$ at a temperature where the liquid viscosity was not great, then cooled to the desired temperature. Direct condensation at very low temperatures yielded viscous liquids

TABLE I. Observed frequencies of ethane, with a possible assignment.

| Observed wave-length mu | Observed frequency $cm^{-1}$ | Intensity* | Assigned frequency $cm^{-1}$ | Calculated frequency $cm^{-1}$ | $D_{3h}$ | $D_{3d}$ |
|---|---|---|---|---|---|---|
| 12.09 | 827 | *s* | Fund | 827 | $E'$ | $E_u$ |
| 8.22 | 1216 | *vw* | 1460−275 | 1185 | $E'$ | $E_u$ |
| 7.25 | 1380 | *m* | Fund | 1380 | $A''_2$ | $A_{2u}$ |
| 7.14 | 1400 | | — | — | — | — |
| 6.80 | 1470 | *s* | Fund | 1470 | $E'$ | $E_u$ |
| 6.50 | 1538 | *vw* | — | — | — | — |
| 5.84 | 1712 | *w* | 1460+275 | 1735 | $E'$ | $E_u$ |
| 5.46 | 1831 | *w* | 827+993 | 1820 | $E'$ | $E_u$ |
| 4.97 | 2012 | *vw* | 1170+827 | 1997 | $A''_1+A''_2+E''$ | $A_{1u}+A_{2u}+E_u$ |
| 4.50 | 2222 | *w* | 1375+827 | 2202 | $E'$ | $E_u$ |
| 4.25 | 2353 | *m-s* | 1380+993 | 2377 | $A''_2$ | $A_{2u}$ |
| | | | (1170)² | 2340 | $A'_1+A'_2+E'$ | — |
| 3.74 | 2674 | *w* | 2960−275 | 2685 | $E'$ | $E_u$ |
| 3.64 | 2750 | *m* | 1380+1375 | 2755 | $A''_2$ | $A_{2u}$ |
| 3.36 | 2980 | *s* | Fund | 2980 | $E'$ | $E_u$ |

* Meaning of symbols: *s* = strong, *m* = medium, *w* = weak, *vw* = very weak.

which collected in drops and showed little tendency to spread into a thin film.*

## MATERIALS

Ethane was prepared by Mr. E. Manning of this laboratory by hydrogenation of Ohio Chemical Company's ethylene at room temperature using a platinum catalyst. The ethylene was stated to be 99.5 percent pure, the hydrogen 99.9 percent. Analysis of the ethane by Mr. E. Gelus of this laboratory using a method of isothermal distillation showed the purity to be 99.8 percent or better.

Propylene obtained from the Ohio Chemical Company was stated to be 99.95 percent pure. The purity was confirmed within the limits of error of the isothermal distillation, and it was used without further purification.

2, 2-dimethyl butane was prepared from a petroleum fraction by Mr. W. H. Marsh of the Rice Institute by repeated azeotropic distillation with a 100 plate Hicks-Brunn column. The melting point was −102.0°C and the boiling point 49.80°C.

## ETHANE

Because of its significance in the determination of the potential restricting rotations of the methyl groups, ethane has been the subject of several recent investigations.[3–5] The existence of a barrier of about 3000 calories is now well established but spectroscopic evidence still is conflicting with regard to the orientation of the methyl groups. The low temperature results were expected to be of interest for their bearing on this question.

The spectrum of ethane has been obtained at room temperature, at −170°C and at −195°C, the pressures used ranging from 50 to 500 mm.

The spectrum found at room temperature is presented in Fig. 2. The wave-lengths and frequencies of the bands are presented in Table I (columns 1 and 2). The bands at 1216, 1538 and 2012 $cm^{-1}$ have not been found by previous investigators. However, all these bands are weaker than the weakest ethane bands previously reported. They were found on every record at 500 mm and their positions do not correspond to bands of any likely impurities. Column 3 lists the relative intensities of the bands, 4 presents the probable assignment, 5 the frequency calculated for the combination or overtone bands listed in 4. Columns 5 and 6 give the symmetry for the point groups $D_{3h}$ and $D_{3d}$.

TABLE II. Low temperature spectrum of ethane.

| Wave-length mu | Frequency $cm^{-1}$ | Frequency difference $cm^{-1}$ | Intensity* |
|---|---|---|---|
| 13.6 | 735 | 87 | *vw* |
| 12.22 | 818 | | *s* |
| 12.11 | 826 | 79 | |
| 11.10 | 901 | 84 | *w* |
| 10.15 | 985 | | *vw* |
| 8.3 | 1205 | 77 | *vw* |
| 7.80 | 1282 | 88 | *w* |
| 7.30 | 1370 | | *s* |
| 6.84 | 1462 | 76 | *s* |
| 6.50 | 1538 | | *m* |
| 5.67 | 1764 | | *w* |
| 5.50 | 1818 | | *vw* |
| 5.00 | 2000 | | *vw* |
| 4.52 | 2212 | | *w* |
| 4.25 | 2353 | | *m* |
| 3.85 | 2597 | 77 | *m* |
| 3.74 | 2674 | 76 | *m-s* |
| 3.64 | 2750 | | *m-s* |
| 3.45 | 2900 | | *s* |
| 3.20 | 3125 | | *m* |

* Meaning of symbols: *s* = strong, *m* = medium, *w* = weak, *vw* = very weak.

Figure 3 presents the spectra of ethane observed at −170 and −195°C. In Table II the wave-lengths and frequencies are listed.

## DISCUSSION

Stitt[3] has recently discussed in full the assignment of frequencies in ethane. He concluded that the available spectroscopic evidence provided no clue to the orientation of the methyl groups. Although three new ethane bands have been discovered in this work, no evidence has been adduced which alters Stitt's conclusions. As is indicated in Table I, the bands at 1200 and 2012 $cm^{-1}$ may be assigned to either of the point groups $D_{3h}$ or $D_{3d}$. No assignment is apparent for the minimum observed in the gas at 1538 $cm^{-1}$. The 1400 $cm^{-1}$ band was found at 1414 by

* In a few experiments at low temperatures the gas was first condensed in the side arm, the reflecting surface next cooled to −195°C and the gas then allowed to vaporize to the surface.

[3] F. Stitt, J. Chem. Phys. **7**, 297 (1939).

[4] B. L. Crawford, Jr., W. H. Avery, and J. W. Linnett, J. Chem. Phys. **6**, 682 (1938).

[5] J. Karweil and C. Schafer, Zeits. f. physik. Chemie **B40**, 376 (1938).

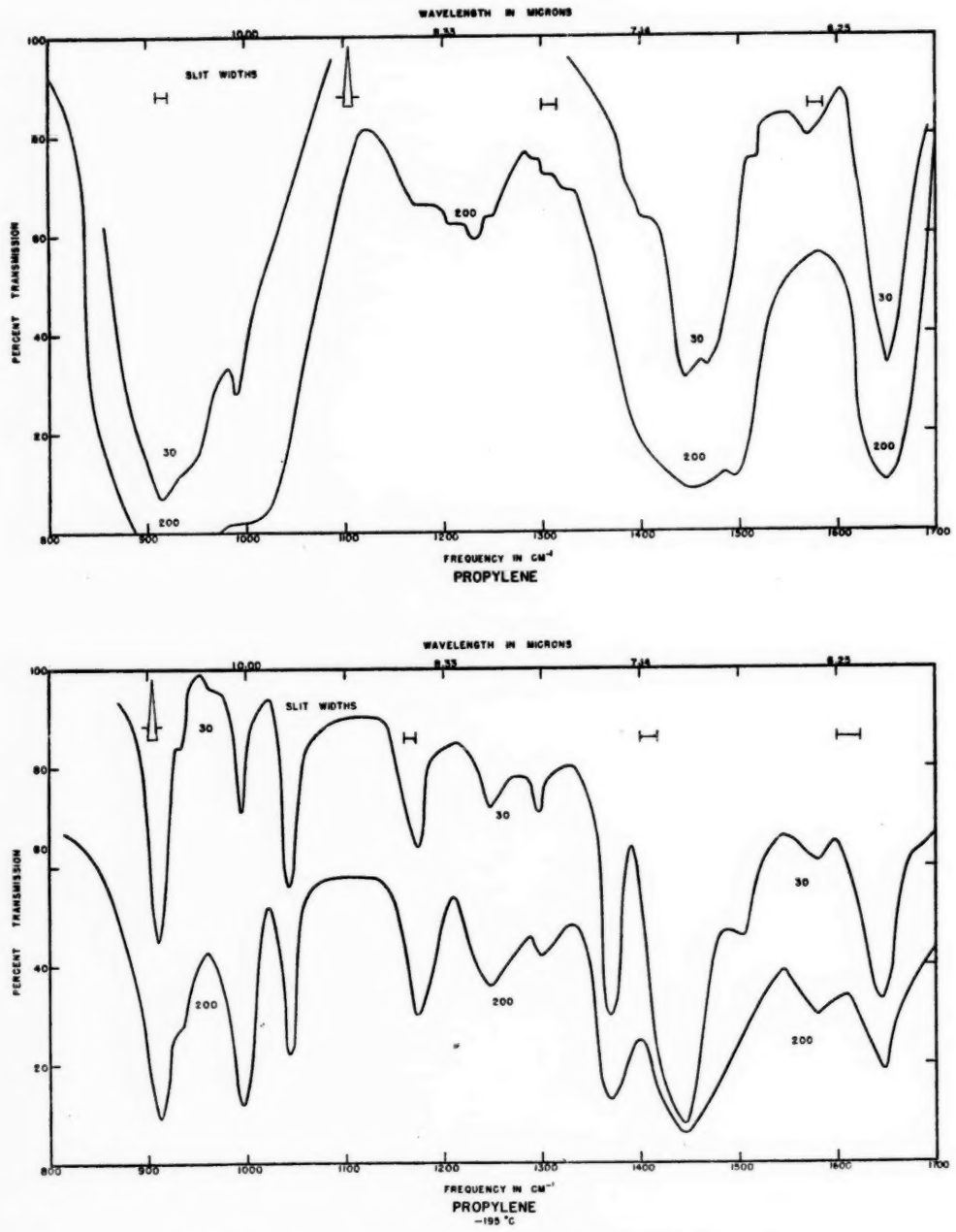


FIG. 4. Room temperature and low temperature spectra of propylene.

Crawford, Avery, and Linnett using a spectrometer of less resolving power. The value 1400 $cm^{-1}$ agrees with the calculated frequency of the $P$ branch of the 1380 $cm^{-1}$ band and leaves little doubt as to the origin of this minimum. Stitt suggested this assignment of the band. It is interesting to note that three assignments involve the torsional frequency.

Before discussing the data obtained at liquid nitrogen temperature it is well to consider briefly how the spectrum of a gas might be affected by a lowering of the temperature.

(1) In a gas the band "width"** should vary

** In parallel type bands the band width may be defined as the wave number separation of the $P$ and $R$ branches. In a perpendicular band of a symmetrical top molecule,

as the square root of the absolute temperature as the temperature is lowered. When condensation to a liquid takes place, we should expect the positions and shapes of the bands to be altered through intermolecular interactions and restrictions on the rotation. In the solid, rotations should be further restricted if not prevented, producing a further change in the band shape.

(2) In general, three translational and three rotational degrees of freedom of each molecule would be converted upon solidification to lattice vibrations. Since intermolecular forces in hydrocarbon molecules would be expected to be considerably smaller than intramolecular forces, these vibrations would be of too low frequency to appear as fundamentals in the near infra-red even in the absence of restrictions imposed by the selection rules. However, combination bands would be possible.

(3) As a rule we should not expect the symmetry of the solid lattice to conform to that of the gas, so that vibrations which are degenerate in the gas might not be so in the solid. Gas phase selection rules might also be altered by liquid or solid interactions.

(4) Since overtones are possible only for anharmonic types of vibration and since intermolecular interactions might affect the character of the potential functions, overtone bands obtained at low temperatures might be expected to show a change in intensity or position relative to the room temperature results.

Comparison of Figs. 2 and 3 shows that most of the above anticipations are verified. The reduction in the width of the bands and the attendant increase in resolution are striking. The perpendicular 827 $cm^{-1}$ band is suitable for a semi-quantitative estimate of the temperature dependence. Considering the width at 60 percent transmission, this band is 141 $cm^{-1}$ wide at room temperature, 56 $cm^{-1}$ at $-170°C$ (measured as twice the wave numbers separation between the center and low frequency edge) and 27 $cm^{-1}$ at $-195°C$. The predicted widths for the gas would be 141, 83, and 80 $cm^{-1}$. These measurements are, of course, very rough but the fact that the band widths are less than the predicted values suggests that there is some hindrance to molecular rotation in the liquid and considerable hindrance in the solid. The doublet structure of the band at $-195°C$ suggests that the vibration is no longer degenerate in the crystal lattice. This interpretation is strengthened by the lack of structure of the band in the liquid at $-170°C$. However, the doubling could also be ascribed to the appearance of a new band at $-195°C$.

Comparing the spectra obtained at room temperature and liquid nitrogen temperature we note that all the major bands found at room temperature also appear in the liquid and solid spectra. The lowest degenerate fundamental is found at 822 $cm^{-1}$, 5 $cm^{-1}$ lower than the gas value. The $A_2$ fundamental appears at 1370 $cm^{-1}$ and the second degenerate fundamental at 1462 $cm^{-1}$, the frequencies being lower than the gas phase values by 10 and 8 $cm^{-1}$. The resolution of the spectrometer at 3000 $cm^{-1}$ is too small to permit conclusions to be drawn regarding any

TABLE III. Partial vibrational spectrum of propylene.

| Room temperature | | −195°C | | | | |
|---|---|---|---|---|---|---|
| Frequency $cm^{-1}$ | Wavelength mu | Frequency $cm^{-1}$ | Wavelength mu | Wells and Wilson | Raman Effect | Calculated |
| Not investigated | | Not investigated | | 417 | 432 | 428 |
| Not investigated | | Not investigated | | 578 | 580 | 574 |
| Not investigated | | Not investigated | | 755 | — | — |
| 915 | 10.93 | 912 | 10.96 | 919 | 920 | 917 |
| 940 | 10.64 | 936 | 10.68 | — | — | 932 |
| — | — | 963 | 10.38 | — | — | 1015 |
| 991 | 10.09 | 994 | 10.06 | *ca.* 996 | — | 976 |
| — | — | 1043 | 9.59 | — | — | 1022 |
| 1170 | 8.55 | 1172 | 8.53 | 1166 | — | 1170 |
| 1206 | 8.30 | — | — | — | — | — |
| — | — | 1224 | 8.17 | 1224 | | |
| 1236 | 8.09 | — | — | — | — | — |
| 1250 | 8.00 | 1246 | 8.03 | 1244 | — | — |
| 1288 | 7.76 | — | — | 1287 | — | — |
| 1304 | 7.67 | 1297 | 7.71 | — | 1297 | 1287 |
| 1320 | 7.58 | — | — | 1317 | — | — |
| — | — | 1370 | 7.30 | — | — | — |
| 1400 | 7.14 | — | — | 1399 | — | 1386 |
| — | — | — | — | 1416 | 1415 | 1429 |
| 1444 | 6.93 | 1445 | 6.92 | 1448 | 1448 | 1471 |
| 1466 | 6.82 | — | — | 1472 | — | 1474 |
| | | | | 1489 | | |
| 1516 | 6.60 | 1506 | 6.64 | 1508 | — | — |
| | | | | 1520 | | |
| 1650 | 6.06 | 1648 | 6.07 | 1647 | 1648 | 1681 |

maxima are observed only if the moment of inertia about the symmetry axis is not less than one-third of the other moment. However, the separation of points on the band where the intensity has a given value should show the same dependence. See S. L. Gerhard and D. M. Dennison, Phys. Rev. **43**, 197 (1933). Similar considerations apply to bands of asymmetric top molecules. R. M. Badger and L. R. Zumwalt, J. Chem. Phys. **6**, 711 (1938).

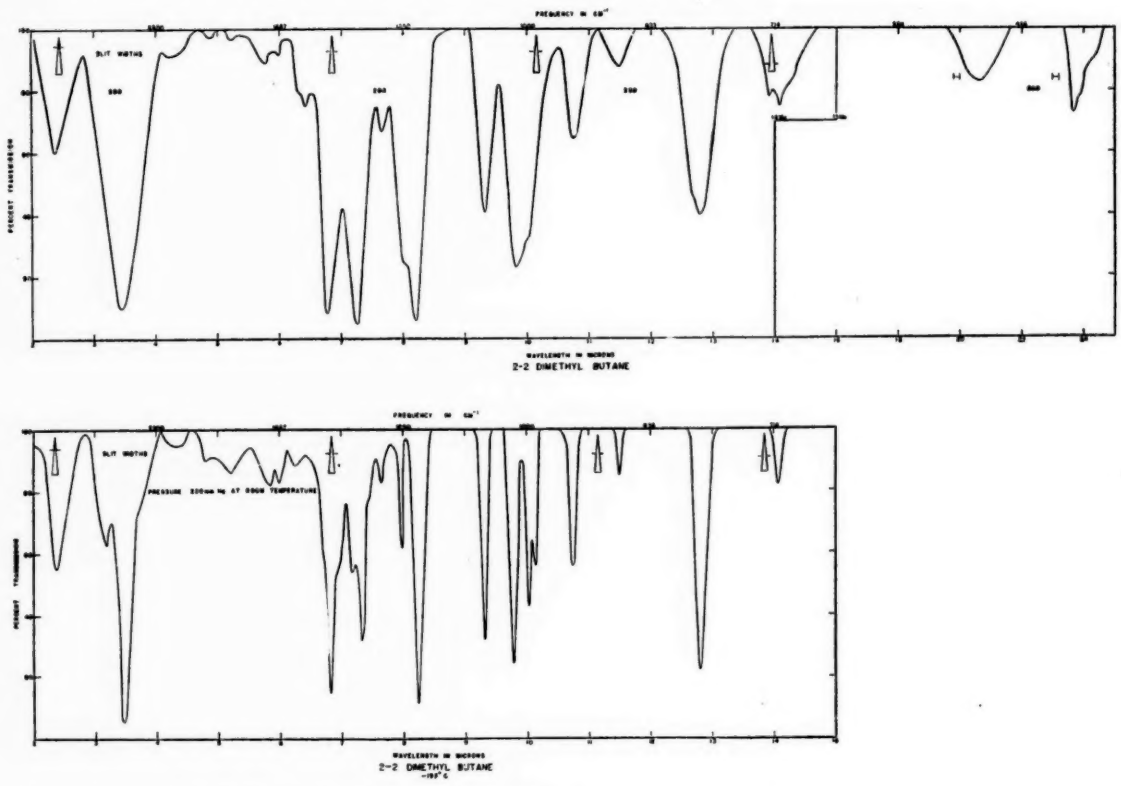


FIG. 5. Room temperature and low temperature spectra of 2-2 dimethyl butane.

shifts in this region. The weaker bands all appear at −170°C and −195°C with the exception of the minimum found at 1400 $cm^{-1}$. This is to be expected from the assignment of this minimum to the $P$ branch of the 1380 $cm^{-1}$ band, the lowering of the temperature reducing the band width so that the branches of the band are no longer resolved.

Several bands appear at −170°C and −195°C which are not found at room temperature. In every case the bands are separated from strong bands by multiples of roughly 80 $cm^{-1}$. Such a low frequency cannot correspond to a fundamental vibration of the ethane molecule and must, therefore, be ascribed to a lattice vibration, possibly a restricted rotation of the ethane molecule in the crystal or liquid.

Some differences in the intensities and positions of the overtone bands have been observed, but in view of the large scattering correction mentioned above we reserve comment until more data have been obtained.

## PROPYLENE

The study of the spectrum of ethane disclosed that no significant shifts in the positions of the bands occurred when the temperature was lowered to −195°C. Since it is well known that the spectra of strongly polar compounds are affected by the change from gaseous to liquid state it was interesting to investigate the temperature shift in a more polar hydrocarbon. Propylene was chosen for study because, in addition to being somewhat polar it has been the subject of a recent theoretical analysis by Wells and Wilson.[6] They found that the overlapping of the bands at room temperature prevented a complete assignment of the frequencies. Thus, a low temperature measurement of the compound might be of interest from two standpoints.

The region 6 to 12.5 mu was chosen for examination; for a ready comparison with the

[6] A. J. Wells and E. Bright Wilson, Jr., J. Chem. Phys. 9, 319 (1941).

data of Wells and Wilson, transmissions have been plotted as a function of frequency rather than of wave-length. The curves are presented in Fig. 4. Numbers on the curves indicate pressures in mm of Hg. The low temperature cell was used for all measurements.

In Table III are presented the frequencies and wave-lengths of bands observed in propylene at room temperature and −195°C (columns 1, 2, 3 and 4). In column 5 the results of Wells and Wilson are presented. Column 6 lists the frequencies observed in the Raman effect and column 7 the calculated positions of the absorption bands. A comparison of column 3 with column 5 shows that three bands were found in this research which were not reported by Wilson and Wells, i.e., 936, 963 and 1043 $cm^{-1}$. It is interesting to observe that the theoretical analysis of the spectrum of propylene predicts four bands, which Wilson and Wells, on the basis of their data, were unable to correlate with observed frequencies. The unknown frequencies were computed by them to be at about 920, 1015, 1020 and 1100 $cm^{-1}$. There seems to be little doubt that the bands brought out by the low temperature experiments correspond to three of the predicted frequencies.

TABLE IV. Wave-lengths and frequencies of significant bands in 2, 2-dimethyl butane.

| Room temperature Wave-length mu | Room temperature Frequency $cm^{-1}$ | −195°C Wave-length mu | −195°C Frequency $cm^{-1}$ | Raman effect* Frequency $cm^{-1}$ |
|---|---|---|---|---|
| | | | | 259 (1) |
| | | | | 335 (0) |
| | | | | 361 (1) |
| 24.4 | 410 | | | |
| 23.9 | 418 | | | |
| 23.7 | 422 | | | |
| 20.64 | 484 | | | 485 (1) |
| 14.3 | 700 | | | |
| 14.09 | 710 | 14.07 | 711 | 711 (10-*b*) |
| 13.91 | 719 | | | |
| 12.9 | 775 | | | |
| 12.79 | 782 | 12.81 | 781 | |
| 12.68 | 789 | | | |
| 11.48 | 871 | 11.50 | 870 | 869 (3) |
| 10.75 | 930 | 10.74 | 931 | 927 (3-*b*) |
| 10.0 | 1000 | 10.14 | 986 | |
| 9.82 | 1018 | 10.03 | 997 | 1017 (2-*b*) |
| | | 9.78 | 1022 | |
| 9.32 | 1073 | 9.31 | 1074 | 1075 (2) |
| 8.22 | 1216 | 8.23 | 1215 | 1217 (3-*d*) |
| 8.0 | 1250 | 7.99 | 1251 | 1251 (2-*b*) |
| 7.65 | 1307 | 7.65 | 1307 | 1304 (1-*d*) |
| | | 7.45 | 1340 | |
| 7.27 | 1376 | 7.33 | 1364 | |
| | | 7.17 | 1395 | |
| | | 6.95 | 1439 | 1447 (6) |
| 6.78 | 1475 | 6.82 | 1466 | 1468 (6) |
| | | 6.75 | 1480 | |
| 6.42 | 1558 | 6.25 | 1600 | |
| 6.32 | 1582 | | | |
| 5.99 | 1669 | 6.00 | 1667 | |
| 5.77 | 1733 | 5.86 | 1706 | |
| 5.22 | 1916 | 5.22 | 1916 | |
| 4.88 | 2049 | 4.80 | 2083 | |
| 4.30 | 2326 | 4.32 | 2315 | |
| | | 3.7 | 2700 | 2720 (1) |
| | | | | 2760 (1) |
| | | | | 2860 (3) |
| 3.45 | 2899 | 3.47 | 2882 | 2874 (10) |
| | | | | 2903 (3-*d*) |
| | | | | 2936 (3-*d*) |
| | | | | 2965 (6-*d*) |
| | | | | 2980 (3-*d*) |
| | | 3.19 | 3135 | |
| 2.37 | 4219 | 2.37 | 4219 | |

* E. J. Rosenbaum, A. V. Grosse and H. F. Jacobson, J. Am. Chem. Soc. **61**, 689 (1939). Note: Numbers in parentheses refer to intensity; *b* means broad, *d* diffuse.

The frequency shifts associated with lowering of the temperature are seen to be small with the exception of the band at 1370 $cm^{-1}$. The explanation of this displacement is not clear but it may be related to another phenomenon which is produced by a lowering of the temperature: a variation in the intensity of certain bands. Thus, a preliminary series of curves obtained at temperature intervals of about 5°C from −195 to −170°C in the spectral region 900 to 1050 $cm^{-1}$ show a pronounced temperature dependence of the relative intensities of the bands. The disappearance of the band at 1466 $cm^{-1}$ and the apparent shift in the position of the 1400 $cm^{-1}$ band may well be other examples of this temperature dependence, but a definite explanation requires a more thorough investigation than was possible in this survey. Perhaps the minima at 1466 and 1444 $cm^{-1}$ are *P* and *R* branches of a single band whose center is shifted to 1445 $cm^{-1}$ at −195°C.

### 2, 2-DIMETHYL BUTANE

This compound was examined because it is fairly representative of the higher hydrocarbons and because the liquid may be supercooled to

TABLE V. Comparison of widths of bands at room temperature and −195°C.

| Frequency of band center ($cm^{-1}$) | Room temperature | −195°C | Ratio | Transmission |
|---|---|---|---|---|
| 782 | 25 | 13 | 0.52 | 60 |
| 930 | 24 | 12 | 0.50 | 80 |
| 1073 | 24 | 12 | 0.50 | 60 |
| 1216 | 56 | 28 | 0.50 | 60 |

−195°C without crystallization. The spectrum is presented in Fig. 5, the wave-lengths and frequencies of the bands at the two temperatures are given in Table IV in columns 1 through 4. Column 5 presents the Raman spectrum obtained by Rosenbaum, Grosse, and Jacobson.

The increase in resolution obtained by the use of low temperatures is particularly evident in this spectrum. It is interesting to note that the group of bands of 10 mu appear in the Raman effect only as a single broad line. The positions of the bands are affected only slightly if at all by the temperature change, except in the overtone region, and the agreement between the Raman and infra-red frequencies is excellent. As is shown in Table V, the reduction in the width of the bands at −195°C is in close agreement with the theoretical value. Column 4 gives the ratio between the width at room temperature and that at −195°C. The ratio predicted for a gas is 0.51. Column 5 gives the value of the percentage transmission at which the width of the band was determined.

The close agreement between calculated and observed band widths and gas and liquid frequencies suggests that the vibrational and rotational partition functions for 2, 2-dimethyl butane are unaffected by the change from the gaseous to the liquid state and that the entropy change on vaporization could be accurately correlated with the change in free volume.

## CONCLUSION

Although the experiments described above are intended only to serve as an introduction to low temperature spectroscopy, they indicate that the method promises to be very valuable in several types of problems. In the spectroscopic analysis of molecular structure, it provides a better basis for comparison of Raman and infra-red data and a means of distinguishing bands unresolved by conventional methods. It provides a very useful tool for the study of the liquid state. The range of analytical applications of infra-red spectroscopy should be greatly enlarged by the use of low temperature technique.

## ACKNOWLEDGMENT

We are greatly indebted to Dr. Harold Gershinowitz for his interest and advice. Professor Paul C. Cross and Dr. E. J. Rosenbaum read the manuscript of the paper and we are grateful for their comments.

---

JANUARY, 1942 JOURNAL OF CHEMICAL PHYSICS VOLUME 10

# Raman Spectra of Dialkyl Ketones

FORREST F. CLEVELAND, *Department of Physics,*
M. J. MURRAY, J. R. COLEY, AND V. I. KOMAREWSKY, *Department of Chemistry,*
*Illinois Institute of Technology, Chicago, Illinois*

(Received October 22, 1941)

Displacements, estimated intensities and depolarization factors have been measured for acetone, 2,6-dimethyl-4-heptanone, 5-nonanone, 7-tridecanone, 8-pentadecanone and 5-tetradecanone. The results for acetone are compared with the previous data: Eight lines previously reported by one or more investigators are believed to be non-existent. A new weak line was observed at 1676 $cm^{-1}$. The depolarization factors obtained agree well with those reported by Simons, except that the 1356 line was found to be considerably less polarized and data for five additional lines were obtained.

## INTRODUCTION

THE dialkyl ketones, 2,6-dimethyl-4-heptanone, 5-nonanone, 7-tridecanone, 8-pentadecanone and 5-tetradecanone were prepared in another investigation by a new and convenient method of ketone production and it seemed desirable to obtain their Raman spectra while they were available. In searching the literature, it was noted that there were some discrepancies in the Raman data reported by many investi-

TABLE I. Raman spectrum of acetone as obtained by several investigators.

| N | Mean values Δν | I | ρ | Kohlrausch Köppl Δν | I | Sirkar Δν | I | Present results Δν | I | ρ | Probable values Δν | I | ρ |
|---|---|---|---|---|---|---|---|---|---|---|---|---|---|
| 1 | 360 | 0 | | | | | | | | | | | |
| 8 | 389 | 2 | 0.87 | 391 | 1 | 392 | 1.5 | 390 | 2 | 0.9 | 391 | 2 | 0.87 |
| 7 | 489 | 1 | | 486 | ½ | 487 | ½ | 492 | 1 | 0.9 | 488 | 1 | 0.9 |
| 12 | 528 | 2 | 0.70 | 532 | 3*b* | 527 | 2 | 531 | 4 | 0.7 | 530 | 3 | 0.70 |
| 1 | 544 | 1 | | | | | | | | | | | |
| 1 | 594 | 00 | | 594 | 00 | | | 580 | 0 | | 587 | 0 | |
| 1 | 727 | | | | | | | 735 | 0 | | 731 | 0 | |
| 15 | 788 | 7 | 0.20 | 787 | 8 | 789 | 5 | ± 786 | 8 | 0.1 | 787 | 7 | 0.20 |
| 1 | 821 | | | | | | | | | | | | |
| 5 | 903 | ½ | | 902 | 00 | 903 | 0 | 899 | ½ | | 901 | ½ | |
| 3 | 930 | 1 | | | | | | | | | | | |
| 12 | 1068 | 2 | 0.64 | 1066 | 2 | 1065 | 1 | 1066 | 4 | *P* | 1066 | 2 | 0.64 |
| 1 | 1093 | 0 | | | | | | | | | | | |
| 2 | 1192 | 3 | 0.88 | | | | | | | | | | |
| 12 | 1223 | 3 | 0.88 | 1220 | 2 | 1221 | 1 | 1221 | 5 | 0.8 | 1221 | 3 | 0.88 |
| 1 | 1247 | | | | | | | | | | | | |
| 9 | 1350 | 1 | 0.23 | 1354 | ½ | 1358 | 0 | 1355 | 2 | 0.6 | 1356 | 1 | 0.6 |
| 11 | 1429 | 3*b* | 0.90 | 1423<br>1438 | 3<br>4 | 1423 | 3*b* | 1427 | 6*b* | 0.8 | 1423<br>1438 | 3<br>4 | 0.90 |
| 1 | 1489 | | | | | | | | | | | | |
| | | | | | | | | 1676 | 0 | | 1676 | 0 | |
| 12 | 1711 | 4 | 0.38 | 1706 | 5*b* | 1705 | 5 | 1710 | 7 | 0.5 | 1710 | 6 | 0.38 |
| 1 | [1748] | 1 | | | | | | 1751 | ¼ | | 1750 | ¼ | |
| 3 | 2692 | 1 | | 2689 | 00 | 2689 | 0 | 2697 | 1 | *P* | 2692 | 1 | *P* |
| 5 | 2849 | 1 | | 2838 | 1 | 2857 | 0*b* | 2843 | 3 | *P* | 2840 | 3 | *P* |
| 1 | 2879 | | | | | | | 2865 | 2 | | 2871 | 2 | |
| 14 | 2924 | 7 | 0.22 | 2922 | 12*vb* | 2923 | 10 | 2921 | 10 | 0.1 | 2922 | 10 | 0.22 |
| 6 | 2967 | 4 | | 2965 | 5 | 2964 | 4 | 2963 | 4 | 0.9 | 2965 | 4 | 0.9 |
| 8 | 3005 | 4 | | 3005 | 4*b* | 3006 | 4 | 3004 | 5 | 0.8 | 3005 | 4 | 0.8 |

Δν = displacement in cm⁻¹, *I* = estimated intensity, ρ = depolarization factor, ± = Stokes and anti-Stokes, brackets enclose data in regard to which there is some uncertainty, the brace joins lines that were unresolved on the polarization spectrogram, *b* = broader than usual, *vb* = very much broader than usual, *P* = somewhat polarized but a quantitative estimate of the depolarization factor was not possible, *N* = number of times the line has been reported by independent investigators.

gators for acetone, the simplest dialkyl ketone, and that the depolarization factors for several strong lines had not been reported. Consequently, the Raman spectrum of this compound was obtained from carefully purified samples.

## EXPERIMENTAL

The apparatus and experimental technique were essentially the same as described in previous papers.[1] A few changes have been made: The mercury arc now has tungsten-Pyrex seals at the electrodes and was baked out for two hours at 450°C, under high vacuum, before the mercury was distilled into it. The side tube, which now has a somewhat larger diameter than previously in order to increase its effectiveness as a condenser was then sealed off while still on the pumps. The arc thus prepared has been in practically continuous operation for six months and shows no sign of leakage or deterioration. The arc is now started without changing the series resistance by placing the tip of a high frequency coil (commonly used for testing vacuum assemblages for leakage) near the mercury surface at the negative terminal.[2]

In the depolarization measurements, the Polaroid disk has been replaced by a Nicol prism, on account of the rather strong absorption of light by the Polaroid.

The ketones which were solids at room temperature were kept in the liquid state during exposure by means of an electric heating element wrapped loosely about the glass tube containing the sample. The width of the slit of the spectrograph was set at 0.08 mm for the regular expo-

[1] F. F. Cleveland, M. J. Murray, H. H. Haney, and J. Shackelford, J. Chem. Phys. **8**, 153 (1940); Forrest F. Cleveland and M. J. Murray, J. Chem. Phys. **7**, 396 (1939).

[2] We are indebted to Professor Paul L. Copeland, Department of Physics, for assistance in preparing the mercury arc and for suggesting this convenient method of starting it.

TABLE II. Raman spectra of some dialkyl ketones.

| Desig-nation | 2,6-dimethyl-4-heptanone Δν | I | ρ | 5-nonanone Δν | I | ρ | 7-tridecanone Δν | I | ρ | 8-pentadecanone Δν | I | 5-tetradecanone Δν | I | ρ | Desig-nation |
|---|---|---|---|---|---|---|---|---|---|---|---|---|---|---|---|
| | | | | | | | | | | | | 224 | 2*b* | | |
| | ±262 | 4 | 0.7 | 257 | 2 | 0.6 | | | | | | | | | |
| | 295 | 2 | | 271 | 2 | | | | | | | | | | |
| *a* | ±349 | 3*b* | | | | | | | | 394 | 1 | | | | |
| *b* | ±419 | 4 | 0.6 | | | | | | | | | | | | |
| | 533 | 2*b* | | | | | | | | | | | | | |
| | | | | 715 | 1 | | | | | | | 715 | 2*b* | | |
| *c* | 779 | 3*b* | 0.3 | 772 | 1 | | | | | | | 776 | 1 | | |
| | 815 | 2 | *P* | 823 | 2*b* | 0.6 | | | | | | 819 | 3*b* | *P* | *c* |
| *d* | 840 | 6 | 0.3 | | | | 843 | 1 | | 842 | 1 | 835 | 2*b* | | |
| | 870 | 1 | | 874 | 3 | 0.6 | 863 | 2 | | 872 | 2 | 872 | 3*b* | *P* | *d* |
| | | | | 892 | 2 | | 889 | 3 | 0.6 | 893 | 2 | 893 | 3*b* | *P* | *e* |
| | 929 | 1 | | | | | | | | | | | | | |
| *e* | 962 | 5 | 0.8 | | | | 970 | 1 | 0.9 | | | 962 | 2 | | |
| | 994 | ½ | | | | | | | | | | | | | |
| *f* | 1039 | 1 | | | | | 1020 | 1*b* | 0.9 | | | | | | *f* |
| | 1059 | 1 | | 1056 | 5 | 0.7 | | | | | | 1062 | 5 | 0.6 | |
| | | | | | | | | | | | | | | | *g* |
| | 1074 | 1 | | 1065 | 3 | | 1074 | 4*b* | 0.7 | 1074 | 5*b* | 1083 | 5 | 0.6 | |
| *h* | 1133 | 5*b* | 0.7 | 1121 | 4 | 0.5 | 1119 | 4 | 0.6 | 1120 | 5 | 1123 | 5 | 0.4 | *h* |
| *i* | 1171 | 4 | 0.9 | | | | | | | 1168 | 1 | 1167 | 1 | | *i* |
| | 1215 | 1 | | | | | | | | | | | | | |
| | | | | 1301 | 4 | 0.7 | 1308 | 5 | 0.7 | 1303 | 6 | 1301 | 7 | 0.6 | *k* |
| *l* | 1333 | 4 | 0.8 | | | | | | | | | | | | |
| | 1411 | 3 | 0.7 | 1413 | 3 | 0.7 | 1411 | 2 | 0.7 | 1411 | 1 | 1405 | 3 | 0.9 | |
| | 1449 | 8 | | 1452 | 7 | | 1441 | 7 | | 1438 | 8 | 1441 | 8 | | |
| *m* | | | 0.8 | | | 0.7 | | | 0.7 | | | | | 0.7 | *m* |
| | 1465 | 8 | | 1462 | 4 | | 1456 | 5 | | 1455 | 6 | 1455 | 8 | | |
| | 1714 | 6 | 0.6 | 1717 | 5 | 0.6 | 1717 | 3 | 0.4 | 1713 | 3 | 1718 | 4 | 0.7 | |
| *n* | 2719 | 3 | *P* | | | | | | | | | | | | |
| | | | | 2736 | 2 | *P* | 2731 | 1 | 0.6 | 2731 | 2 | 2732 | 2 | 0.7 | *n* |
| | 2762 | 2 | | | | | | | | | | | | | |
| | | | | | | | 2858 | 10 | 0.1 | 2852 | 10 | 2853 | 10 | 0.1 | *o* |
| *o* | 2870 | 10 | 0.3 | 2869 | 10*b* | 0.2 | 2884 | 10 | | [2865 | 6] | 2870 | 10 | | |
| | | | | | | | | | 0.4 | | | | | 0.6 | |
| *p* | 2904 | 9*b* | 0.6 | 2911 | 9 | 0.6 | 2907 | 10 | | 2904 | 8 | 2897 | 10 | | *p* |
| | 2930 | 5 | *P* | 2936 | 10 | 0.2 | 2933 | 8 | 0.1 | 2931 | 9 | 2933 | 10 | 0.1 | *q* |
| *r* | 2966 | 10 | 0.9 | 2965 | 5 | 0.9 | 2965 | 4 | 0.9 | 2960 | 6 | 2967 | 5 | 0.9 | *r* |
| | 2983 | 3 | | | | | | | | | | | | | |
| | C.M.[a] | | | C.W. | | | C.W. | | | C.W. | | C.M. | | | |

[a] C.M. =continuum medium, C.W. =continuum weak; **bold type** indicates previously observed lines.

sures and 0.12 mm for the polarization exposures. The time of the exposures was 7–10 hours. Excitation was by Hg 4358A.

The ketones used in this investigation, with the exception of acetone and 2,6-dimethyl-4-heptanone which were both Carbide and Carbon Chemical Corporation products, were prepared by a catalytic method,[3] involving the simultaneous dehydrogenation and condensation of primary alcohols. The liquid ketones were purified by distillation in a column equivalent to twelve theoretical plates. The solid ketones were purified by recrystallization and finally were melted and distilled in vacuum directly into the Raman tube. The boiling or melting points were as follows: Acetone, b. p. 56.1°C, 2,6-dimethyl-4-heptanone, b. p. 168°, 5-nonanone, b. p. 187–188°, 7-tridecanone, m. p. 32.5–33.0°, 8-pentadecanone, m. p. 39–40°, 5-tetradecanone, m. p. 25.5–26.0°. Two samples of acetone were used, one of which was purified by use of the sodium bisulfite addition compound.

## RAMAN SPECTRUM OF ACETONE

The Raman data for acetone, as obtained by many investigators[4] are summarized in the first

[3] V. I. Komarewsky and J. R. Coley, J. Am. Chem. Soc. **63**, 700 (1941).

[4] See bibliography in *Der Smekal-Raman Effekt, Ergänzungsband* (Julius Springer, Berlin, 1938), p. 220.

columns of Table I. The depolarization factors are those measured by Simons.[5] In several of the earlier investigations unfiltered light was used. This made it difficult to decide which of the mercury lines was the exciting line and frequently non-existent lines were reported. With this in mind, the later work of Kohlrausch and Köppl[6] and of Sirkar[7] are listed separately in Table I. Finally, the present results and the values which seem to the authors to be the most probable ones are listed in the columns at the right. Frequencies that have been observed by only one of the investigators must be regarded as questionable and have for the most part not been included in the list of probable values.

Kohlrausch and Pongratz[8] have pointed out that the line 1192 is not real, but corresponds to the 2965 $cm^{-1}$ line excited by Hg 4047A. This conclusion is supported by the present results in which, not only was the 1192 line absent, but also the depolarization factor of the 2965 line (previously unknown) was found to be the same, within experimental error, as that of the line measured by Simons as 1192. The line 930, observed by three investigators, probably corresponds to the 2692 line excited by Hg 4047A.

The polarization data agree quite well with those of Simons, except that the 1356 line was found to be considerably less polarized and data for five additional lines were obtained.

### RAMAN SPECTRUM OF 2,6-DIMETHYL-4-HEPTANONE

To facilitate comparison, the spectra of the other five dialkyl ketones are listed side by side in Table II. Of these, the spectrum was most complete for the 2,6-dimethyl-4-heptanone. Displacements and estimated intensities have been reported for this compound by Kohlrausch and Köppl.[6] Displacements which agree within experimental error with their results appear in **bold type** in Table II. The weak lines at 1276 and 1619 $cm^{-1}$ were not observed in the present investigation, but nine new lines were found. The doublet 1449, 1465 corresponds to the broad line at 1456 $cm^{-1}$ in the previous report.

The lines designated by the letters *a*, *b*, etc. are those listed by Kohlrausch and Köppl[6] as characteristic of isobutyl compounds. They were obtained by examination of the spectra of eight compounds containing the $(CH_3)_2CHCH_2$-group. The surprisingly large intensities of the 2870 and 2966 lines may result from coincidence of $CH_3$ and $CH_2$ frequencies, since acetone, containing only $CH_3$ groups, had frequencies at 2871 and 2965 $cm^{-1}$.

### KETONES OF THE TYPE $CH_3(CH_2)_nCO(CH_2)_mCH_3$

In general, the spectra of the four ketones of this type are not as complete as for the one just discussed. The frequencies given by Kohlrausch and Köppl[6] as characteristic of $C_nH_{2n+1}$ are indicated by the letters in the right-hand column of Table II. A new frequency, not observed for acetone or 2,6-dimethyl-4-heptanone, appears near 1303 $cm^{-1}$. It is somewhat polarized and seems to become more intense as the length of the chain increases. The possibility that this may be a chain frequency is suggested by the fact that Whitcomb, Nielsen and Thomas[9] have calculated values of 385, 1106, 1354, 1463, 2320 and 2778 $cm^{-1}$ for the chain frequencies of straight chain paraffins. Values observed by them in the infra-red spectrum of undecane were 1066, 1308, 1463, 2320 and 2778 $cm^{-1}$, the exact coincidence of the last three observed values with the calculated values being explained by the fact that these frequencies were used to adjust the force constants. Frequencies observed here for the normal ketones which may correspond to these are 394 (observed for only one), 1075, 1303 and 2733 $cm^{-1}$.

In the 3000 $cm^{-1}$ region an exceedingly intense, polarized line appears at 2855 $cm^{-1}$ for the last three ketones and the 2983 line, found for the 2,6-dimethyl-4-heptanone, was not observed for any of the four normal ketones.

[5] L. Simons, Soc. Scient. Fenn. Com. Phys. Math. **6**, No. 13 (1932).
[6] K. W. F. Kohlrausch and F. Köppl, Zeits. f. physik. Chemie **B24**, 370 (1934).
[7] S. C. Sirkar, Ind. J. Phys. **7**, 61 (1932).
[8] K. W. F. Kohlrausch and A. Pongratz, Zeits. f. physik. Chemie **B27**, 180 (1934).
[9] S. E. Whitcomb, H. H. Nielsen, and L. H. Thomas, J. Chem. Phys. **8**, 143 (1940).

# The Polymerization of Ethylene Photosensitized by $5^1P_1$ Cadmium Atoms

E. W. R. STEACIE AND D. J. LEROY
*Division of Chemistry, National Research Laboratories, Ottawa, Canada*

(Received October 21, 1941)

An investigation has been made of the reactions of ethylene photosensitized by $5^1P_1$ cadmium atoms, i.e., using the resonance line at 2288A. It is found that reaction occurs readily, in contrast to the action of $5^3P_1$ atoms, which have been previously shown to be ineffective. The products of the reaction are butene, hexene, and higher olefins, together with smaller amounts of acetylene and hydrogen. No pressure rise is detectable in the early stages of the reaction, and acetylene is a much less important product than is the case with mercury photosensitization. It is concluded that the primary step may be either

$$Cd(^1P_1)+C_2H_4=Cd(^1S_0)+C_2H_3+H$$

or

$$Cd(^1P_1)+C_2H_4=Cd(^1S_0)+C_2H_4^*.$$

Subsequent polymerization probably occurs by a free radical mechanism.

IN recent years we have made a number of investigations of reactions photosensitized by $5^3P_1$ cadmium atoms, the atoms being excited by absorption of the resonance line at 3261A.[1-4] These results are of interest by comparison with mercury photosensitization, since the magnitude of the excitation energy of the photosensitizer is much smaller, *viz.*, 87 kcal. as compared with 112 kcal. for $Hg(6^3P_1)$. In view of this it seemed worth while to extend the investigations to a number of excitation energies of different magnitudes, and experiments have accordingly been made with $Cd(5^1P_1)$, $Zn(4^3P_1)$, and $Zn(4^1P_1)$ atoms. The results with zinc will appear shortly.[5] The present paper deals with photosensitization by $Cd(5^1P_1)$, the atoms being excited by absorption of the lower resonance line at 2288A. The excitation energies, etc., corresponding to the use of both resonance lines for zinc, cadmium, and mercury are given in Table I.[6]

In view of the interest attaching to the photosensitized polymerization of ethylene, we have chosen this reaction as the initial investigation of photosensitization with $Cd(5^1P_1)$ atoms.

A number of investigations of the mercury photosensitized reactions of ethylene have been made, largely by Taylor and his collaborators. Virtually all investigators adopt for the primary step the suggestion of Taylor and Bates[7,8]

$$C_2H_4+Hg(^3P_1)=C_2H_2+H_2+Hg(^1S_0).$$

It is then assumed that the subsequent reactions are the photosensitized polymerization of acetylene, together with reactions of hydrogen atoms and of radicals with ethylene, *viz.*,

$$H+C_2H_4=C_2H_5$$
$$C_2H_5+C_2H_4=C_4H_9, \text{ etc.}$$

The main evidence for this mechanism is the detection of large amounts of acetylene in the products of the reaction, and the fact that the pressure *rises* considerably in the early stages of the reaction, passes through a maximum, and then decreases.

We have recently[9] made a more detailed investigation of the reaction with special emphasis on the early stages. It was found that in the initial stages the pressure rise and acetylene production were exactly equivalent, but that the initial rate of acetylene production (or of pressure increase) decreased with increasing

[1] E. W. R. Steacie and R. Potvin, Can. J. Research **B16**, 337 (1938).
[2] E. W. R. Steacie and R. Potvin, J. Chem. Phys. **7**, 782 (1939).
[3] E. W. R. Steacie and R. Potvin, Can. J. Research **B18**, 47 (1940).
[4] E. W. R. Steacie, D. J. LeRoy and R. Potvin, J. Chem. Phys. **9**, 306 (1941).
[5] E. W. R. Steacie and H. Habeeb, unpublished.
[6] E. W. R. Steacie, Ann. N. Y. Acad. Sci. **41**, 187 (1941).
[7] H. S. Taylor and J. R. Bates, Proc. Nat. Acad. Sci. (Washington) **12**, 714 (1926).
[8] J. R. Bates and H. S. Taylor, J. Am. Chem. Soc. **49**, 2438 (1927).
[9] D. J. LeRoy and E. W. R. Steacie, J. Chem. Phys. **9**, 829 (1941).

TABLE I. Excitation energies, etc.

| Substance | Resonance line, A | Transition | Energy of excited atom, kcal. | Heat of dissociation of hydride, kcal. | "Maximum energy available" to split off H atom, assuming intermediate hydride formation, kcal. |
|---|---|---|---|---|---|
| Mercury | 1849 | $6^1S_0-6^1P_1$ | 153.9 | 8.5 | 162.4 |
| | 2537 | $6^1S_0-6^3P_1$ | 112.2 | 8.5 | 120.7 |
| Cadmium | 2288 | $5^1S_0-5^1P_1$ | 124.4 | 15.5 | 139.9 |
| | 3261 | $5^1S_0-5^3P_1$ | 87.3 | 15.5 | 102.8 |
| Zinc | 2139 | $4^1S_0-4^1P_1$ | 133.4 | 23.1 | 156.5 |
| | 3076 | $4^1S_0-4^3P_1$ | 92.5 | 23.1 | 115.6 |

pressure. This points definitely to an excited molecule type of mechanism, *viz.*,

$$C_2H_4+Hg(^3P_1)=Hg(^1S_0)+C_2H_4^*$$
$$C_2H_4^*=C_2H_2+H_2$$
$$C_2H_4+C_2H_4^*=2C_2H_4.$$

One of the most striking features of the investigation was the explanation afforded for the subsequent pressure decrease. It has usually been assumed that the decrease was caused by the photosensitized polymerization of acetylene formed in the early stages of the reaction. It was found that this was definitely contrary to the facts, since the acetylene concentration increased without interruption after the pressure had begun to fall. It was found that hydrogen was responsible for the pressure decrease, presumably by an atom and radical sensitized polymerization of ethylene, *viz.*,

$$H_2+Hg(^3P_1)=Hg(^1S_0)+2H$$
$$H+C_2H_4=C_2H_5$$
$$2C_2H_5=C_4H_{10}$$
$$C_2H_4+C_2H_5=C_4H_9, \text{ etc.}$$

Acetylene proved to be surprisingly stable to attack by excited mercury atoms in the presence of ethylene, its concentration in some cases rising to 30 percent of the total gas mixture.

Bates and Taylor[10] made the first investigation of the cadmium photosensitized reactions of ethylene-hydrogen mixtures, using the resonance line at 3261A, i.e., $5^3P_1$ cadmium atoms. A more detailed investigation of the reactions photosensitized by $Cd(5^3P_1)$ atoms has recently been made by one of us.[11] The results are striking in that they indicate a quantum efficiency of about 0.5 for a 1 : 1 ethylene-hydrogen mixture, but a yield of only about 0.015 for pure ethylene. Furthermore, this does not seem to be due to a lack of quenching by ethylene, since qualitative indications are that ethylene quenches reasonably strongly.

Two possible explanations suggest themselves for the difference between the results with $Cd(^3P_1)$ and $Hg(^3P_1)$ atoms. The reaction

$$C_2H_4=C_2H_2+H_2 \qquad (1)$$

is endothermic to the extent of 42.9 kcal.[12] The activation energy of the reaction has not been determined, but Taylor and van Hook[13] have found that of the reverse reaction to be roughly 42 kcal. Combining these results we obtain a value of approximately 85 kcal. for the activation energy of reaction (1). It is therefore possible that the 112 kcal. associated with a $^3P_1$ mercury atom can cause reaction, while the 87-kcal. excitation energy of a $^3P_1$ cadmium atom cannot be used efficiently enough to do so.[14]

On the other hand, there is a great deal of evidence that the polymerization of ethylene can be induced by free radicals, and this suggests the possibility of the thermal reaction proceeding by a free radical mechanism.[15] It also suggests the possibility of the photosensitized reaction

[10] J. R. Bates and H. S. Taylor, J. Am. Chem. Soc. **50**, 771 (1928).
[11] E. W. R. Steacie and R. Potvin, Can. J. Research **B16**, 337 (1938).
[12] F. R. Bichowsky and F. D. Rossini, *Thermochemistry of Chemical Substances* (New York, 1936).
[13] H. A. Taylor and A. van Hook, J. Phys. Chem. **39**, 811 (1935).
[14] For a discussion of this point and of the mechanism of quenching from the standpoint of potential energy surfaces and the theory of absolute reaction rates see K. J. Laidler, J. Chem. Phys. **10**, 34 (1942).
[15] See, e.g., H. D. Burnham and R. N. Pease, J. Am. Chem. Soc. **62**, 453 (1940).

involving a primary split into radicals, i.e.,

$$C_2H_4+M^*=C_2H_3+H+M$$
$$\text{or}=C_2H_3+MH.$$

If this is the case, the $Cd(^3P_1)$ photosensitized reaction would be ruled out if the strength of the C−H bond in ethylene is greater than 103 kcal. It is, however, impossible to reconcile this with the facts as far as the mercury photosensitized reaction is concerned. However, it seemed possible that such a mechanism might hold for other sensitizers, and accordingly we have investigated the polymerization of ethylene photosensitized by $Cd(5^1P_1)$ atoms.

## EXPERIMENTAL

### The Light Source

The cadmium resonance lamp was similar to one previously described[1,2] except that the emitting portion of the lamp was made of quartz rather than of Corex D glass, in order to transmit λ2288. The lamp consisted of a 6-inch length of 11 mm outside diameter quartz tubing connected by graded seals to Pyrex tubing of the same diameter. To the ends of this were sealed electrode chambers of Pyrex, 1 inch in diameter and 3 inches long. These contained standard neon sign "coated" sheet iron electrodes in the form of hollow cylinders ½ inch in diameter and 1½ inches long. The ends of the electrodes contained annular porcelain insulators to prevent excessive sputtering. The lamp contained a piece of cadmium, weighing about 0.1 gram, and was filled with neon at a pressure of 3 mm at room temperature. Mercury vapor was excluded during the evacuation and filling. The filling of the tube, outgassing, etc., was done by the usual neon sign technique.

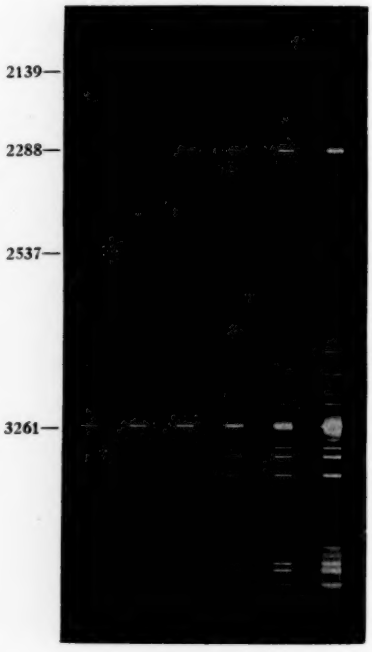


FIG. 1. Spectrogram of cadmium resonance lamp. Successive exposures 60, 10, 2, 1, ½, and ⅕ sec.

The lamp was operated at 120 milliamperes from a 6000-volt sign transformer.

A set of spectrograms of the lamp, taken with a Hilger intermediate quartz spectrograph, is shown in Fig. 1. Considering the diminished plate sensitivity in the short ultraviolet it is apparent that the two resonance lines, 2288A, and 3261A, are much more intense than any other lines. The zinc resonance line 2139A, and the mercury line at 2537A appear, but their intensities are far too low to have any appreciable effect. The zinc line at 3076A is probably present also, but is masked by the fairly strong cadmium line, 3082A. It is evident that the lamp is highly efficient for photosensitization purposes, since the intensity is mainly in the two resonance lines. In this respect it compares very favorably with commercial high voltage mercury lamps.

When desired the lower resonance line could be completely filtered out, and λ3261 almost completely transmitted by surrounding the lamp with a filter consisting of an 8-inch length of Corex D tubing with a wall thickness of about 2 mm.

The output of the lamp was determined only very roughly, since it is intended to make quantum yield determinations of this and other cadmium photosensitized reactions in the near future. There appears to be no suitable actinometer for 2288A which could be used at 300°C. The intensity was therefore merely estimated geometrically from the amount emerging from a quartz window on the side of the furnace. This indicated that the amount of λ2288 entering the reaction vessel was of the order of $10^{-6}$ to $10^{-7}$ einstein per sec.

The output was very constant, and a series of measurements with a thermopile, and with a

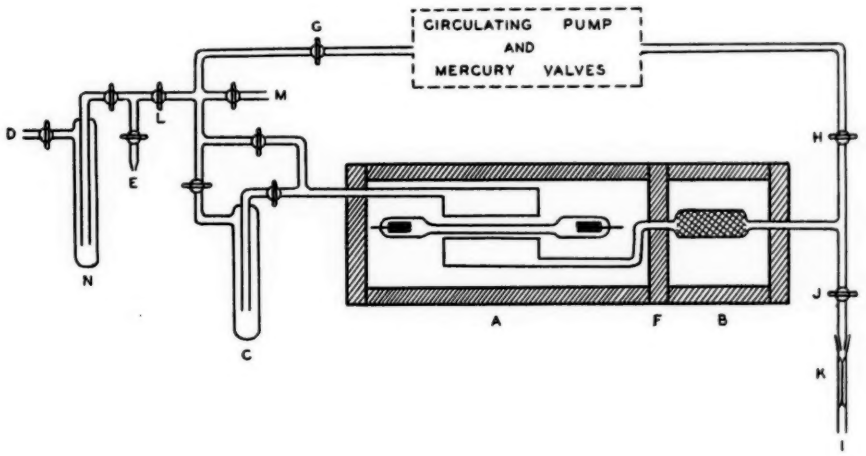


FIG. 2. Apparatus.

General Electric F.J. 405 sodium photo-tube indicated that the output was constant to within 5 percent over long periods of time.

More accurate measurements were made of the relative intensities of λ2288 and λ3261. In these a beam of radiation from the quartz window was defined by stops (but without lenses, to avoid focal isolation) and then used in various ways:

(a) A uranyl oxalate actinometer was used with and without a chlorine filter. Allowing for the transmission of the filter this gave approximately $\lambda 3261/\lambda 2288 = 1.5$.

(b) A sodium photo-tube was used together with various combinations of chlorine and Corex D filters. Allowing for the transmission, and for the variation of the sensitivity of the photo-tube with wave-length, this gave in 4 determinations

$$\lambda 3261/\lambda 2288 = 0.75,\ 0.97,\ 0.97,\ 1.04.$$

This value of the ratio will be somewhat low on account of the presence of other lines in the region of 2800A where the photo-tube has maximum sensitivity.

(c) A thermopile was used with various filter combinations. This gave a value for the ratio of 2.3, which will be somewhat high since some of the long ultraviolet will appear as λ3261.

(d) Photographic determinations were made using Eastman 40 U. V. sensitized plates. With rough corrections for the falling off in plate sensitivity at the shorter wave-lengths these indicated a value of about 2 for the ratio.

It thus appears that the ratio of the intensities of λ3261 to λ2288 is not far from 1.5.

For the interpretation of the results of photosensitization experiments, some knowledge of quenching efficiencies is required. An investigation of the quenching of cadmium resonance radiation by a number of gases is in progress, and pending the completion of this work only rough "absorption" measurements were made. For these cadmium turnings were placed directly in the reaction cell, and the intensity of the resonance radiation transmitted at 225°C was measured photographically, and also in some cases with the photo-tube or thermopile and suitable filter combinations. These approximate measurements indicated a rather low absorption of λ3261 by ethylene, i.e., with a 4-cm path there was about 30 percent absorption at 35-mm pressure, while under the same circumstances over 90 percent of λ2288 was absorbed.

### The Reaction System

The reaction system is shown diagrammatically in Fig. 2. The lamp was contained in a furnace *A*, which was cylindrical in shape and was heated electrically. The lamp was surrounded by an annular fused quartz reaction vessel, 10 cm long, 8 cm in diameter, with a 4-cm diameter hole through the middle. The tube leading from the right-hand end of the reaction vessel passed into a second furnace *B*, and was connected through a graded quartz to Pyrex seal to a Pyrex tube 1 inch in diameter and 1 foot

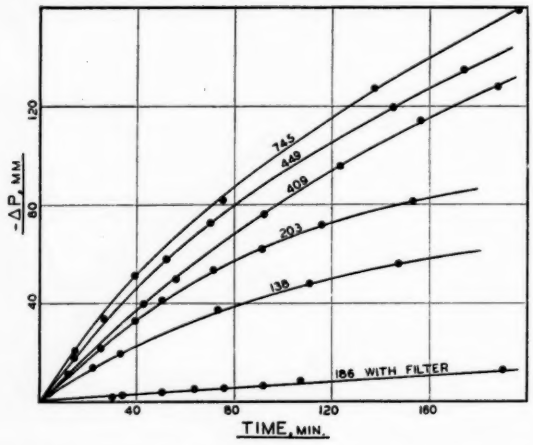


FIG. 3. Pressure decrease—time curves for ethylene alone. Ethylene pressures in mm as shown. The lowest curve shows the rate with the filter on, i.e., with λ3261 only.

long which contained cadmium turnings. This acted as a saturator to furnish cadmium vapor to the reaction system. The temperatures of *A* and *B* could be independently varied. The furnace *A* contained a fused quartz window opposite the reaction vessel through which spectroscopic observations of the lamp could be made.

The temperatures of the two furnaces were measured by means of copper-constantan thermocouples. The temperatures were regulated by Cenco bimetallic regulators. We have found that these can be lengthened to over three feet without affecting their operation. This is done by merely sawing the outer tube and inner rod in half, and brazing on an additional length of brass tube and of drill rod with silver solder.

The experimental arrangement could be used for static, circulatory, or single-pass flow runs. For circulatory runs a circulating pump was used which consisted essentially of two Toepler pumps with mercury reservoirs on a rocker which alternately raised and lowered them. This arrangement avoided volume, and pressure, changes in the system during the cycle of operation of the pumps. The pumps had a speed of about 500 cc per minute. A system of mercury bubblers was used as valves, so that the gas always circulated in the same direction, i.e., through the saturator and then the furnace. After leaving the furnace the gases passed through a trap *C*. This could be maintained at any desired low temperature by an arrangement which has been previously described.[9] After passing the trap the gases returned to the circulating pump.

A manometer was connected to the system at *M*. By a suitable manipulation of stopcocks the trap *C* could be isolated or by-passed when desired. The usual oil pump, mercury vapor pump, McLeod gauge, gas reservoirs, etc., were connected at *D*. Gaseous or liquid products could be removed through *E*. The total apparent volume of the circulating system, when the furnaces were at 300°C, was 945 cc.

Static runs could be made when desired by sealing off the tubing between the reaction vessel and the saturator at the point *F*, putting cadmium turnings in the reaction vessel, and shutting the stopcocks leading to the circulating pump. The apparent volume of the system when used in this way was 512 cc.

To make single-pass runs stopcocks *G* and *H* were closed. A cylinder of ethylene with a regulating valve set at about 5 lb. was connected at *I*, stopcock *J* was opened, and gas flowed into the apparatus at a rate determined by the size of the capillary *K*. The gas passed through the saturator, reaction vessel, and the trap *C*, and then through the file-scratched stopcock *L* to a liquid-air trap *N*. The filed stopcock was adjusted until the desired pressure was indicated on the manometer. In the absence of permanent gases all the gas flowing through the apparatus

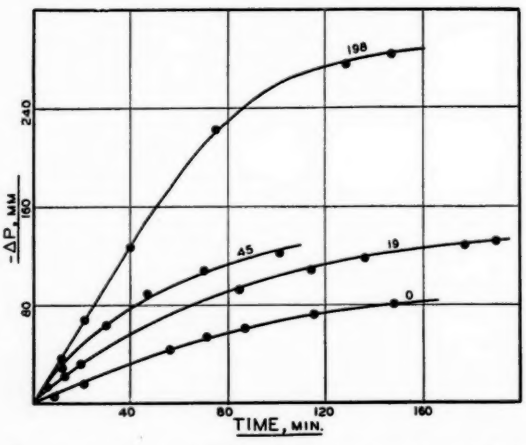


FIG. 4. Pressure decrease—time curves for ethylene-hydrogen mixtures. Ethylene pressure approximately 200 mm. Hydrogen pressures in mm as shown.

was collected in $N$. If, however, hydrogen were formed in appreciable quantity it was necessary to pump out $N$ occasionally during a run. The apparent volume of the single-pass system was 738 cc.

### Analysis of Products

The gaseous products of the reaction were analyzed in a small-capacity low temperature distillation apparatus of the Podbielniak type. The liquid products were fractionated in a micro-distillation apparatus, and the fractions were analyzed by more or less conventional micro-analytical methods. Acetylene was determined as previously described.[9]

TABLE II. Acetylene production in static runs at 280°C.

| Initial ethylene pressure, mm | Time, min. (corrected for change in transmission of cell) | Pressure decrease, mm | Acetylene formed cc | Acetylene formed mm | $\frac{-\Delta P}{C_2H_2}$ |
|---|---|---|---|---|---|
| 438.5 | 9 | 12.5 | 0.28 | 0.41 | 30.0 |
| 440 | 23 | 29.5 | 0.58 | 0.86 | 34.4 |
| 201.5 | 10.5 | 8.5 | 0.40 | 0.59 | 14.4 |
| 199.5 | 16.5 | 14.0 | 0.48 | 0.71 | 19.8 |
| 201 | 23 | 17.5 | 0.69 | 1.02 | 17.2 |
| 199.5 | 23.5 | 20.0 | 0.67 | 0.99 | 20.2 |
| 201 | 46 | 33.0 | 0.95 | 1.41 | 23.4 |
| 201 | 88 | 51.5 | 1.00 | 1.48 | 34.8 |
| 100.5 | 10 | 5.5 | 0.39 | 0.58 | 9.5 |
| 99.5 | 38 | 19.0 | 0.70 | 1.04 | 18.3 |
| 101 | 10 | 5.0 | 0.33 | 0.48 | — (A) |
| 51.5 | 10.5 | 3.0 | 0.43 | 0.64 | 4.7 |
| 50.5 | 18.5 | 6.5 | 0.56 | 0.83 | 7.8 |
| 50.5 | 20 | 7.0 | 0.56 | 0.83 | 8.5 |
| 51.0 | 31 | 11.0 | 0.61 | 0.91 | 12.1 |
| 51.0 | 58 | 16.5 | 0.59 | 0.88 | 18.8 |
| 23.0 | 10.5 | 2.5 | 0.40 | 0.59 | 4.2 |
| 24.2 | 21.5 | 4.4 | 0.52 | 0.77 | 5.7 |
| 11.0 | 5.0 | 0.65 | 0.20 | 0.30 | 2.2 |
| 10.1 | 10.5 | 1.3 | 0.30 | 0.45 | 2.9 |
| 10.0 | 23 | 2.0 | 0.33 | 0.49 | 4.1 |
| 94.7 +4.8 mm of $H_2$ | 10 | 9.0 | 0.26 | 0.39 | — (B) |
| 93.7 +4.8 mm of $H_2$ | 43 | 25.5 | 0.48 | 0.71 | — (B) |

(A) In this run the products were allowed to stand, after turning off the lamp, for 15 hours in the reaction system at 280°C before withdrawing the sample for analysis. The results show that any loss of acetylene due to thermal reactions is negligible in the length of time required for an ordinary run.

(B) These runs show that the addition of an amount of hydrogen much larger than that which might be formed in the reaction cuts down acetylene production only by about 30 percent, probably merely owing to quenching by hydrogen as well as ethylene.

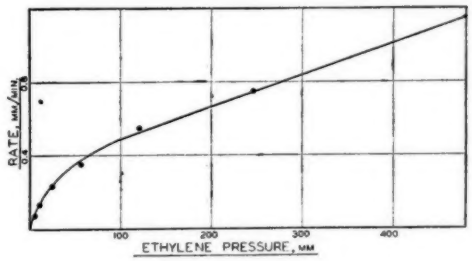


FIG. 5. Static runs—initial rates.

### Materials

The cadmium used was the purest commercial grade. It contained a small amount of zinc. The metal was cast into thick rods and turned on a lathe into thin coherent turnings.

Ethylene was obtained in cylinders from the Ohio Chemical and Manufacturing Company, and was purified by simple bulb to bulb distillation. For single-pass runs it was taken direct from the cylinder.

Hydrogen was of commercial grade. It was passed over hot copper and through a liquid-air trap.

## RESULTS

### (1) Static Runs

A series of static runs was first made at 280°C with various pressures of ethylene. The results are given in Fig. 3, and show that the rate of pressure decrease increases strongly with increasing pressure. The lowest curve represents runs made with the Corex D filter in place, so that only λ3261 was transmitted. It is evident that λ3261 is relatively inefficient compared to λ2288, and that when both lines are present little error will be introduced if we disregard the effect of λ3261, and attribute any effects observed to λ2288 alone.

It will be noted that the curves show no indications of a pressure *rise* in the initial stages of the reaction, as occurs in the mercury photosensitized reaction. However, the total rise in the case of mercury is small, amounting to from 1 to 2 millimeters at the pressures employed here. In view of the difficulties in thermostating at 300°C, such small effects would be difficult to establish. However the absence of any signs of an induction period in the pressure-time curves is proof that if a rise does occur it is considerably

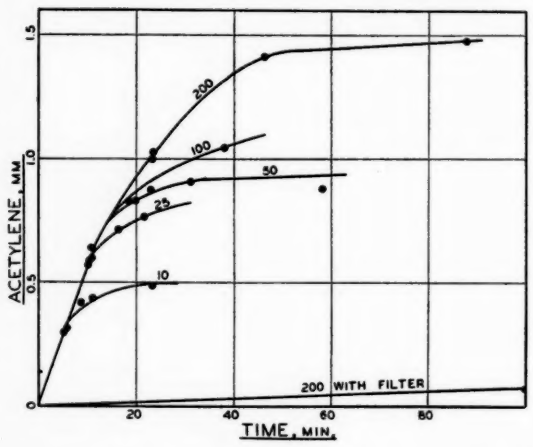


FIG. 6. Acetylene production in static runs. Ethylene pressures in mm as shown.

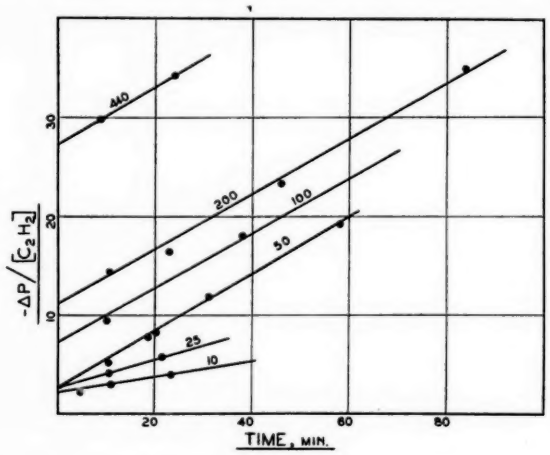


FIG. 7. Ratio of pressure increase to acetylene production in static runs.

smaller than in the case of mercury. An initial rise of 0.5 mm or less at a total pressure of 200 mm might, however, have escaped detection.

Figure 4 shows the results of a series of runs made with 200 mm of ethylene and varying amounts of hydrogen at 280°C. The rate is obviously strongly increased by hydrogen, presumably largely because, as shown previously, the photosensitized reaction with λ3261 occurs readily in the presence of hydrogen, but not in its absence. Since the result is a reaction in which both resonance lines participate the situation is complex, and no further work was done with ethylene-hydrogen mixtures.

The results given in Fig. 3 show the general trend of the effect of pressure on the rate of pressure decrease. They are not very accurate since a layer of brown polymer very slowly forms on the walls of the reaction vessel and cuts down the intensity of the radiation entering the cell. The effect is, however, quite slow and only becomes troublesome when a series of long runs are being made. To correct for this a series of runs were made with the vessel freshly cleaned. The duration of these was as short as possible, and only initial rates of pressure decrease were determined. These are given in Fig. 5. The total time of illumination for the whole series was short enough so that no appreciable polymer deposition occurred. Figure 5 was then used as a calibration curve for future runs to correct for the loss of intensity due to polymer formation. In all cases this correction was only applied until the intensity had fallen off about 30 percent, after which the cell was cleaned by taking the apparatus apart, washing with fuming nitric acid, and flaming in a stream of oxygen. Check runs were made from time to time during all phases of the investigation to correct for the variation in transmission of the cell due to polymer formation.

The static runs indicated that liquid products boiling in the butene-hexene range were formed, but on account of the small quantity of material available they were not suitable for an investigation of the liquid products of the reaction. However the quantity of gas available was ample for acetylene determinations, and in view of the importance of acetylene as a product of the mercury photosensitized reaction an extended series of runs was made to determine the relative magnitudes of acetylene formation and of the pressure decrease under various conditions. The results of these runs are given in Table II. The fourth column of the table gives the amount of acetylene found, and the fifth column the partial pressure this would exert in the system. The last column gives the ratio of the pressure decrease to the acetylene formed, both quantities being expressed in mm.

The results on the production of acetylene are shown in Fig. 6. This shows that, within the experimental error, the initial rate of acetylene production is independent of the ethylene

pressure. As a run proceeds and ethylene is used up, the acetylene production falls off and as would be expected this effect occurs sooner with low pressure runs, where the total amount of ethylene in the system is relatively small. The initial rate of acetylene production is about 0.056 mm per min., or $2.7\times10^{-8}$ mole per sec. This corresponds to a quantum yield of acetylene production of the order of 0.05 to 0.1.

Figure 7 shows the ratio of the pressure decrease to acetylene production, both expressed in mm. It will be seen (a) that the ratio increases as a run proceeds, and (b) that the initial ratio is approximately constant up to 50-mm pressure and equal to about 2, and that at higher pressures it increases rapidly to nearly 30 at 440-mm pressure. Assuming that the pressure decrease in the early stages of the reaction is due solely to the formation of butene, this means that at pressures below 50 mm in the early stages of the reaction about 6 ethylene molecules disappear by forming butene for every one which disappears by forming acetylene. At 440-mm pressure on the same basis about 58 molecules of ethylene disappear by polymerization for each one disappearing by forming acetylene.

It may be noted from Fig. 6 that the acetylene concentration in any run eventually reaches a constant value. Thus, for example, at 200-mm initial ethylene pressure acetylene builds up to about 1.5 mm in 60 min. and then remains sensibly constant. Calculation shows that at 60 min. slightly less than half the ethylene has disappeared, mostly by polymerization. Since the initial rate of acetylene formation is independent of the pressure, it follows that the drop in acetylene production is not due merely to the decreasing concentration of ethylene. It must therefore be due to (a) competing processes which destroy acetylene, (b) to a reaction of hydrogen, or (c) to a diminished formation of acetylene owing to quenching by butene rather than ethylene. It seems unlikely that the effect is due to a loss of acetylene by direct photosensitized polymerization, since the quantity of acetylene present is always very small compared with that of ethylene and butene, and acetylene cannot have a much larger quenching cross section than the olefins. The indications are that hydrogen atoms have little action on acetylene,[16–19] although no experiments have been made at high temperatures. Acetylene may, however, disappear indirectly through a reaction of hydrogen atoms, i.e.,

$$H+C_2H_4=C_2H_5$$
$$C_2H_5+C_2H_2=\text{polymer}.$$

It may also disappear by reaction with higher radicals produced from butene.

It appeared possible that the small amount of acetylene formed might arise by a reaction involving λ3261 rather than λ2288. To check this runs were made in the static system at 200-mm pressure with the filter on. These showed a production of acetylene of 0.03 cc of acetylene per hour. This is negligible as far as the present investigation is concerned.

As mentioned previously, acetylene is surprisingly inert to the action of excited mercury atoms in the presence of ethylene. This suggests an excited molecule mechanism for the acetylene polymerization, with efficient deactivation by ethylene.

TABLE III. Production of liquid products in circulating runs. Temperature = 290°C; trap temperature = −130°C; saturator temperature = 300°C; ethylene pressure = approximately 20 cm.

| Run No. | $-\Delta P$ mm per hr | Time, min. | Liquid products, cc per min. $\times10^4$ | Remarks |
|---|---|---|---|---|
| 1 | 0.57 | 280 | 8.7 | |
| 2 | 0.43 | 275 | 7.0 | |
| 3 | 0.42 | 245 | 7.4 | |
| 4 | 0.38 | 272 | 5.8 | |
| 5 | 0.33 | 330 | 5.3 | |
| 6 | 0.29 | 305 | 4.7 | |
| 7 | 0.64 | 250 | 10.0 | System cleaned out and |
| 8 | 0.55 | 275 | — | reaction vessel flamed |
| 9 | 0.46 | 275 | 7.5 | in oxygen after run 6. |
| 10 | 0.40 | 280 | — | |
| 11 | 0.39 | 275 | — | |
| 12 | 0.32 | 280 | — | |
| 13 | <0.02 | 350 | 0.0 | Filter on. Only λ3261 transmitted. |
| 14 | <0.02 | 280 | 0.0 | Blank run. Lamp not on. |

[16] K. F. Bonhoeffer and P. Harteck, Zeits. f. physik. Chemie **139**, 64 (1928).
[17] H. v. Wartenberg and G. Schultze, Zeits. f. physik. Chemie **B2**, 1 (1929).
[18] K. H. Geib and E. W. R. Steacie, Zeits. f. physik. Chemie **B29**, 215 (1935).
[19] J. R. Bates and H. S. Taylor, J. Am. Chem. Soc. **49**, 2438 (1927).

To test this point further runs were made in the circulating system with the 3261A line alone (i.e., with a Corex D filter). This has previously been shown to have very little effect on pure ethylene. With acetylene alone at 200-mm pressure, the acetylene consumption was 90 cc per hour in a two-hour run. This will be a minimum rate since the transmission of the cell was greatly diminished by the deposition of polymer on the walls, and the initial rate must have been much higher. After cleaning the reaction vessel an experiment was made with 200-mm total pressure of a mixture consisting of 77 percent ethylene and 23 percent acetylene. In one hour 1.9 cc of acetylene was consumed, together with a trace of ethylene. It follows that in a 3 to 1 mixture of ethylene and acetylene the rate of polymerization of acetylene has fallen to less than 1/47 of the rate for pure acetylene. It seems highly unlikely that the quenching cross section of ethylene for $^3P_1$ cadmium atoms can be 10 times greater than that of acetylene, and it must therefore be concluded that excited acetylene molecules are easily deactivated by collision with ethylene.

### (2) Circulating and Single-Pass Runs

The runs in the circulating and single-pass systems were mainly of long duration, and were designed to accumulate products for analysis, especially liquid products. During such long runs a very thin film of highly polymerized material built up on the walls of the vessel and cut down the light transmission. Examples of the over-all rates of successive runs of about 4 hours duration are given in Table III. These runs were made primarily for the purpose of collecting liquid products, and the trap was maintained at −130°C to diminish secondary reactions of the products of higher molecular weight.

The results on the production of acetylene in circulating and single-pass runs are given in Fig. 8. The times given in the figure have been corrected for the drop in transmission of the reaction cell in successive runs, using the data of Table III. In these runs the temperature of the reaction vessel was 290°C, and that of the saturator was 300°C. The pressure was 20 cm in both cases. In the circulating runs the trap

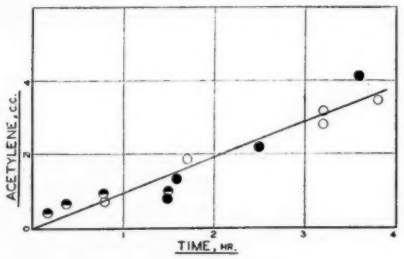


FIG. 8. Acetylene production in all types of run; open circles = circulating runs; filled circles = single-pass runs; half-filled circles = static runs.

temperature was −130°C. In the single-pass runs the flow rate was 20 cc per min. at N.T.P., corresponding to a contact time of about 2.0 min. Some single-pass runs were also made at higher flow rates, *viz.*, 136 and 394 cc per min. In these runs, however, considerable difficulty was encountered in obtaining satisfactory saturation with cadmium vapor. The results were therefore rather unreliable and are not reported, but as far as they went they indicated that the change in flow rate made no appreciable change in the rate of acetylene production. In the single-pass runs all the gas flowing was condensed in a liquid-air trap and an aliquot was analyzed for acetylene.

Some explanation is required of the fact that the maximum acetylene production in static runs of long duration is approximately 1 cc, while in circulating runs it rises to above 4 cc. (Obviously it will increase linearly with time indefinitely in single-pass runs.) There are several factors which together will account for the larger acetylene production in circulating runs of long duration.

(a) The volume of the circulating system is larger by a factor of nearly 2. Hence if the maximum occurred at the same partial pressure it would be nearly 2 cc in the circulating system.

(b) The vapor pressure of acetylene is about 10 mm at −130°C, which corresponds to 12 cc of acetylene in the gas phase. However, it is probable that some solubility of acetylene in the butene, etc., in the trap will occur, and thus acetylene may be removed from the system, and its apparent steady-state concentration increased.

(c) The destruction of acetylene may involve reaction with butene or higher hydrocarbons, as pointed out previously. Since these are trapped

out in the circulating system, acetylene can accumulate to a greater extent.

(d) In the circulating system the total pressure was kept constant throughout a run at 20 cm by changing the level of the mercury reservoirs of the circulating pump. Since higher products were trapped out this 20 cm consisted only of hydrogen, ethylene, acetylene, and a trace of butene. Hence the partial pressure of ethylene was maintained much higher than in the later stages of a static run. It follows that acetylene should build up to a greater extent if the relative amount of quenching by ethylene and acetylene is the deciding factor.

However, in spite of the differences discussed above, and of the lower accuracy of circulating and especially of single-pass runs, it appears from Fig. 8 that the initial rate of acetylene production is approximately the same in static, circulating, and single-pass runs. It may be concluded, therefore, that the initial rate observed in static runs is not influenced by secondary reactions involving butene, higher olefins, or hydrogen.

### (3) The Products of the Reaction

#### (*a*) *Acetylene*

The production of acetylene has already been discussed in detail.

#### (*b*) *Hydrogen*

The detection of an amount of hydrogen of the same order of magnitude as that of acetylene is very difficult, and hence it was determined merely as "non-condensable" gas. Thus in a typical $3\frac{1}{2}$-hour circulating run at 290°C and 20-cm pressure the gas non-condensable at −180°C was determined. This, including the vapor pressure of ethylene, was equivalent to 2.0 cc of gas at N.T.P. In a corresponding blank run the non-condensable gas, including the vapor pressure of ethylene, was 0.4 cc. Hence the non-condensable products amounted to 1.6 cc or 0.46 cc per hour. The acetylene formed was 1.0 cc per hour under the same conditions. The hydrogen formed therefore appears to be equivalent to approximately half the acetylene. It would appear from this result, which was typical of a number of determinations, that some of the hydrogen formed with acetylene is used up. However, in view of the very small amount of hydrogen the possibility of its loss by adsorption, solubility, etc., cannot be excluded.

#### (*c*) *Propylene*

In low temperature distillations of the products some indications of the presence of propylene were obtained. Thus in 2 nine-hour single-pass runs at 20-cm pressure distillation analyses indicated 74 and 91 cc of propylene at N.T.P. A nine-hour blank under the same conditions, however, gave 86 cc, and hence the propylene appears to be merely an impurity in the ethylene. This is not a large amount of impurity, since in such a single-pass run over 11 liters of ethylene is used. As might be expected, little propylene was found in circulating runs where the amount of ethylene used was much smaller. Here blank runs and ordinary runs both indicated the presence of about 0.5 percent propylene as an impurity in the ethylene. It may therefore be concluded that propylene is not produced in the reaction in appreciable amounts.

#### (*d*) *Butene and Higher Olefins*

A typical distillation analysis of the accumulated products from 7 circulating runs each of approximately 4 hours duration, with the trap at −125°C and an initial pressure of 200 mm gave

| | | | | | |
|---|---|---|---|---|---|
| Sample 1 | $C_3H_6$ | b.p. −53° to −44°C | 19 cc at N.T.P. | =0.03 g |
| Sample 2 | $C_4H_8$ | b.p. − 8° to + 4°C | 266 cc | =0.61 g |
| Sample 3 | "$C_6H_{12}$" | b.p. 17° to 70°C | | 1.01 g |
| Sample 4 | | b.p. >70°C | | 0.40 g |

These results suggest that the products other than hydrogen and acetylene are about $\frac{1}{3}$ butene and the remainder higher olefins. Analytical data are given later to substantiate this.

A number of circulating runs were made specifically to determine the rate of production of butene. In these a distillation analysis of the products of each run was made in the low temperature still. Only butene could thus be determined: the remaining liquid products were merely weighed. The results are given in Table IV.

The data of Table IV are in general agreement with those reported above, i.e., from 25 to 30 percent of the olefinic products appear to be butenes. From these results we can make an

TABLE IV. Distillation analyses of products of circulating runs. Temperature = 290°C; trap temperature = −125°C; initial pressure-200 mm.

| Time, min. | $C_2H_4$, cc | $C_4H_8$, cc | $C_4H_8$, g | Liquids, g | Remarks |
|---|---|---|---|---|---|
| 250 | 252 | 26.5 | 0.063 | 0.16 | |
| 235 | — | 20 | 0.047 | 0.14 | |
| 220 | 195 | 31 | 0.072 | 0.19 | System cleaned after |
| 245 | 248 | 35 | 0.082 | 0.21 | second run, hence |
| Blank | 294 | 2.5 | — | 0.00 | higher transmission in |
| Blank | 278 | 0.0 | — | 0.00 | following runs. |

approximate check of the relative rates of acetylene production and of pressure decrease. From Table IV for a four-hour run in a clean reaction vessel the rate of butene production is about 9 cc per hour. The liquid products are about 2.7 times this by weight. Assuming that they are hexene, this corresponds to 16 cc. Now the pressure decrease, expressed as cc of gas disappearing is given by

$$-\Delta P = 1 \times C_4H_8 + 2 \times C_6H_{12}$$
$$= 41 \text{ cc per hour.}$$

From Fig. 8 the production of acetylene is approximately 1.0 cc per hour. Hence for the circulating runs

$$-\Delta P / C_2H_2 = 41.$$

Actually, from Fig. 7 the ratio in the static runs is 35 at 90 min. and is rising with time. The agreement between the static and circulating runs is thus excellent.

As a check on the composition of the fraction of the products boiling at about 0°C, which has been reported as butene above, a molecular weight determination was made by combusting a known volume of gas and determining the weights of carbon dioxide and water formed.[20] Two determinations gave 53.58 and 53.79, as compared with the theoretical value for butene of 54.1. For the composition of the gas the combustion analyses gave

C = 84.44, 84.96 percent
H = 14.78, 14.56
C/H = 5.75, 5.87.

(Theoretical C/H for $C_4H_8 = 6$, for $C_4H_6 = 8$, for $C_4H_{10} = 4.8$.)

[20] L. Marion and A. E. Ledingham, Ind. Eng. Chem. Anal. Ed. **13**, 260 (1941).

As a further check on the composition of the 0° fraction, a "butene" cut of −8° to +4° was further separated by distillation into two cuts, (a) 70 percent of the total, boiling in the range −8° to 0°, and (b) 30 percent boiling in the range 0° to +4°. Samples (a) and (b) were then quantitatively brominated.

The results were:

| | Percent of double bonds assuming a molecular weight of 56 |
|---|---|
| Sample (a) | 92.4 |
| (b) | 90.5 |

It thus appears probable that a small amount of butane is present with the butene. Pentene or hexene with the butene would give a similar result, but this seems unlikely in view of the agreement between the two fractions.

### (e) *Higher Liquids*

As pointed out above the higher liquids amounted to about twice the butene. Most of these were in the 17° to 70° cut. The small amount of material made it difficult to fractionate this cut further, but the indications were that it was largely hexene, with some pentene. There was also a small amount of liquid product which boiled in the range 70° to 120°C, and a still smaller amount which boiled above this.

The liquid products from a number of circulating runs were roughly fractionated into cuts boiling in the ranges 30° to 40°C, 60° to 75°C, 100° to 120°C, and over 120°C. These were analyzed by combustion with the following results:

| | |
|---|---|
| 30° to 40° cut | C/H = 5.97, 6.07 |
| 60° to 75° cut | C/H = 5.97, 5.92, 6.14, 5.97 |
| 100° to 120° cut | C/H = 6.03, 6.14 |
| over 120° cut | C/H = 6.10, 6.09. |

Since all olefins give C/H = 6, these results strongly confirm the previous conclusion that the liquid products are olefinic.

As a further check on the olefinic nature of the products, a number of brominations were made followed by fractional distillation of the bromides and micro-analyses of the fractions for bromine. The products used were a composite sample from a number of circulating runs.

(a) The analysis of the bromides from the 0° fraction was

Found Br = 76.15 percent
calc. for $C_4H_8Br_2$ = 74.06
calc. for $C_4H_6Br_4$ = 85.57.

Hence if any diolefins are present they are not in large amount.

(b) The 60° to 75° fraction was brominated in about 25 cc of carbon tetrachloride and the product, after removal of excess bromine and solvent under reduced pressure at 50°C, was fractionated. Fraction I was a colorless oil with b.p. 75°/2 mm. This was the bulk of the product. On redistillation it again gave b.p. 75°/2 mm. Fraction II was of relatively small amount, with b.p. 80° to 120°/2 mm. The bromides from fraction I were analyzed with the results shown in Table V. Fraction I was then redistilled twice and a fraction of about ½ the amount, coming over at about 68° to 70°/2 mm, was again analyzed. This gave C = 28.48, 28.48, H = 4.75, 4.79, Br = 68.07. The results suggest that the bulk of the product is a single $C_6$ compound, i.e., hexene, but that some diolefins or pentene may be present. The latter is probably the more likely alternative.

## DISCUSSION

The main facts established above are:

(a) The products of the reaction are olefins, together with smaller amounts of hydrogen and acetylene.

(b) Since circulating runs with the trap at −80° and −125°C and single-pass runs all give much hexene, it appears that hexene is not merely formed by secondary reactions of butene, but arises in reactions which are an integral part of the mechanism.

(c) The concentration of acetylene rises to a maximum and then remains sensibly constant. The initial rate of acetylene formation is approximately independent of pressure.

(d) The ratio of pressure decrease to acetylene formation is high at high pressures and falls to about 2 at lower pressures, i.e., the rate of pressure decrease rises rapidly with increasing pressure.

(e) There is no measurable pressure rise at the beginning of the reaction as occurs with mercury.

There appear to be 4 possible mechanisms for the primary step:

$$C_2H_4+Cd(^1P_1)=Cd(^1S_0)+2CH_2 \quad (2)$$

$$=Cd(^1S_0)+C_2H_2+H_2 \quad (3)$$

$$=Cd(^1S_0)+C_2H_4^* \quad (4)$$

$$\left.\begin{array}{l}=Cd(^1S_0)+C_2H_3+H\\ \text{or}=CdH+C_2H_3\end{array}\right\}. \quad (5)$$

Reaction (2) appears to be unlikely on energetic grounds. In any case the predominance of $C_4$ and $C_6$ olefins in the products and the absence of propylene and methane seem to rule it out.

Reaction (3) can certainly be ruled out as the primary step since acetylene is not the major product of the reaction, and evidence has been cited above to show that acetylene is surprisingly inert in the presence of ethylene.

Reaction (4) is favored by analogy with the mercury photosensitized reaction, and reaction (5) is favored by analogy with other cadmium photosensitized reactions.

As we have seen, in the case of the mercury photosensitized reaction the main steps are

$$C_2H_4^*=C_2H_2+H_2, \quad (6)$$

$$C_2H_4+C_2H_4^*=2C_2H_4 \quad (7)$$

and the subsequent polymerization arises by a free radical mechanism based on H atoms formed by

$$H_2+Hg(^3P_1)=Hg(^1S_0)+2H. \quad (8)$$

In view of the large amount of polymerization compared with acetylene formation in the present investigation, it does not seem possible to explain all the polymerization on this basis. However, it is possible that the higher excitation energy in the case of cadmium causes (7) to be largely replaced by

$$C_2H_4+C_2H_4^*=C_4H_8. \quad (7a)$$

TABLE V.

| Found | Calculated for $C_6H_{12}Br_2$ | $C_6H_{10}Br_4$ | $C_8H_{10}Br_2$ |
|---|---|---|---|
| C 28.48, 28.75 | 29.52 | 22.55 | 26.10 |
| H 4.77, 4.91 | 4.92 | 2.35 | 4.35 |
| Br 67.71, 67.64 | 65.55 | 75.11 | 69.55 |

It seems more likely, however, that by virtue of the higher excitation energy reaction (5) is also an important primary step. If so the subsequent polymerization can proceed simply by a free radical mechanism involving H and $C_2H_3$, e.g.,

$$H+C_2H_4=C_2H_5$$
$$C_2H_4+C_2H_5=C_4H_9$$
$$C_2H_4+C_4H_9=C_6H_{13}, \text{ etc.}$$

As a matter of fact a mechanism could be devised based on reaction (5) as the only primary step, provided that we assume acetylene to be formed by disproportionation,

$$C_2H_3+C_2H_4=C_2H_2+C_2H_5.$$

However, all this is entirely speculative. The main features of the work are that there is practically no polymerization of ethylene by $Cd(5^3P_1)$, while polymerization proceeds efficiently with the higher energy associated with $Hg(6^3P_1)$ and $Cd(5^1P_1)$.

We are indebted to Dr. L. Marion and Mr. A. E. Ledingham of this laboratory for making the micro-analyses.

---

JANUARY, 1942 JOURNAL OF CHEMICAL PHYSICS VOLUME 10

# The Mechanism of Processes Initiated by Excited Atoms

## I. The Quenching of Excited Sodium*

KEITH J. LAIDLER
*National Research Laboratories, Ottawa, Canada*
(Received October 30, 1941)

The potential-energy surfaces relevant to a number of simple processes involving excited ($^2P$) sodium have been constructed, and the mechanism of the reactions discussed in terms of them and of the theory of absolute reaction rates. It is shown that quenching by atoms is normally a very inefficient process, the effect of additional atoms in a quencher being to stabilize a quenched complex, commonly a polar compound, which finally decomposes to give the deactivated atom and a vibrationally excited product. The activated state may be either at the top of a rotational-energy barrier or at a crossing point to a polar surface, and the theory is shown to be consistent with the experimental values of the quenching cross sections. In the cases examined the quenching is of a physical nature, the energy passing chiefly into vibrational energy, with a certain amount going into translational and rotational degrees of freedom. Saturated hydrocarbons appear to quench like hydrogen except that there is probably a small energy of activation, but the unsaturated ones quench by means of an interaction between the sodium atom and the unsaturated group, and the efficiency is considerably higher.

### INTRODUCTION

AFTER an atom in the gas phase has absorbed energy and become excited electronically, three distinct processes may ensue:

(1) The electronic energy may be re-emitted in the form of radiation (fluorescence);

(2) The atom may collide with an atom or molecule and become deactivated, the excitation energy passing into translational, rotational or vibrational degrees of freedom, but not inducing reaction (quenching); or

(3) The atom may collide with another atom or molecule and initiate chemical reaction in the latter (photosensitization). All of these processes may, and frequently do, occur simultaneously in a given reaction system, and the individual rate constants may be separated by investigating the effects of changing the concentrations of the reacting species on the intensity of the emitted fluorescent radiation or on the rate of formation of the reaction products. Thus if A denotes the atom which is excited electronically to A* by the absorption of radiation, and M is a foreign gas molecule, possible reactions, with their corre-

* Contribution No. 1031 from the National Research Laboratories, Ottawa, Canada.

sponding rate coefficients, are

$$A+h\nu=A^* \quad (k_1), \tag{1}$$

$$A^*+A=A'+A' \quad (k_2), \tag{2}$$

$$A^*+M=A'+M' \quad (k_3), \tag{3}$$

$$A^*=A+h\nu \quad (k_4). \tag{4}$$

A′ denotes an A atom which has an abnormal amount of translational energy, while M′ may be excited translationally, vibrationally or rotationally, and may subsequently undergo reaction. The assumption of a steady state for the excited atom leads at once to the equation[1]

$$\frac{I}{I_0}=\frac{k_4}{k_4+k_2c_A+k_3c_M} \tag{5}$$

$$=\frac{1}{1+k_2\tau c_A+k_3\tau c_M}, \tag{6}$$

where $\tau(=1/k_4)$ is the mean life of A*; $I_0$ is the intensity of radiation emitted in the absence of foreign gas and extrapolated to zero concentration of A, and $I$ is that in the presence of A and M at concentrations $c_A$ and $c_M$. Since $\tau$ can usually be determined readily, $k_2$ and $k_3$ can be found from the effect on the ratio $I/I_0$ of varying the concentrations of A and M.

The rates of such processes as (2) and (3) have previously been discussed almost entirely in terms of classical collision theory according to which the number of collisions per second per cubic centimeter, for unit concentration (in molecules per cc) of the two colliding molecules, is given by

$$Z=\sigma^2\left[8\pi kT\left(\frac{m_A+m_B}{m_Am_B}\right)\right]^{\frac{1}{2}}, \tag{7}$$

where $\sigma$ is the distance between centers on collision, and $m_A$ and $m_B$ are the actual masses of the colliding species. This is related to the velocity coefficient $k$ by the equation

$$k=Ze^{-E/RT} \text{ cc molecule}^{-1} \text{ sec.}^{-1}, \tag{8}$$

and if the activation energy $E$ can be assumed to be zero, as is probably the case in most of these reactions, $k$ and $\sigma$ are related by

$$k=\sigma^2\left[8\pi kT\left(\frac{m_A+m_B}{m_Am_B}\right)\right]^{\frac{1}{2}}. \tag{9}$$

The experimental results for quenching and primary photosensitization processes are frequently expressed in terms of $\sigma^2$, known as the "quenching cross section," and derived from $k$ by means of this equation. It will later be shown that this equation is also obtained when the theory of absolute reaction rates is applied to the processes, and that values of the quenching cross section in satisfactory agreement with experiment can be derived when the potential-energy surfaces have been constructed.

Most of the experimental work on quenching and photosensitization has been done with excited sodium, mercury and cadmium. The simplest reactions to interpret theoretically are those of sodium, since the potential-energy surfaces are fewest in this case, and because the quenching of a $^2P$ sodium atom must involve the formation of sodium in its lowest, $^2S$, state since this is the only lower state; with mercury and cadmium, on the other hand, quenching often occurs by the transfer of the atoms from their $^3P_1$ levels to the metastable $^3P_0$ levels (see Part II, following paper). A further simplification in the case of sodium arises from the fact that the amount of energy, 48.3 kcal. per mole, liberated when an excited ($^2P$) sodium atom becomes deactivated to the normal ($^2S$) state is not sufficient to dissociate the average quenching molecule.

The quenching of excited ($^2P$) sodium by a number of gas molecules has recently been studied by Norrish and Smith.[2] Some of the data are given in Table I, which also includes, for comparison, the data for mercury and cadmium. The values given for sodium are those of Norrish and Smith, and of Terenin and Prileshajewa (the halogens).

Of the previous theoretical treatments of reactions of this type, most have been of a general

[1] O. Stern and M. Volmer, Physik. Zeits. **20**, 183 (1919).

[2] R. G. W. Norrish and W. MacF. Smith, Proc. Roy. Soc. **A176**, 295 (1940); see also R. Mannkopff, Zeits. f. Physik **36**, 315 (1926); J. G. Winans, *ibid.* **60**, 631 (1930); A. Terenin and N. Prileshajewa, Zeits. f. physik. Chemie **B13**, 72 (1931), Physik. Zeits. Sowjetunion **2**, 337 (1932); and B. Kisilibasch, V. N. Kondratjew, and A. Leipunsky, *ibid.* **2**, 201 (1932).

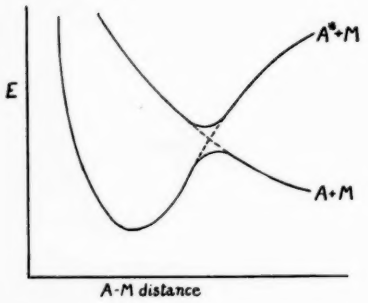


FIG. 1. Potential-energy curves for the quenching of an excited atom A* by an atom M (Case I; cf. Eq. (10)).

nature. Teller[3] has discussed the general principles involved in the dissipation of electronic into other types of energy, while Kallmann and London,[4] and Morse and Stuechelberg,[5] have made calculations based upon assumed potential-energy surfaces. Recently, a number of papers have treated special aspects of the application of the theory of absolute reaction rates to reactions involving excited electronic states,[6] and in particular Magee and Ri[7] have discussed the quenching of sodium by hydrogen. In the remainder of the present paper the general forms of the potential-energy surfaces upon which the simpler reactions involving excited sodium atoms take place will be deduced, and the mechanisms and rates of the reactions discussed in the light of them.

## QUENCHING BY ATOMS

The set of potential-energy curves for the two-atom system formed from the interaction of the excited and the quenching atom belongs to one of at least three classes. In the first place the interactions between the atoms may be of such a nature that the lowest curve for the interaction of A* with M is intersected by one of the curves for A−M; this case is illustrated in Fig. 1 in which the rounding-off of the curves due to resonance between them is shown. If the probability of crossing from the upper to the lower surface is equal to $\rho$, the probability that atoms A* and M approaching one another along the upper curve will separate along the lower can readily be shown to be[8]

$$\kappa = 2\rho(1-\rho). \tag{10}$$

Since $1>\rho>0$, $\kappa$ has a maximum value of $\frac{1}{2}$ when $\rho=\frac{1}{2}$, while, when $\rho\sim1$ or $\rho\sim0$, $\kappa$ is very small. If there is no difference of multiplicity between the two states the interaction energy will usually be large owing to a considerable overlapping of orbitals; $\rho$ will therefore be $\sim0$ and the rate of quenching low. The reaction is also slow for the same reason in the rather common case of a change of multiplicity, when $\rho\sim1$. Only in especially favorable cases, therefore, will the quenching efficiency be appreciable.

In the second case the upper and lower curves do not intersect, but both are intersected by a third curve, so that quenching can occur by means of two transitions; this case is illustrated in Fig. 2. The curve *HBFK* is usually a polar curve, for the ionic molecule $A^+M^-$. In order to derive an explicit expression for the transmission coefficient of such a reaction, an expression is first obtained for the fraction of systems which, beginning at *A*, find themselves traveling towards *F* on the polar curve *BF*, and then for that fraction of the latter which finally arrive at *E*. The first fraction is found to be $2(1-\rho)/(2-\rho)$, where $\rho$ is the probability of crossing at *B*; the second fraction is

$$\frac{2\sigma(1-\sigma)}{1-\rho^2\{\sigma^2+(1-\sigma)^2\}},$$

where $\sigma$ is the probability of crossing at *F*. The

TABLE I. Quenching cross sections ($A^2$).

| Quenching gas | Na($^2P$) | Hg($^3P_1$) | Cd($^3P_1$) |
|---|---|---|---|
| Inert gases | ~0 | ~0 | ~0 |
| $H_2$ | 7.4 | 6.01 | 0.67 |
| $N_2$ | 14.5 | 0.192 | 0.021 |
| CO | 28.0 | 4.07 | 0.14 |
| $I_2$ | 40.0 | — | — |
| $Br_2$ | 100.0 | — | — |
| I | 40.0 | — | — |
| $CH_4$ | 0.11 | 0.059 | 0.012 |
| $C_2H_6$ | 0.17 | 0.421 | — |
| $C_2H_4$ | 44.0 | 48.0 | — |
| $C_3H_6$ | 52.0 | — | — |

[3] E. Teller, J. Phys. Chem. **41**, 109 (1937); Ann. N. Y. Acad. Sci. **41**, 173 (1941); see also J. v. Neumann and E. P. Wigner, Physik. Zeits. **30**, 467 (1929).
[4] H. Kallmann and F. London, Zeits. f. physik. Chemie **B2**, 207 (1929).
[5] P. M. Morse and E. C. G. Stuechelberg, Ann. d. Physik **9**, 579 (1931).
[6] For a summary, with references, see S. Glasstone, K. J. Laidler, and H. Eyring *The Theory of Rate Processes* (McGraw-Hill Book Co., 1941), Chapter VI.
[7] J. L. Magee and T. Ri, J. Chem. Phys. **9**, 638 (1941).
[8] W. A. Noyes and F. C. Henriques, J. Chem. Phys. **7**, 767 (1939).

net transmission coefficient is therefore

$$\kappa=\frac{2(1-\rho)}{2-\rho}\cdot\frac{2\sigma(1-\sigma)}{1-\rho^2\{\sigma^2+(1-\sigma)^2\}}. \qquad (11)$$

Other things being equal this function is greatest when $\rho=0$; its maximum value is $\frac{1}{2}$ when $\rho=0$ and $\sigma=\frac{1}{2}$, while it is zero when $\sigma=0$ or $\sigma=1$. When there is no change of multiplicity the resonance energies are usually large so that $\rho\sim0$ and $\sigma\sim0$; $\kappa$ is therefore small in this case. Otherwise, if there is a change of multiplicity, $\sigma\sim1$ so that $\kappa\sim0$.

The third possible case is when the polar curve does not lie sufficiently low to cut both curves; quenching is extremely inefficient in this case. In general, therefore, atoms are poor quenchers, owing to the high probability of the dissociation of the complex formed by the two atoms to give the original excited atom; the efficiency with which electronic energy passes into translational is thus low. That atoms are poor quenchers seems to be confirmed by experiment; thus the inert gases quench very weakly.[9] The case of the quenching of excited sodium and thallium by iodine atoms appears, however, to be in contradiction to this conclusion, since Terenin and Prileshajewa[10] give values of 40 and 30A², respectively, for $\sigma^2$. It is conceivable that this arises from the case of $\sigma\sim\frac{1}{2}$ and $\rho=0$, but in view of the indirect method by which the results were obtained it would seem to be more likely that the results are in error, the quenching actually being effected by iodine molecules.

## QUENCHING BY HYDROGEN

### Quenching by Hydrogen Atoms

Before considering the quenching of excited sodium by hydrogen molecules, it is necessary to construct the potential-energy curves for the system Na−H; these are shown in Fig. 3.[11] A $^2P$ sodium atom interacts with a $^2S$ hydrogen atom to give $^1\Sigma^+$, $^3\Sigma^+$, $^1\Pi$ and $^3\Pi$ states, of which the first is the lowest and attractive. The curve for this state can be plotted making use of the spectroscopic data;[12] the value of $D_0$, the dissociation energy plus the zero-point energy, is 34.15 kcal. The form of the curve is remarkable in that in spite of being very shallow at its minimum it rises sharply in the region of 4–6A;[13] this arises from resonance with the ionic state, its effect being to give negative values for the band-spectrum constants $\alpha_e$ and $x_e\omega_e$.

A normal ($^2S$) sodium atom interacts with a hydrogen atom to give an attractive $^1\Sigma^+$ state and

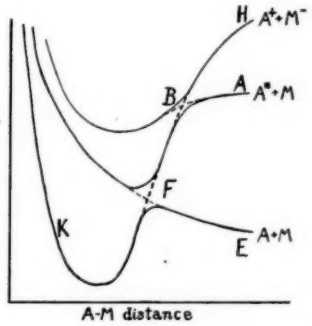


FIG. 2. Potential-energy curves for quenching by an atom M, the process involving the intermediate formation of a polar complex (case II; cf. Eq. (11)).

a repulsive $^3\Sigma^+$ state, of which the former can be constructed from the spectroscopic data. The only other curve for the system which falls sufficiently low to be of any interest is that for the ionic $Na^+-H^-$ state. For an infinite $Na^+-H^-$ separation this is higher than the curve for $Na(^2S)-H(^2S)$ by an amount $I(Na)-E(H)$ where $I(Na)$ is the ionization potential of sodium and $E(H)$ is the electron affinity of the hydrogen atom; this quantity has the value 101.5 kcal. The form of the curve for the ionic state is given approximately by the expression

$$V=-\epsilon^2/r+br^{-n}, \qquad (12)$$

where $V$ is the energy relative to the separated ions, $\epsilon$ is the electronic charge, $r$ the distance between the $Na^+$ and $H^-$ ions, and $b$ and $n$ are constants; the first term represents the Coulombic attraction of the ions, while the second is the repulsive contribution due to exchange forces. The values of $b$ and $n$ can be evaluated from the crystal data collected by Sherman;[14] at values of $r$ greater than 4A the influence of the second term becomes negligible, and the energy in kcal. per

[9] R. Mannkopff, Zeits. f. Physik **36**, 315 (1926); L. V. Hámos, *ibid.* **74**, 379 (1932).
[10] A. Terenin and N. Prileshajewa, Zeits. f. physik. Chemie **B13**, 72 (1931); Physik. Zeits. Sowjetunion **2**, 337 (1932).
[11] Cf. R. S. Mulliken, Rev. Mod. Phys. **4**, 7 (1932).
[12] Values from H. Sponer, *Molekülspektren* (J. Springer, Berlin, 1935), Vol. I.
[13] Cf. R. S. Mulliken, Phys. Rev. **50**, 1028 (1936), who treats LiH similarly.
[14] J. Sherman, Chem. Rev. **11**, 93 (1932).

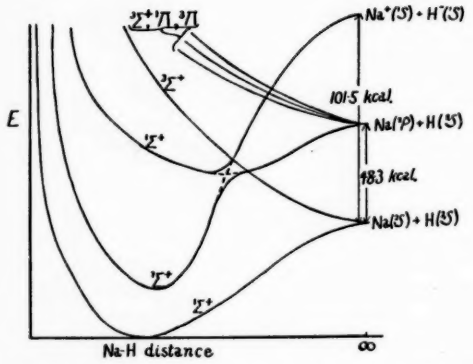


FIG. 3. Potential-energy curves for the system Na−H.

mole may be written as $V=-330/r$, where $r$ is expressed in angstroms.

Examination of the curves in Fig. 3 shows that for quenching to take place the system must proceed along the $Na(^2P)+H(^2S)$ curve and either make a direct transition to the repulsive $^3\Sigma^+$ curve, with the ultimate formation of $Na(^2S)+H(^2S)$ which will move away from one another with an extra relative kinetic energy equal to the excitation energy of sodium, or make two transitions, first to the polar curve and then to the repulsive curve. The first possibility is case I of the previous section (Fig. 1 and Eq. (10)); as there is a change of multiplicity $\rho\sim1$, so that $\kappa\sim0$ and the rate is low. The second possibility is case II (Fig. 2 and Eq. (11)) with $\rho\sim0$ and $\sigma\sim1$, so that again $\kappa\sim0$. The normal course of events is therefore that the colliding atoms readily form a polar compound $Na^+H^-$, but that this, being unable to get rid of its excess of vibrational energy, redissociates at once.

### Quenching by Hydrogen Molecules

The potential-energy surfaces for the three-body system Na−H−H may be represented in a three-dimensional diagram in which the coordinates are potential energy, Na−H distance and H−H distance. The two profiles of the surfaces which correspond to infinite separation of Na and H and of H and H are shown on two sides of the cube in Fig. 4. The process of interest, the quenching of $Na(^2P)$ to $Na(^2S)$ is represented by a transition from $B$ to $A$ in this figure. The manner in which the curves are connected by surfaces may now be discussed.

When a hydrogen molecule in a $^1\Sigma^+_g$ state interacts with a $^2S$ sodium atom to give a linear complex, the resulting state is a $^2\Sigma^+$ state, which is therefore the lowest for the system, the surface describing it connecting the two lowest curves. This surface corresponds to that upon which the reaction $H+H_2$ takes place and is of the same general form; its energy may be expressed by the London equation[15] taking the negative sign:

$$E=Q-\left[\tfrac{1}{2}\{(\alpha-\beta)^2+(\beta-\gamma)^2+(\gamma-\alpha)^2\}\right]^{\frac{1}{2}}, \quad (13)$$

where $Q$ is the sum of the three Coulombic energies and $\alpha$, $\beta$ and $\gamma$ are the exchange energies. The form of the surface has been calculated using the semi-empirical method, the potential-energy curves being estimated from the data given by Sponer.[12] The proportion of Coulombic energy was taken as 12 percent for the H−H bond and 22 percent for the Na−H bond; this latter figure is the average of 12 percent for H−H and 32 percent for Na−Na, these being the most satisfactory figures for bonds involving electrons having principal quantum numbers of 1 and 3, respectively.[16] The interactions of the higher states are neglected.

The interaction of a $^2S$ sodium atom with a $^3\Sigma^+_u$ hydrogen molecule gives rise to two states, $^4\Sigma^+$ and $^2\Sigma^+$; similarly $H(^2S)+NaH(^3\Sigma^+)$ gives $^4\Sigma^+$ and $^2\Sigma^+$. The two repulsive curves in Fig. 4 for $H_2$ and NaH are therefore connected by two

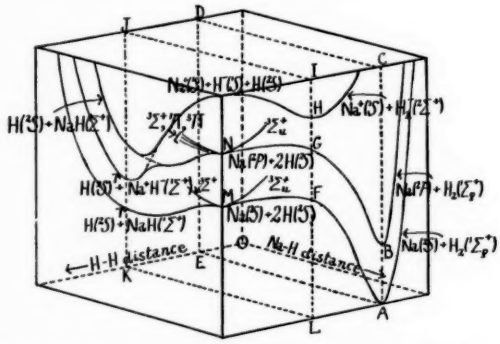


FIG. 4. Potential-energy surfaces for the system Na−H−H (linear configuration). The curves on the left- and right-hand faces are for Na−H and H−H, respectively, and the manner in which they are connected by surfaces within the cube is described in the text. $AB=MN=48.3$ kcal.

[15] F. London, *Probleme der modernen Physik* (*Sommerfeld Festschrift*) (1928), p. 104; Zeits. f. Elektrochemie **35**, 552 (1929).

[16] J. H. Bartlett and W. H. Furry, Phys. Rev. **38**, 1615 (1931); N. Rosen and S. Ikehara, *ibid.* **43**, 5 (1933).

surfaces. The same conclusions have been arrived at by the method of bond eigenfunctions;[17] neglecting double-exchange integrals, and making other approximations, the energy of the $^2\Sigma^+$ state is found to be

$$E=Q+[\tfrac{1}{2}\{(\alpha-\beta)^2+(\beta-\gamma)^2+(\gamma-\alpha)^2\}]^{\frac{1}{2}}, \quad (14)$$

while that of the $^4\Sigma^+$ state is

$$E=Q-\alpha-\beta-\gamma. \quad (15)$$

As the exchange integrals are of negative sign these surfaces represent highly repulsive states; this being so, and since the energy of $Na(^2S)+2H$ ($M$ in Fig. 4) is considerably higher than that of $Na(^2P)+H_2(^1\Sigma^+_g)$ ($B$ in Fig. 4) it is clear that a quenching process utilizing one of these states would have a very high activation energy. As such energies are not involved the surfaces are not used, but it will be seen later that the repulsive surfaces are of significance in the reactions of excited mercury and cadmium.

Of the surfaces involving excited sodium, only the lowest, connecting the curves for $Na(^2P)+H_2(^1\Sigma^+_g)$ and $NaH(^1\Sigma^+)+H(^2S)$, and of designation $^2\Sigma^+$, is of any interest. As Magee has shown,[18] the triangular configuration of atoms is probably the most stable in this case, but the error in assuming linearity is not large. A plot of the surface for the linear configuration has been made in the same manner as for the lowest

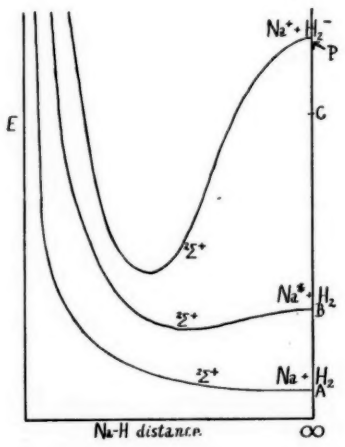


FIG. 5. Potential-energy profiles in the plane *ABCDE* of Fig. 4, corresponding to the normal H—H separation. $AB$=48.3 kcal., $BP$=c. 200 kcal.

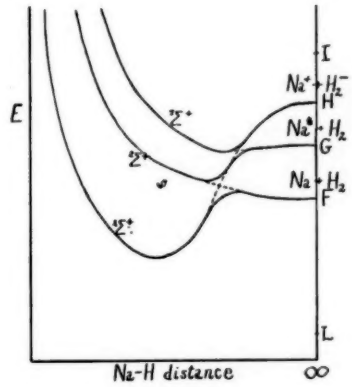


FIG. 6. Potential-energy profiles in the plane *FGHIJKL* of Fig. 4, corresponding to an extension of the H—H bond.

surface, of sufficient accuracy to establish two facts. The first is that the lowest point in the valley representing the approach of $Na(^2P)$ to $H_2$ runs parallel to the Na—H axis up to small (c. 1A) values of the Na—H distance; on this surface the excited sodium atom therefore approaches close to the hydrogen molecule without appreciable extension of the bond in the latter. The second point is that the surface is at all points well above the lowest surface, a conclusion that can also be accepted for the triangular configuration. The possibility was originally envisaged that the interaction between excited sodium and hydrogen might be so different from that between normal sodium and hydrogen that the two surfaces might cut, with the result that quenching would involve a simple transition from the upper to the lower surface.[19] Such a possibility is, however, excluded.

The only remaining possibility is that the surface representing the ionic state $Na^+-H^--H$ cuts both upper and lower surfaces, so that the reaction proceeds *via* a transition first from the upper to the polar surface, and then from the polar to the lower surface. The curves representing $Na^+H^-(^1\Sigma^+)$ and $H^--H(^2\Sigma^+)$ are shown in Fig. 4. The construction of the former has already been discussed. The molecule $H_2^-$ has been treated theoretically by Eyring, Hirschfelder, and Taylor[20] who find a dissociation energy of 37.4 kcal. and an equilibrium separation of 1.8A. At the separation of 0.74A, equal to

[17] J. C. Slater, Phys. Rev. **38**, 1109 (1931).
[18] J. L. Magee, J. Chem. Phys. **8**, 677 (1940); J. L. Magee and T. Ri, *ibid.* **9**, 638 (1941).
[19] Cf. M. G. Evans, Trans. Faraday Soc. **35**, 59 (1939).
[20] H. Eyring, J. O. Hirschfelder, and H. S. Taylor, J. Chem. Phys. **4**, 484 (1936).

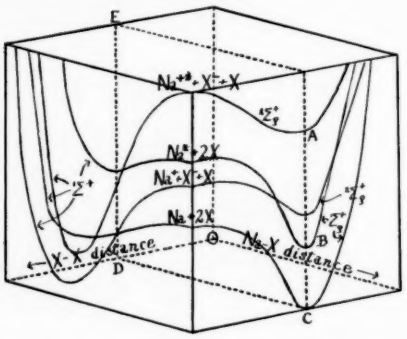


FIG. 7. Potential energy surfaces for the linear system Na−X−X, where X is a halogen atom.

the separation in $H_2$, the energy is considerably (by more than 50 kcal.) higher than corresponds to dissociation into $H+H^-$. The sodium ion $Na^+(^1S)$ interacts with the $H_2^-$ ion ($^2\Sigma^+$) to give a single $^2\Sigma^+$ state in which it is assumed for the purpose of calculation that the charge is located at the center of the hydrogen molecule. The surface is best constructed by assuming that the interaction between $Na^+$ and $H_2^-$ obeys the same law of force as that between $Na^+$ and $H^-$, which is justifiable as the exchange forces in the region of interest are negligible in comparison with the coulombic ones. Owing to the high repulsion in $H_2^-$ at the separation of 0.74A the polar surface does not cut the upper surface in the profile that corresponds to the normal H−H distance; this profile is shown schematically in Fig. 5, in which the curve for the upper surface is drawn with a slight minimum which Magee and Ri have shown to exist for the triangular configuration. For crossing to take place there must be an extension of the H−H bond until the polar surface cuts the upper one. This extension is clearly not as great as to 1.8A, the normal distance in $H_2^-$; if it were, the effect would be to bring the polar surface down as low as possible, but the activation energy would be high (Fig. 6). The value of $r_c$ at the crossing point in this profile is about 8A. The crossing point through which reaction actually proceeds will clearly correspond to a smaller extension of the bond, so that the value of $r_c$ will be only slightly greater than 2.4A, the value of $r$ at the minimum of the polar surface.

Before considering the nature of the activated complex of the reaction it is necessary to consider the rate equation. If the transmission coefficient is unity and the activation energy zero, the theory of absolute reaction rates[21] gives for the rate expression for a non-linear complex,[22]

$$k=\frac{kT}{h}\cdot\frac{\dfrac{(2\pi m_\ddagger kT)^{\frac{3}{2}}}{h^3}\cdot\dfrac{8\pi^2(8\pi^3ABC)^{\frac{1}{2}}(kT)^{\frac{3}{2}}}{2h^3}\prod^{2}(1-e^{-h\nu_\ddagger/kT})^{-1}}{\dfrac{(2\pi m_{Na}kT)^{\frac{3}{2}}}{h^3}\cdot\dfrac{(2\pi m_{H_2}kT)^{\frac{3}{2}}}{h^3}\cdot\dfrac{8\pi^2IkT}{2h^2}\cdot(1-e^{-h\nu_i/kT})^{-1}}. \qquad (16)$$

From the fact that the activation energy is zero, it follows that the hydrogen molecule retains its two rotational and one vibrational degrees of freedom in the activated state, and that one of the vibrational degrees of freedom in the initial state becomes replaced by a vibrational degree for the complex as a whole. With these assumptions the rate equation becomes

$$k=r_\ddagger^2\left[8\pi kT\left(\frac{m_A+m_B}{m_Am_B}\right)\right]^{\frac{1}{2}}, \qquad (17)$$

the same reduction being here obtained as in the case of a reaction between atoms; $r_\ddagger$ is the separation in the activated state. This equation is equivalent to Eq. (9), so that the calculated value of $r_\ddagger$ may be compared directly with the experimental value of $\sigma$.

Magee and Ri take the activated complex to be at the top of the rotational-energy barrier, the value for $r_\ddagger$ being 7.64A. However, in view of the fact that a stretching of the H−H bond has to take place before there can be a transition to the polar state, it also appears possible that the configuration of highest free energy may be at the crossing point, particularly as the entropy is lower here. If this is so, $r_\ddagger$ for the activated com-

[21] For reviews, see H. Eyring, Chem. Rev. **17**, 65 (1935); Trans. Faraday Soc. **34**, 41 (1938); S. Glasstone, K. J. Laidler, and H. Eyring, reference 6, p. 184 ff.

[22] Cf. S. Glasstone, K. J. Laidler, and H. Eyring, reference 6, p. 309.

plex should be only slightly greater than 2.4A. The experimental value of 2.7A for $\sigma$ suggests that this interpretation is to be preferred.

The probability of transition to the polar surface will be of the order of unity, since the interatomic separation is small and the overlapping of orbitals therefore considerable. In order that reaction shall proceed to completion further extension may be necessary in order that the polar surface shall cut the lower surface, and from the form of the polar surface it is seen that this can take place without expenditure of energy. The value of the transmission coefficient depends upon the ease with which the system passes from the polar surface to the lower surface as compared with the probability that it returns to the upper surface. In the case of such a reaction as the one under consideration the mass point representing the system will perform a circular movement within the basin representing the polar surface, so that the probability of a return to the upper state is small; the transmission coefficient of the over-all reaction may therefore be taken as unity. Physically this means that owing to the presence of the additional hydrogen atom the excitation energy passes readily into vibrational energy, so that the atom has the effect of stabilizing the polar "quenched complex" with respect to decomposition to give the initial reactants once again.

## QUENCHING BY HALOGEN MOLECULES

The potential-energy surfaces for the quenching of sodium radiation by halogen molecules are shown schematically in Fig. 7. The curves on the left-hand face of the cube, for the molecules NaX, are all for $^1\Sigma^+$ states; these will not interact appreciably with the repulsive $^3\Sigma^+$ states which have therefore been omitted for simplicity. The curves for $X_2$, on the right-hand face, may readily be constructed from the spectroscopic data, although this is not necessary here. The curve for

TABLE II. Calculated quenching radii (A). $I(\mathrm{Na})=118.2$.

| Halogen | $E(\mathrm{X})$ | $D(\mathrm{X}_2)$ | $r_c$ |
|---|---|---|---|
| Fluorine | 95.3 | 64.6 | 5.97 |
| Chlorine | 86.5 | 57.2 | 5.47 |
| Bromine | 81.5 | 45.4 | 5.55 |
| Iodine | 74.3 | 35.5 | 5.34 |

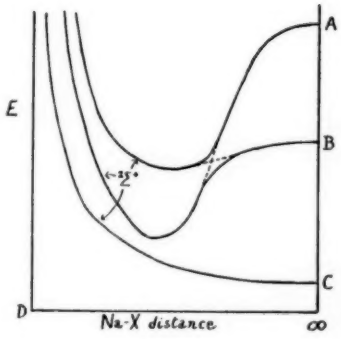


FIG. 8. Potential-energy profiles in the plane $ABCDE$ of Fig. 7, corresponding to the normal X−X separation.

$X_2^-$ has been constructed on the assumption[23] that the binding energy is one-half of that in $X_2$, and the equilibrium separation the same. The designations of the states are indicated in the figure.

The quenching process involves a transition from the point $B$ to the point $C$, and the only surface which intersects both of the valleys beginning at $B$ and $C$ is that corresponding to the polar state $Na^{++}-X^{-}-X$; reaction will therefore proceed initially in the plane including the points $A$, $B$ and $C$ and running parallel to the Na−X axis. The energy profiles in this plane are shown in Fig. 8. The distance between the points $A$ and $B$ is readily seen to be $I(\mathrm{Na})-E(\mathrm{X})+\frac{1}{2}D(\mathrm{X}_2)-48.3$ kcal., where $I(\mathrm{Na})$ is the ionization potential of sodium, $E(\mathrm{X})$ the electron affinity of the atom X, and $D$ is the energy of dissociation of the halogen molecule. Neglecting exchange forces, as is here permissible owing to the high value of $r_c$, the value of $r_c$ is given by

$$r_c=\frac{330}{I(\mathrm{Na})-E(\mathrm{X})+\frac{1}{2}D(\mathrm{X}_2)-48.3}\text{A}. \quad (18)$$

The values of $E$ and $D$ (in kcal.) and of $r_c$ (in A) for the four halogens are given in Table II.

Since the activation energy is zero and the transmission coefficient probably unity, the rate equation again reduces to Eq. (17); the values of $r_\ddagger$ may therefore be compared directly with those of $\sigma$. There is here no rotational-energy barrier, since the surface is polar in the region in which it would appear (c. 5A) and the rapidly varying angular momentum $(1/r^2)$ cannot introduce a maximum into the polar state $(1/r)$.[23] The acti-

[23] Cf. J. L. Magee, J. Chem. Phys. 8, 687 (1940).

vated state should therefore be at the crossing point, i.e., $r_{\ddagger}=r_c$.

The only data available for quenching by the halogens are those of Terenin and Prileshajewa,[2] whose values of $\sigma$ (cf. Table I) are 10 for $Br_2$ and 6.3 for $I_2$; the values are only rough but are appreciably higher than the calculated. However, in view of the approximations involved the agreement is not unsatisfactory. In particular the calculations explain the observed decrease in rate on passing from bromine to iodine; simple collision theory would give an increase owing to the increased diameter.

It is clear from Fig. 8 that, as in the case of quenching by hydrogen, the reaction is not completed in the profile *ABCDE*, but that extension of the X−X bond has to take place until the polar and lower surfaces cross; this can be effected without expenditure of energy.

## QUENCHING BY HYDROCARBONS

From the point of view of the efficiency with which they quench excited sodium atoms, the hydrocarbons appear to fall into two distinct classes, corresponding to whether or not an unsaturated group is present.[2] The saturated hydrocarbons are only weakly effective, their quenching cross sections being only a fraction of a square angstrom, while the unsaturated hydrocarbons have quenching cross sections of 40–50A² (see Table I). The explanation of these differences can only be inferred from a consideration of the evidence with regard to the quenching of excited mercury and cadmium atoms, which is discussed in the last section of Part II (following paper). From the fact that triplet mercury and cadmium atoms remove hydrogen atoms from saturated hydrocarbons, one may conclude that a saturated hydrocarbon molecule interacts with an excited sodium atom in the same manner as does a hydrogen atom, the sodium atom approaching one of the hydrogen atoms of the hydrocarbon (H−R) to give a complex $Na(^2P)-H-R$, with a slight extension of the carbon-hydrogen bond. The surface corresponding to this complex is cut by a polar surface for $Na^+-H^--R$, and reaction is completed by a transition, probably with a considerable extension of the carbon-hydrogen bond, from the polar to the lowest surface. The explanation of the low quenching efficiency is probably that a slight activation energy is involved, since there would seem to be little possibility of a restriction at either of the crossing points.

The simple saturated hydrocarbons do not absorb except at very low wave-lengths; they therefore have no singlet levels of excitation energy less than the excitation energy of sodium. It is thus clear that electronic excitation of the hydrocarbons does not take place; probably most of the energy passes into vibrational energy, with a small amount going into translational and rotational degrees of freedom.

As it does not appear that triplet mercury or cadmium atoms in general remove hydrogen atoms from unsaturated hydrocarbons it is inferred that the interaction, with these atoms and with sodium, is not between the metal atom and a hydrogen atom, but rather between the metal atom and the double bond. The interactions can hardly be worked out in detail at the present stage, but it would again seem likely that the first surface is cut by a polar surface, which is probably low-lying since the double-bond system readily takes up an additional electron; the crossing point of the two surfaces therefore corresponds to a high value of $r_c$, so that the quenching efficiency is high.

From the fact that ethylene does not absorb at wave-lengths greater than about 2100A[24] it can be concluded that there is no electronic energy state of ethylene which will combine with the ground state (i.e., no singlet state) having an energy less than about 135 kcal. Since only a singlet state could be produced by collision with an excited sodium atom, electronic excitation cannot take place, all of the energy going into vibrational, rotational and translational degrees of freedom, the majority probably going into vibrational.

[24] R. B. Mooney and E. B. Ludlam, Trans. Faraday Soc. **25**, 442 (1929).

# The Mechanism of Processes Initiated by Excited Atoms

## II. Photosensitization by Excited Mercury and Cadmium*

KEITH J. LAIDLER
*National Research Laboratories, Ottawa, Canada*

(Received October 30, 1941)

The treatment of the preceding paper is extended to the reactions of excited mercury and cadmium in their triplet and singlet states. It is shown that with the hydrogen molecule quenching of a physical nature is prohibited for the triplet atoms by the necessity for conservation of spin angular momentum, and that dissociation must take place with the initial formation of the metal hydrides. In the reactions of Hg $^3P_0$, Cd $^3P_1$, and Cd $^3P_0$ these are also final products, but with Hg $^3P_1$ and the singlet excited atoms, dissociation of the hydride into the metal and a hydrogen atom takes place at once. Quenching to the metastable state is found to be usually inefficient. The atoms react with saturated hydrocarbons by splitting off a hydrogen atom, but the unsaturated ones usually interact with the initial formation of an excited molecule which when activated by singlet atoms have vibrational energy only, but which with triplet atoms are excited to triplet electronic states. The subsequent reactions of the excited olefines are discussed with reference to the experimental material.

### INTRODUCTION

OF recent years a considerable amount of work has been done on the reactions of excited mercury and cadmium.[1] Mercury possesses important resonance lines at 2537A and 1849A, but most of the experimental work has been done with the former, which corresponds to the transition $6^1S_0-6^3P_1$. The amount of energy liberated when a triplet mercury atom passes into its lowest state is 112.2 kcal. per mole, which is sufficient to cause dissociation of many molecules, particularly as a further amount (8.5 kcal. per mole in the case of hydrogen) of energy may be liberated simultaneously if the quenched atom combines with one of the products of the dissociation. The corresponding energy for triplet excited cadmium is somewhat less, 87.3 kcal. per mole, but this again may be increased, by 15.5 kcal., if cadmium hydride is formed. The energies liberated by the four excited atoms are summarized in Table I.

TABLE I.

| Metal | Line A | Transition | Energy of excited atom kcal. | Total available energy if hydride is formed kcal. |
|---|---|---|---|---|
| Mercury | 2537 | $6^1S_0-6^3P_1$ | 112.2 | 120.7 |
| Cadmium | 3261 | $5^1S_0-5^3P_1$ | 87.3 | 102.8 |
| Mercury | 1849 | $6^1S_0-6^1P_1$ | 153.9 | 162.4 |
| Cadmium | 2288 | $5^1S_0-5^1P_1$ | 124.4 | 139.9 |

Quenching experiments have so far only been carried out with mercury[2] and cadmium[3] in their triplet states. The data are given in Table I of Part I (preceding paper). The chemical reactions which are initiated by the excited atoms have been studied, using the usual kinetic methods, with mercury and cadmium in both the triplet and singlet states, although the majority are with the triplet atoms. Most of the work has been with hydrogen and the hydrocarbons.

In the remainder of this paper the treatment of Part I is extended to the simpler primary reactions occurring between excited mercury and cadmium atoms and other substances.

* Contribution No. 1031 from the National Research Laboratories, Ottawa, Canada.

[1] For reviews, see E. W. R. Steacie, Ann. N. Y. Acad. Sci. **41**, 187 (1941); W. A. Noyes and P. A. Leighton, *Photochemistry of Gases* (Reinhold Publishing Corporation, 1941), Chapter V.

[2] H. A. Stuart, Zeits. f. Physik **32**, 262 (1925); W. A. Noyes, J. Am. Chem. Soc. **49**, 3100 (1927); A. C. G. Mitchell, Zeits. f. Physik **49**, 228 (1928); J. R. Bates, Proc. Nat. Acad. Sci. **14**, 849 (1928); J. Am. Chem. Soc. **52**, 3825 (1930); *ibid.* **54**, 569 (1932); M. W. Zemansky, Phys. Rev. **36**, 919 (1930); M. G. Evans, J. Chem. Phys. **2**, 445 (1934); E. W. R. Steacie, Can. J. Research **B18**, 44 (1940).

[3] H. C. Lipson and A. C. G. Mitchell, Phys. Rev. **48**, 625 (1935).

## REACTIONS OF TRIPLET EXCITED MERCURY

### Reaction with Hydrogen

The potential-energy surfaces for the reaction $Hg(^3P_1)+H_2(^1\Sigma^+_g)$ are shown in Fig. 1, the curves on the left-hand face of the cube being those for an infinite H−H separation, those on the right for an infinite Hg−H separation. The reaction $Hg(^3P_1)+H$ may first be discussed in terms of the former curves.

The curves for the homopolar states may be constructed from the spectroscopic data;[4] it should be noted that there is no repulsive state which dissociates into normal Hg and H. An $Hg^+(^2S)$ ion interacts with an $H^-(^1S)$ ion with the formation of a polar $^2\Sigma^+$ state, but the corresponding curve cannot be constructed owing to lack of information from crystal data; however, neglecting the exchange interactions it is found that the polar curve cuts the $^2\Pi$ curve, the lowest formed from $Hg(^3P_1)$ and $H(^1\Sigma^+)$, at a separation of about 3A. Since the curve for the polar state does not cut that for the lowest $(^2\Sigma^+)$ state of the HgH molecule, which is known to be the case from the fact that the lowest state is homopolar, and since there is no other (repulsive) state, it is clear that quenching by the hydrogen atom can only arise from a jump from the polar to the $^2\Sigma^+$ state; as these are probably well separated the quenching efficiency is low.

The surfaces connecting the two sets of curves in the interior of the figure may now be discussed. If a hydrogen atom $(^2S)$ approaches linearly an HgH molecule in its lowest state $(^2\Sigma^+)$ the resulting states are $^1\Sigma^+$ and $^3\Sigma^+$, and of these, on account of the relationships

$$Hg(^1S)+H_2(^1\Sigma^+_g)=HgH_2(^1\Sigma^+) \qquad (1)$$

and

$$Hg(^1S)+H_2(^3\Sigma^+_u)=HgH_2(^3\Sigma^+), \qquad (2)$$

the $^1\Sigma^+$ state arises from the attractive state of hydrogen and the $^3\Sigma^+$ from the repulsive. The curves for $HgH(^2\Sigma^+)$ and $H_2(^1\Sigma^+_g)$ are therefore connected by a $^1\Sigma^+$ surface which has the same general form as the lowest surface in the $Na+H_2$ reaction. A second, $^3\Sigma^+$, surface connects the curves for $HgH(^2\Sigma^+)$ and $H_2(^3\Sigma^+_u)$; this is a highly repulsive surface, its lowest point being the lowest point on the curve for $HgH(^2\Sigma^+)$ when the second hydrogen atom is at infinity.

The lowest state of HgH which arises from $Hg(^3P_1)$ and a normal hydrogen atom is $^2\Pi$, and this interacts with a second hydrogen atom to give $^3\Pi$ and $^1\Pi$ states. In view of the further relationships

$$Hg(^3P_1)+H_2(^1\Sigma^+_g)=HgH_2(^3\Pi, {}^3\Sigma^+) \qquad (3)$$

and

$$Hg(^3P_1)+H_2(^3\Sigma^+_u) = HgH_2(^5\Pi, {}^3\Pi, {}^1\Pi, {}^5\Sigma^+, {}^3\Sigma^+, {}^1\Sigma^+) \qquad (4)$$

the $^3\Pi$ surface is clearly the lowest, and the only one of immediate interest. For the triangular configuration it may be assumed that the corresponding state is slightly attractive.

There are two comparatively low-lying surfaces representing ionic states of the $HgH_2$ complex. The lowest state of the $H_2^-$ molecule is $^2\Sigma^+$, and this interacts with a normal $(^2S)$ $Hg^+$ ion to give $^3\Sigma^+$ and $^1\Sigma^+$ states; similarly the lowest ionic state of HgH $(^2\Sigma^+)$ interacts with a $^2S$ hydrogen atom to give $^3\Sigma^+$ and $^1\Sigma^+$ states. Two surfaces therefore connect the $Hg^+H^-(^2\Sigma^+)$ and $H_2^-(^2\Sigma^+)$ curves in Fig. 1, of which that for the $^1\Sigma^+$ is lower and corresponds roughly to the electron being on the hydrogen atom nearer to the mercury atom; the $^3\Sigma^+$ state corresponds to the electron being on the farther atom. In the isosceles-triangular configuration the polar states have no such simple significance.

The potential-energy profiles drawn parallel to the Hg−H axis for the linear configuration, and corresponding to the normal H−H separation in hydrogen, are shown schematically in Fig. 2, in which only states corresponding to

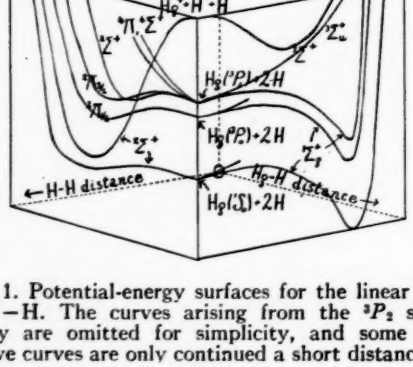


FIG. 1. Potential-energy surfaces for the linear system Hg−H−H. The curves arising from the $^3P_2$ state of mercury are omitted for simplicity, and some of the repulsive curves are only continued a short distance.

[4] Cf. R. S. Mulliken, Rev. Mod. Phys. 4, 1 (1932).

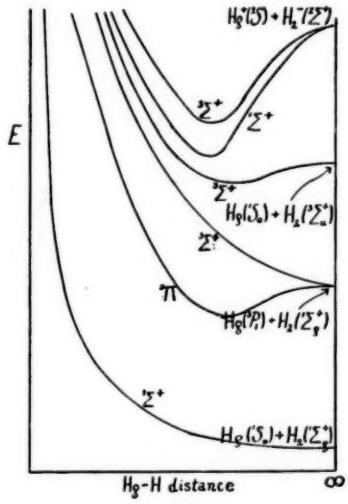


FIG. 2. Potential-energy profiles for $HgH_2$ in the plane corresponding to the normal H—H distance.

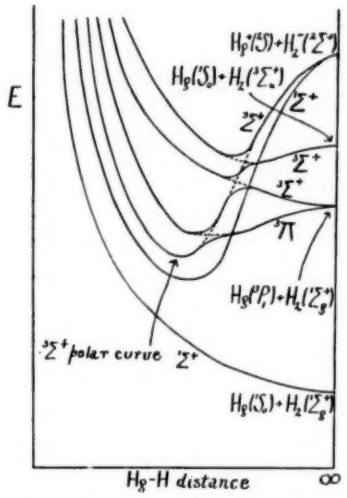


FIG. 3. Potential-energy profiles for $HgH_2$ corresponding to an extension of the H—H bond. Reaction initially proceeds along the $^3\pi$ homopolar surface, followed by a crossing to the $^3\Sigma^+$ polar surface. The transition to the $^3\Sigma^+$ repulsive surface takes place after an even greater extension of the H—H bond has taken place.

excited mercury in the $^3P_1$ state are shown. It is seen that owing to the high energy of the $H_2^-$ ion at this H—H separation the polar curves do not cut the homopolar ones; extension of the bond must therefore take place for reaction to occur in some section such as that shown in Fig. 3. As in the case of the quenching of sodium the activated state may be either at the top of the rotational-energy barrier, or at a point where the homopolar $^3\Pi$ surface is cut by the polar $^3\Sigma^+$ one, there being a restriction to crossing to the $^1\Sigma^+$ polar surface owing to the change of multiplicity. In either case there is a statistical factor of $\frac{1}{2}$ in the rate expression due to the fact that the $Hg^+$ and $H_2^-$ may approach one another initially either on the $^3\Sigma^+$ or the $^3\Pi$ surface of which only the latter leads to rapid reaction. The theoretical value of $r_\ddagger$ must therefore be divided by $\sqrt{2}$ to be directly comparable with $\sigma$. The value of $\sigma$ is about 2.5A (Table I, Part I) so that $r_\ddagger$ should be about 3.5A. This distance is a reasonable one for a crossing point but rather smaller than the value at the top of the rotational-energy barrier (4–5A). Agreement in the latter case could, however, be given by a value of $\kappa$ of less than one-half.

The mechanism by which the reaction proceeds to the final state may now be discussed, and this will be done in terms of the linear configuration of atoms. It has been seen that the polar surface on which the system finds itself is for a $^3\Sigma^+$ state, so that a transition to the lowest, $^1\Sigma^+$, state can only take place with difficulty owing to the change of multiplicity. Reaction therefore occurs more readily by a transition from the $^3\Sigma^+$ polar surface to the $^3\Sigma^+$ repulsive homopolar surface connecting the $HgH(^2\Sigma^+)$ and $H_2(^3\Sigma^+_u)$ curves. At large H—H separations, which may readily take place on the polar surface, this transition may be effected at a point below that corresponding to the first crossing point. The subsequent path of the system corresponds to its finding its way to the lowest part of this repulsive, $^3\Sigma^+$, surface, that is to that part which corresponds to $HgH(^2\Sigma^+)$ and $H(^2S)$. The quenching of excited mercury by hydrogen is therefore of a chemical rather than a physical nature, the H—H bond being broken.[5]

The exact mechanism by which the process takes place is, of course, extremely complex and could not, at the present stage, be treated theoretically. One can be fairly certain, however, that a large fraction of the energy set free, 17.7 kcal., passes into vibrational energy of the HgH molecule, the dissociation energy of which is 8.5 kcal. per mole; the alternative suggestion that it becomes relative translational energy implies

[5] G. Cario and J. Franck, Zeits. f. Physik **11**, 161 (1922).

that the mass point proceeds along the lowest point of the valley, which would seem improbable in view of the complicated form of the surfaces. The HgH molecule will therefore decompose within the period of one vibration, so that the over-all reaction is indistinguishable from[6]

$$Hg+H_2=Hg+2H. \qquad (5)$$

This conclusion is in accord with the findings of Olsen,[7] who showed spectroscopically that HgH is not produced in the reaction in the normal state, but only excited, presumably by secondary reactions. It is interesting to note that in the case of the reaction between hydrogen and mercury in the metastable ($^3P_0$) state the energy available for transfer into vibrational energy, 12.7 kcal., may not be converted efficiently enough into vibrational energy to permit dissociation of the HgH molecule; it might, therefore, be possible to detect HgH in its normal state in a system in which this reaction is occurring.

In view of the application of these principles that is made below to the reactions of the hydrocarbons, the mechanism of the reaction of hydrogen may be considered from a slightly different point of view. The "physical" type of reaction,

$$Hg(^3P_1)+H_2(^1\Sigma^+_g)=Hg(^1S_0)+H_2, \qquad (6)$$

analogous to that which takes place with sodium, is here restricted by the necessity for conservation of spin angular momentum (the "Wigner spin conservation rule") unless the hydrogen on the right-hand side is in a triplet state; if this condition is satisfied, however, the molecule at once dissociates, so that the reaction is not of a physical nature. There is therefore little possibility of the hydrogen molecule taking up the excitation energy in the form of vibrational, rotational or relative translational energy, as it was able to do with excited sodium; reaction can only proceed effectively by a dissociation of the hydrogen. The detailed examination which has been made of the mechanism shows the most probable reaction path to be

$$\begin{aligned} Hg(^3P_1)+H_2(^1\Sigma^+_g)&\rightarrow HgH_2(^3\Pi) \\ &\rightarrow Hg^+H_2^-(^3\Sigma^+)\rightarrow HgH_2(^3\Sigma^+) \\ &\rightarrow HgH(^2\Sigma^+)+H(^2S)\rightarrow Hg(^1S_0)+2H(^2S). \end{aligned} \qquad (7)$$

It is to be particularly noted that the over-all change has taken place without there being, at any stage, a restriction due to change of multiplicity, compensating changes in the hydrogen molecule taking place to preserve spin angular momentum. It will be seen in dealing with the reactions of hydrocarbons that arguments of this kind are frequently extremely useful in excluding mechanisms which might otherwise be considered. It may be mentioned that the selection rules imposed upon these molecular systems by the necessity of conserving spin angular momentum are obeyed almost rigorously.

### Quenching to the Metastable State

Apart from quenching by hydrogen, oxygen and the hydrocarbons, the other gases given in Table I of Part I quench by transferring the excited mercury atom to the metastable state; this is known to be true as the presence of the metastable atoms can be demonstrated spectroscopically. A potential-energy profile for quenching by a molecule M to the metastable state, which lies 5.03 kcal. below the $6^3P_1$ state, is shown in Fig. 4. The system first finds itself in the dip of the middle curve. If M is an atom the quenching process is clearly inefficient, but otherwise the dip is a section through a de-

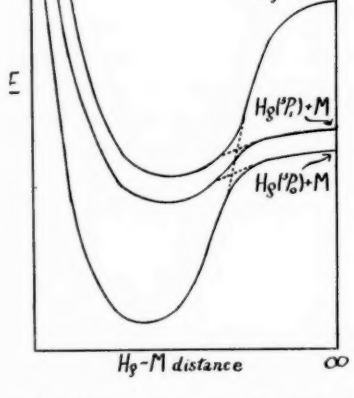


FIG. 4. Potential-energy curves for the quenching of $Hg(^3P_1)$ to the metastable state by an atom or molecule M.

[6] Cf. J. Franck and H. Sponer, Nachrichten Göttingen 241 (1928); H. Beutler and E. Rabinowitch, Zeits. f. physik. Chemie **B8**, 403 (1930).

[7] L. O. Olsen, J. Chem. Phys. **6**, 307 (1938).

pression in three or more dimensional space, and owing to the possibility of a redistribution of energy the complex will not necessarily redissociate into $Hg(^3P_1)+M$, but may perform a series of vibrations until a transition to the lower surface is possible. The efficiency of quenching to the metastable state is lower than generally obtains for quenching to the normal state since, owing to the small difference between the energies of the $^3P_1$ and $^3P_0$ levels, the rate with which the complex redissociates into $Hg(^3P_1)$ and M is by no means negligible. The apparent quenching efficiency is also lowered in reactions of this kind by the fact that $^3P_0$ mercury atoms may become excited to the $^3P_1$ state by collisions.

Zemansky[8] has attempted to show a relationship between the efficiency of quenching to the metastable state and the nearness of a vibrational level of the quencher to 5.03 kcal., the energy of the transition $^3P_1 \rightarrow {}^3P_0$. The hydrocarbons must, however, be removed from his figure as they are now known to quench by a chemical mechanism (see below), and when they are removed the existence of the relationship can hardly be maintained. In any case it is doubtful whether such a connection has any theoretical justification, as the restriction to crossing caused by a failure of levels to fit is probably usually only slight.[9] It would appear from the present treatment that the problem requires a detailed construction of the potential-energy surfaces relevant to each individual case, and a calculation from them of the course of reaction. This could hardly be attempted at the present stage.

## REACTIONS OF TRIPLET EXCITED CADMIUM

The potential-energy surfaces for the quenching of the cadmium 3261 line by hydrogen are similar in general form to those for the mercury reaction shown in Fig. 1. The chief difference arises from the fact that, owing to only 87.3 kcal. of energy being liberated in the transition $Cd\,^3P_1 \rightarrow {}^1S_0$, the process

$$Cd(^3P_1)+H_2=Cd(^1S_0)+2H \qquad (8)$$

is endothermic to the extent of 15.6 kcal., and therefore slow since the activation energy is at least this amount. The reaction which forms CdH,

$$Cd(^3P_1)+H_2=CdH+H, \qquad (9)$$

is much faster since it is only endothermic by c. 0.1 kcal. The quenching reaction is therefore largely reaction (9), which has a slight activation energy of at least 0.1 kcal. This activation energy accounts for the lower value of $\sigma$ as compared with the mercury reaction (see Table I, Part I).

The chief difference between the mechanism of the quenching of cadmium and that of mercury is that in the former case very little energy can pass into vibrational energy of the hydride, any that does so having to be paid for as activation energy. The hydride CdH will therefore not dissociate and should be detectable in its normal state; this has been done spectroscopically by Bender.[10]

The quenching of cadmium atoms in the metastable state will also proceed by a mechanism analogous to (9), but the activation energy will be increased by 1.5 kcal., the difference between the $^3P_1$ and $^3P_0$ levels, and the process is consequently inefficient; this, however, has not been investigated, as the levels are separated so slightly as to be difficult to distinguish experimentally.

Owing to the comparative slowness of the quenching by this mechanism, complications may arise in the form of quenching of other types; thus the quenching may be partly due to a physical type of reaction which took place in the quenching of sodium by hydrogen, although as was seen for mercury such a reaction is restricted by a difference in multiplicity between the polar and the final state. A certain amount of the quenching may also be quenching to the metastable state, although this, as has been seen, is inefficient. In any case a considerable fraction of the total reaction must proceed by the chemical process since hydrogen atoms are known to be formed in quantity.

Apart from the hydrocarbons most of the other quenching reactions proceed by transferring the cadmium atom to the metastable state, and, as this lies only 1.5 kcal. below the

[8] M. W. Zemansky, Phys. Rev. **36**, 1919 (1930).
[9] Cf. J. L. Magee, W. Shand and H. Eyring, J. Am. Chem. Soc. **63**, 677 (1941).
[10] P. Bender, Phys. Rev. **36**, 1535 (1930); cf. L. O. Olsen, reference 7.

$^3P_1$ state, quenching is inefficient owing to the high probability of the system returning to its initial state (cf. Table I, Part I).

### REACTIONS OF THE SINGLET EXCITED ATOMS

Owing to the non-existence of quenching data and the scantiness of the kinetic information, the reactions of singlet ($^1P_1$) excited mercury and cadmium will only be treated briefly; surfaces may, however, readily be constructed if needed. The term relationships required are, for mercury:

$$Hg(^1P_1)+H_2(^1\Sigma^+_g)\rightarrow HgH_2(^1\Sigma^+, {}^1\Pi), \quad (10)$$

$$Hg(^1S_0)+H_2(^1\Sigma^+_g)\rightarrow HgH_2(^1\Sigma^+), \quad (11)$$

$$Hg^+(^2S)+H_2^-(^2\Sigma^+)\rightarrow Hg^+H^-_2(^1\Sigma^+, {}^3\Sigma^+), \quad (12)$$

and

$$HgH(^2\Sigma^+)+H(^2S)\rightarrow HgH_2(^1\Sigma^+, {}^3\Sigma^+), \quad (13)$$

with identical states for the cadmium system. The possibility of physical quenching, without dissociation of the hydrogen, may first be considered. It is seen that this may occur *via* the two $^1\Sigma^+$ states of $HgH_2$ and the $^1\Sigma^+$ state of $Hg^+H_2^-$; reaction (10) first takes place to give $HgH_2(^1\Sigma^+)$, followed by a crossing to the $^1\Sigma^+$ polar state and a second crossing to the lower $^1\Sigma^+$ state of $HgH_2$, which then dissociates into $Hg(^1S)$ and $H_2(^1\Sigma^+_g)$ by the reverse of reaction (11). However in both the mercury and cadmium reactions the hydrogen so produced would probably have sufficient vibrational energy for dissociation to take place at once, so that the overall reaction will be

$$Hg(^1P_1)+H_2(^1\Sigma^+_g)\rightarrow Hg(^1S_0)+2H(^2S). \quad (14)$$

Alternatively, the reaction may be envisaged as taking place *via* $HgH(^2\Sigma^+)$ and $H(^2S)$, which may arise from the lower $^1\Sigma^+$ state of $HgH_2$ (reverse of reaction (13)); however the HgH will probably have sufficient energy to dissociate. There thus seems to be no alternative to assuming that reaction (14) is the one which takes place.

The quenching cross sections for the atoms in the singlet states should be higher than those for the triplet states, since the surfaces upon which the reaction initially moves are higher, and the separation at the crossing-point to the polar state consequently larger; however the very small lifetimes of the singlet states make the actual magnitudes of quenching relatively small.

### PHOTOSENSITIZED REACTIONS OF HYDROCARBONS

#### Reactions of Saturated Hydrocarbons

The evidence from recent investigations on the reactions of ethane,[11] propane[12] and butane[13] photosensitized by triplet mercury and cadmium in all cases indicates an initial carbon-hydrogen bond split. From the theoretical point of view these reactions are very similar to the reactions of hydrogen, the normal state of the hydrocarbons being a singlet state. Quenching of the physical type, the energy being taken up as vibrational energy, is again excluded by the necessity for conservation of spin angular momentum. The possibility of the hydrocarbon becoming excited to a triplet state has to be considered, but this would probably be unstable and decompose to give a hydrogen atom and a free radical. The mechanism is probably much the same as for hydrogen, reaction proceeding *via* a polar complex.

The question of whether the hydrides HgH and CdH are formed is of interest in connection with the strengths of the carbon-hydrogen bonds in the hydrocarbons;[1] if they are, the upper limits to the bond strength are given by the figures in the last column of Table I, while otherwise the upper limits are not so high (fourth column). It has been seen that with hydrogen the hydrides are initially formed, but that if there is sufficient energy available, as in the case of triplet mercury, the hydride decomposes at once. Presumably the situation is much the same with the saturated hydrocarbons; the hydride is formed initially but may decompose. In the absence of additional information, therefore, the upper limit to the strength of the bond

[11] E. W. R. Steacie and N. W. F. Phillips, J. Chem. Phys. **6**, 179 (1938); Can. J. Research **B16**, 303 (1938); E. W. R. Steacie and R. Potvin, J. Chem. Phys. **7**, 782 (1939).

[12] E. W. R. Steacie and D. J. Dewar, *ibid.* **8**, 571 (1940); E. W. R. Steacie, D. J. LeRoy and R. Potvin, *ibid.* **9**, 306 (1941).

[13] E. W. R. Steacie and R. Potvin, *ibid.* **7**, 782 (1939).

is that which corresponds to the formation of the hydride. If, however, it could be satisfactorily proved that the hydride was not formed, the smaller figure might be accepted as a maximum.

Work has not been carried out on the reactions of saturated hydrocarbons photosensitized by singlet excited atoms, but in the light of the treatment in the preceding section there would seem to be no reason to doubt that they proceed by an initial carbon-hydrogen bond split.

### Reactions of Ethylene

The reaction of ethylene photosensitized by triplet mercury atoms has recently been studied by LeRoy and Steacie[14] who obtain evidence for the following reaction scheme:

$$Hg(^3P_1)+C_2H_4=Hg(^1S_0)+C_2H_4^*, \quad (15)$$

$$C_2H_4^*+C_2H_4=2C_2H_4, \quad (16)$$

$$C_2H_4^*=C_2H_2+H_2, \quad (17)$$

$$Hg(^3P_1)+H_2=Hg(^1S_0)+2H, \quad (18)$$

$$H+C_2H_4=C_2H_5, \quad (19)$$

$$2C_2H_5=C_4H_{10}. \quad (20)$$

The most significant facts in favor of this mechanism are the initial pressure increase, which seems to exclude a free radical mechanism, and the increase in acetylene concentration even when the total pressure is decreasing. It is of interest to consider the first three of these reactions in the light of the present treatment.

The lowest electronic state of ethylene is a singlet ($^1A_{1g}$) state, and since it is known from the high quenching cross section of ethylene (cf. Table I, Part I) that reaction (15) occurs without any restriction, it follows that for conservation of spin angular momentum the excited ethylene produced in the reaction must be in a triplet state, so that reaction (15) should be written as

$$Hg(^3P_1)+C_2H_4(^1A_{1g}) = Hg(^1S_0)+C_2H_4(\text{triplet})^*. \quad (15a)$$

Such a triplet state, of designation $^3B_{1u}$, has been shown theoretically[15] to lie about 20 kcal. above the normal state, the next higher being so high as to play no part here. Thus, of the 112 kcal. set free when the $^3P_1$ mercury is deactivated, about 20 kcal. passes into electronic energy, while the majority of the remainder, about 90 kcal., goes into vibrational energy, a small amount being dissipated as translational energy. The excitation of the ethylene molecule to the triplet state is accompanied by a twisting of the double bond through 90°.

The second reaction, the deactivation of excited ethylene by collision with a normal molecule, takes place only with difficulty if the ethylene molecules produced are both in singlet states; however an alternative reaction,

$$C_2H_4(^3B_{1u})^*+C_2H_4(^1A_{1g}) = C_2H_4(^3B_{1u})+C_2H_4(^1A_{1g}), \quad (16a)$$

the removal of vibrational energy from the excited ethylene molecule, leaving the molecule in its triplet state, will take place with greater efficiency, although even here there will be a large negative entropy of activation[16] owing to the loss of rotation in the activated state.[17] Very little polymerization takes place so that the reaction

$$C_2H_4(^3B_{1u})^*+C_2H_4(^1A_{1g})=C_4H_8 \quad (21)$$

is apparently also slow. Since also radiation of triplet excited ethylene is restricted by the change of multiplicity, it appears that the molecule will react chiefly by splitting off hydrogen (reaction (17)).

Reaction (17) as written will be slow for the same reason, but the possibility now arises of an alternative reaction, the formation of acetylene in a triplet state:

$$C_2H_4(^3B_{1u})^*=C_2H_2(\text{triplet})+H_2, \quad (17a)$$

which is not restricted by a low transition probability, but which has an activation energy higher than (17) by the excitation energy of the triplet acetylene molecule. The activation energy for the formation of unexcited acetylene and

[14] D. J. LeRoy and E. W. R. Steacie, J. Chem. Phys. **9**, 829 (1941); cf. H. S. Taylor and J. R. Bates, Proc. Nat. Acad. Sci. **12**, 714 (1926); J. R. Bates and H. S. Taylor, J. Am. Chem. Soc. **49**, 2438 (1927).

[15] J. L. Magee, W. Shand, and H. Eyring, J. Am. Chem. Soc. **63**, 677 (1941).

[16] R. N. Pease, J. Am. Chem. Soc. **53**, 613 (1931); H. D. Burnham and R. N. Pease, *ibid.* **62**, 453 (1940).

[17] F. P. Jahn, J. Am. Chem. Soc. **61**, 798 (1939).

hydrogen from unexcited ethylene has been estimated[18] to be 85 kcal., so that assuming the electronic excitation energy of the triplet acetylene molecule to be the same as that of triplet ethylene, or 20 kcal. (the actual magnitude is unknown), the activation energy for the formation of hydrogen and triplet acetylene from normal ethylene is about 105 kcal. It is thus clear that the excited ethylene has derived from the mercury atom sufficient energy for reaction (17a) to proceed without difficulty.

In the case of the reaction photosensitized by triplet cadmium the energy given to the ethylene, 87 kcal., is not sufficient for reaction (17a) to proceed without an activation energy. This is in accord with the results of Steacie, Potvin and LeRoy,[19] who find that the acetylene formation is only a small fraction of the total reaction, which is chiefly polymerization taking place with a quantum yield of only about 0.01.

The experimental facts with regard to the reaction photosensitized by singlet excited cadmium atoms are rather more difficult to interpret.[20] Polymerization takes place efficiently, but acetylene is a much less important product and there is no initial pressure rise. A possible explanation would seem to be that two initial mechanisms, vibrational excitation of the ethylene, which remains in its lowest electronic state, and the breaking of a carbon-hydrogen bond, are here taking place simultaneously.

### Reactions of Higher Olefines

Preliminary work[21] on propylene, butene-1 and butene-2 with $^3P_1$ cadmium shows that polymerization is extremely slow. Quenching data are not available.

Of the possible initial reactions, the splitting of a carbon-hydrogen bond and the excitation of the double bond to a vibrationally-excited triplet state are the most likely. Of the two the second probably proceeds more rapidly, as is known from the larger quenching cross sections for unsaturated as compared with saturated hydrocarbons; however, subsequent reaction is difficult as polymerization proceeds only with a large negative entropy of activation,[16,22] and triplet cadmium does not provide enough energy for the splitting off of a hydrogen molecule.

The author wishes to express his thanks to Professor G. Herzberg, Professor R. S. Mulliken and Dr. Anthony Turkevich for information regarding molecular electronic states, and to Professor Henry Eyring, Dr. Samuel Glasstone, Dr. D. J. LeRoy and Dr. E. W. R. Steacie for valuable discussions and suggestions in connection with this and the preceding paper.

[18] E. W. R. Steacie, reference 1, p. 195.
[19] E. W. R. Steacie and R. Potvin, Can. J. Research **B16**, 337 (1938); **B18**, 47 (1940); E. W. R. Steacie and D. J. LeRoy, unpublished.
[20] E. W. R. Steacie and D. J. LeRoy, J. Chem. Phys. **10**, 22 (1942).
[21] E. W. R. Steacie and D. J. LeRoy, unpublished.
[22] W. E. Vaughan, J. Am. Chem. Soc. **56**, 3863 (1932); G. B. Kistiakowsky and J. R. Lacher, *ibid.* **58**, 123 (1936); J. B. Harkness, G. B. Kistiakowsky, and W. H. Mears, J. Chem. Phys. **5**, 682 (1937).

# Thermodynamics of High Polymer Solutions[1]

PAUL J. FLORY
*Esso Laboratories of the Standard Oil Development Company, Chemical Division, Linden, New Jersey*

(Received October 15, 1941)

A statistical mechanical treatment of high polymer solutions has been carried out on the basis of an idealized model, originally proposed by Meyer, which is analogous to the one ordinarily assumed in the derivation of the "ideal" solution laws for molecules of equal size. There is obtained for the entropy of mixing of $n$ solvent and $N$ linear polymer molecules (originally disoriented), $\Delta S = -k[(n/\beta)\ln v_1 + N \ln v_2]$ where $v_1$ and $v_2$ are volume fractions and $\beta$ is the number of solvent molecules replaceable by a freely orienting segment of the polymer chain. This expression is similar in form to the classical expression for equal-sized molecules, mole fractions having been replaced by volume fractions. When the disparity between the sizes of the two components is great, this expression gives entropies differing widely from the classical values, which accounts for the large deviations of high polymer solutions from "ideal" behavior. The entropy of disorientation of a perfectly arranged linear polymer is found to be of the order of $R$ cal. per chain segment. After introducing a suitable heat of mixing term, partial molal free energies are computed, and the calculations are compared with experimental data for all concentrations. Phase equilibria have been calculated in the region of partial miscibility. The theory predicts, in agreement with experiment, that the critical composition for partial miscibility lies at a low concentration of polymer. Low intrinsic viscosities of polymers dissolved in poor solvents are attributed to the tendency for the molecule to assume a more compact configuration in such an environment.

## INTRODUCTION

IT is customary to correlate the thermodynamic properties of binary liquid systems with the so-called "ideal" solution laws. These rest fundamentally on an entropy of mixing given by

$$\Delta S_{\text{mixing}} = -R(n_1 \ln X_1 + n_2 \ln X_2), \qquad (1)$$

where $n_1$ and $n_2$ are the numbers of moles of the two components, and $X_1$ and $X_2$ are their mole fractions in the mixture. Partial differentiation of (1) with respect to $n_1$ yields for the partial molal entropy of dilution

$$\Delta \bar{S}_1 = -R \ln X_1. \qquad (2)$$

Although (1) and (2) frequently have been applied indiscriminately, at finite concentrations they can be justified theoretically only when molecules of the two species are equivalent in size and shape, i.e., when molecules of the two species are interchangeable in the liquid. The importance of this limitation has been emphasized by a number of authors during recent years.[2-4]

Meyer and co-workers[5,6] have found that $\Delta \bar{S}_1$ for solutions of long chain compounds dissolved in simple solvents, e.g., for carbon tetrachloride solutions of long chain esters, is much greater than Eq. (2) would predict. In other words, they have found strong negative deviations from Raoult's law, even when $\Delta \bar{H}_1 = 0$. Meyer and Lühdemann[5] suggested that this abnormal entropy effect was due to the ability of sections of a long chain solute molecule to act more or less independently of one another as kinetic units. Thus, the effective mole fraction should be greater than the actual mole fraction. An equivalent explanation has been advanced recently by Powell, Clark and Eyring.[7] Apparently they were unaware of the serious criticisms of this point of view advanced by Hückel,[2] principally on the grounds that it inherently assumes primary validity of the ideal solution laws when applied to mixtures of molecules differing greatly in size. Hückel has also pointed out that the kinetic units cannot be truly independent, nor are they independently interchangeable in the liquid as applicability of (1) or (2) would require. Finally, in order to explain experimental results,

[1] Presented before the Division of Physical and Inorganic Chemistry of the American Chemical Society, at the Atlantic City Meeting, September 11, 1941.
[2] E. Hückel, Zeits. f. Elektrochemie **42**, 753 (1936).
[3] E. A. Guggenheim, Trans. Faraday Soc. **33**, 151 (1937).
[4] R. H. Fowler and G. S. Rushbrooke, Trans. Faraday Soc. **33**, 1272 (1937).
[5] K. H. Meyer and R. Lühdemann, Helv. Chim. Acta **18**, 307 (1935).
[6] Ch. G. Boissonnas, Helv. Chim. Acta **20**, 768 (1937).
[7] R. E. Powell, C. R. Clark, and H. Eyring, J. Chem. Phys. **9**, 268 (1941).

it is necessary to assume a size for the kinetic unit, which, though equal to the entire solute molecule at infinite dilution, decreases rapidly with increasing concentration, approaching a limiting size of some 15 to 30 chain atoms[5,7] at high concentrations.

Recently Meyer[8] has provided a more plausible explanation of the "abnormalities" of solutions of long chain, or polymeric, molecules. He has suggested an idealized model for such solutions, which consists of a quasi-solid lattice, not unlike that customarily used in the derivation of (1) for the case of a mixture of equal-sized molecules. A cell of the hypothetical lattice may be occupied either by a solvent molecule or by a segment of the polymer (solute). The segments of a given polymer chain must occupy a continuous sequence of adjacent cells, which, however, may meander irregularly through the lattice. There will be many such sequences emanating from a given cell, and the polymer molecule may conform to any one of them through suitable rotations about the valence bonds of the chain skeleton. According to Meyer, entropies of mixing in excess of "ideal" values given by (1) are the result of these numerous configurations available to the polymer molecules.

Meyer has discussed his model in qualitative terms only. Recently quantitative statistical mechanical treatments[9–11] of this model have been carried out independently by Huggins and the writer. On the basis of the preliminary accounts which have been published concerning these investigations, the results appear to be in substantial agreement. In this paper the writer's treatment of the problem will be presented in full, with particular emphasis on an extension of the model and applications to hitherto unexplained characteristics of polymer solutions.

## DERIVATION OF THE ENTROPY OF MIXING

Throughout this paper polymer molecules which are linear, i.e., consist of a single linear sequence of structural units, are under consideration. Somewhat arbitrarily, the symmetry number of these molecules is taken to be two, due to (assumed) indistinguishability of the two ends of the molecule. Concurrently with the derivation of the fundamental relationships, special prominence will be given to the assumptions involved.

*Assumption 1:* the mixture of polymer and solvent molecules is assumed to conform to Meyer's model. This involves assumption of (a) a quasi-solid lattice in the liquid, (b) interchangeability of segments (not necessarily identical with the polymer structural units) of the polymer chain with solvent molecules in the lattice cells and (c) independence of lattice constants on composition. Although these assumptions obviously are quite artificial, there is some consolation in the fact that analogous ones are inherent in the model from which Eq. (1) is derived for mixtures of small molecules of equal size.

*Assumption 2:* all polymer molecules are assumed to be of the same size.

*Assumption 3:* the average concentration of polymer segments in cells adjacent to cells unoccupied by the polymeric solute is taken to be equal to the over-all average concentration.

Let $n_0$ = the total number of cells in the lattice.

$N$ = the number of polymer molecules, each composed of $x$ segments, any one of which may replace a solvent molecule in the lattice.

$\gamma$ = a coordination number for the lattice, i.e., the number of "first neighbor" cells in the lattice available to the next consecutive segment of the polymer chain.

In order to determine the total number of possible non-identical configurations, let us first consider the process of successive addition of polymer molecules to the empty lattice containing $n_0$ cells. After $N$ polymer molecules have been added, there will be $n_0 - xN$ cells which may be occupied by the terminal segment of the next polymer molecule to enter the lattice. According to assumption 3, the expected number of available unoccupied cells immediately adjacent to the cell occupied by the terminal segment of this polymer chain will be $\gamma(n_0 - xN)/n_0$. For the third segment the expected number of available cells will be given by $\alpha = (\gamma - 1)(n_0 - xN)/n_0$, since the cell occupied by the terminal segment eliminates one of the neighboring cells.

*Assumption 4:* the expected number of avail-

[8] K. H. Meyer, Zeits. f. physik. Chemie **B44**, 383 (1939); Helv. Chim. Acta **23**, 1063 (1940).
[9] M. L. Huggins, J. Chem. Phys. **9**, 440 (1941).
[10] Paper presented by Dr. Huggins before the Wilder D. Bancroft Colloid Symposium, Ithaca, New York, June 20, 1941.
[11] P. J. Flory, J. Chem. Phys. **9**, 660 (1941).

able positions for each successive segment is taken to be equal to $\alpha \equiv (\gamma-1)(n_0-xN)/n_0$. This is of the nature of an approximation, as it fails to exclude impossible configurations in which two segments, separated by two or more intervening segments but belonging to the same chain, occupy the same cell. Use of this "assumption" obviously will lead to computation of too many configurations.

For the expected number of configurations which the particular chain may assume without shifting the terminal group we have

$$[\gamma/(\gamma-1)]\alpha^{x-1} \tag{3}$$

and for the expected total number of configurations for the chain in the entire lattice

$$\nu_{N+1} = \tfrac{1}{2}(n_0-xN)[\gamma/(\gamma-1)]\alpha^{x-1}, \tag{4}$$

$$\leqq \tfrac{1}{2}(n_0-xN)^x(\gamma-1)^{x-1}, \; n_0{}^{1-x}, \tag{4.1}$$

where the factor $\frac{1}{2}$ has been included in order to eliminate redundancy of configurations due to the indistinguishability of the ends of the polymer chain.

The total number of possible configurations for the system consisting of $N$ polymer and $n$ solvent molecules in a lattice composed of $n_0 = n+xN$ cells is given by

$$W = (1/N!)\prod_{N=1}^{N}\nu_N, \tag{5}$$

where the factor $1/N!$ eliminates redundant configurations which differ only by an interchange of one or more pairs of polymer molecules. Substituting (4.1) in (5) we obtain by suitable rearrangement

$$W = \left(\frac{\gamma-1}{n_0}\right)^{(x-1)N}\left(\frac{x^{xN}}{2^N N!}\right)\left[\frac{(n_0/x)!}{(n_0/x-N)!}\right]^x.$$

Replacing factorials by Stirling's approximation, $N! = (N/e)^N$

$$W = \left(\frac{\gamma-1}{e}\right)^{(x-1)N}(1/2)^N\frac{(n+xN)^{n+N}}{n^n N^N}. \tag{6}$$

For the entropy of mixing, according to the well-known Boltzmann relationship $S = k \ln W$, where $k$ is Boltzmann's constant, we obtain[11]

$$\Delta S_{\text{mixing}} = -k\left[n\ln\left(\frac{n}{n+xN}\right)+N\ln\left(\frac{N}{n+xN}\right)\right]$$

$$+k(x-1)N[\ln(\gamma-1)-1]-kN\ln 2. \tag{7}$$

This expression refers to the entropy change in the process of mixing $n$ pure solvent and $N$ perfectly arranged (or oriented) polymer molecules, subject, of course, to the assumptions introduced above concerning the nature of the solution. When $x=1$, (7) reduces to the classical expression (1), except for the symmetry term.

A few remarks should be made concerning the use in the above derivation of "expected values" for the numbers of configurations, since actual values in many cases may deviate enormously from expectancy. When $\alpha$ is greater than unity (i.e., when the concentration of polymer is not too great) the expected number of available configurations which extend from a given site in the lattice, is, according to Eq. (3), a very large number. (We consider $x$ to be at least of the order of 100.) But the actual number of configurations may be zero; for example, there might be only one cell available for the second segment and none for the third. On the other hand, for a more favorably located initial cell, the number of available configurations may be an exceedingly large number. Since the total number of sites available to the terminal segment of the $N$th polymer molecule to be added to the lattice is very large when $\alpha > 1$, the actual total number of configurations available to the particular molecule will deviate negligibly from the expected number calculated from (4).

When $\alpha$ is appreciably less than unity, i.e., at high concentrations of polymer, the expected number of configurations (Eq. (3)) extending from a given site will be very much less than unity. If $\alpha$ is sufficiently small, e.g., of the order of 0.5, then $\nu_N$ also may be extremely small (for large $x$). That is, at high polymer concentrations the expected number of configurations available for an additional polymer molecule is much less than unity. Of all the possible configurations for the $N-1$ polymer molecules in the lattice, only a small fraction (not exactly equal to $\nu_N$) possess one or more continuous sequences of $x$ vacant cells any place in the entire lattice. According to

this interpretation, $\nu_N$ is the average "yield" of such sequences of unoccupied cells per configuration of the $N-1$ polymer molecules in the lattice. Thus, after a certain concentration is exceeded, addition of more polymer molecules to the lattice (possessing a fixed number of cells) decreases the total number of configurations for the system.[12a] In spite of the use of expected values from which actual deviations may be large, Eq. (6) for the total number of configurations should be a valid approximation at all concentrations, subject only to the original assumptions.

### THE ENTROPY OF DISORIENTATION

The "configurational" entropy of a lattice filled with $N$ polymer molecules in the absence of solvent, which is obtained by setting $n=0$ in (7), is[11]

$$\Delta S^* = kN \ln (x/2) + kN(x-1)[\ln (\gamma-1)-1]. \quad (8)$$

When $x$ is large

$$\Delta S^*/Nx \cong k \ln [(\gamma-1)/e]. \quad (9)$$

That is, the entropy change per mole of segments is of the order of $R$.[12b] These relationships express the entropy change for the transformation of $N$ polymer molecules from a state of perfect orientation and arrangement in the lattice to the state of random entanglement. This probably is the source of an appreciable portion of the entropy of fusion of polymer crystallites (e.g., in rubber, polyesters, etc.). Obviously, other terms arising from change in the lattice constants and in the arrangements and motions within the segments when fusion occurs also contribute to the total entropy of fusion.

It can be shown that the lattice "saturated" with polymer molecules will contain a few vacant cells, equivalent to the "holes"[13] in simple liquids. From the point of view of the equations used above, these vacant cells should be treated as molecules of a second component. However, their concentration is so small that no significant error has been committed in setting $n=0$ in the derivation of (8).

The entropy change on mixing $n$ solvent with $N$ randomly entangled (liquid state) polymer molecules is

$$\Delta S_{\text{mixing}} = \Delta S_{\text{mixing}} - \Delta S^* = -k\left[n \ln \left(\frac{n}{n+xN}\right) + N \ln \left(\frac{xN}{n+xN}\right)\right]. \quad (10)$$

Or

$$\Delta S_{\text{mixing}} = -k[n \ln v_1 + N \ln v_2], \quad (10.1)$$

where $v_1$ and $v_2$ are volume fractions of solvent and polymer, respectively. The pure liquid polymer (disoriented) will be chosen as the standard state for the solute, as is customary for binary liquid mixtures. Equation (10) will serve as the starting point for the derivation of the thermodynamic relationships discussed below.

It is interesting to note that (10.1) is so similar in form to (1); replacement of volume fractions by mole fractions in the logarithms of the former yields the latter. The entropy of mixing of polymer and solvent is greater than (1) would predict, but less than that for mixing the completely dissociated polymer segments with solvent. Meyer's[8] qualitative discussion of the problem leads to the same conclusion.

### PARTIAL MOLAL FUNCTIONS

Differentiating (10) with respect to $n$, there is obtained for the partial molal entropy of the solvent

$$\Delta \bar{S}_1 = -R \ln (1-v_2) - R(1-1/x)v_2 \quad (11)$$

$$= Rv_2(1/x + v_2/2 + v_2^2/3 + \cdots). \quad (11.1)$$

Similarly,

$$\Delta \bar{S}_2 = -R \ln (1-v_1) + R(x-1)v_1. \quad (12)$$

Inasmuch as the forces acting between two polymer molecules, or between a polymer and a simple molecule, obviously are of the same sort as those operating between pairs of simple molecules, the heat of interaction between a polymer

[12a] Alternatively, one may consider that the polymer molecules are continually diffusing in the lattice, i.e., the system is continually changing from one configuration to another. Then $\nu_N$ is the time average number of available sequences of $x$ units.

[12b] H. Mark, J. App. Phys. **12**, 41 (1941), using the statistical theory of the internal configurations of polymer molecules, has arrived at a similar value for the entropy of disorientation *per chain bond* about which there is free rotation.

[13] H. Eyring, J. Chem. Phys. **4**, 283 (1936); H. Eyring and J. O. Hirschfelder, J. Phys. Chem. **41**, 249 (1937).

molecule and its environment should vary linearly with the composition. Consequently, the heat of mixing can be represented by a relationship used by Scatchard[14] for simple molecules

$$\Delta H = BV_1V_2nN/(nV_1+NV_2), \quad (13)$$

where $B$ is a constant for a given pair of liquids and $V_1$ and $V_2$ are the molar volumes of solvent and polymeric solute, respectively. According to the model considered here, $V_2 = xV_1$.

The partial molal heat contents are, according to (13)

$$\Delta\bar{H}_1 = BV_1v_2^2 \quad (14)$$

and

$$\Delta\bar{H}_2 = BV_2v_1^2 = BxV_1v_1^2. \quad (15)$$

Combining these equations with (11) and (12), there is obtained for the partial molal free energy of the solvent

$$\Delta\bar{F}_1 = RT \ln (1-v_2) + RT(1-1/x)v_2 + BV_1v_2^2 \quad (16)$$

$$= -RTv_2[1/x + (1-K)v_2/2 + v_2^2/3 + \cdots], \quad (16.1)$$

where

$$K = 2BV_1/RT$$

and for the partial molal free energy of the solute

$$\Delta\bar{F}_2 = RT \ln (1-v_1) - RT(x-1)v_1 + BV_1xv_1^2. \quad (17)$$

Equations (16.1) and (11.1) reduce to the "ideal" solution relationships at infinite dilution. This is virtually a necessary consequence[3] of the Gibbs-Duhem relationship

$$\partial\Delta\bar{F}_1/\partial \ln X_1 = \partial\Delta\bar{F}_2/\partial \ln X_2.$$

Since for any acceptable model for the system the activity $a_2$ of the solute must be proportional to the concentration at infinite dilution

$$\partial \ln a_2/\partial \ln X_2 \equiv (1/RT)\partial\Delta\bar{F}_2/\partial \ln X_2 = 1$$
$$\partial\Delta\bar{F}_1/\partial \ln X_1 = RT.$$

Or

$$\Delta\bar{F}_1 = RT \ln X_1$$

which at infinite dilution may be replaced by

$$\Delta\bar{F}_1 = -RTX_2 = -RTv_2/x, \quad (16.2)$$

which is identical with (16.1) as $v_2$ approaches zero.

[14] G. Scatchard, Chem. Rev. **8**, 321 (1931).

## THE EFFECT OF SEGMENT SIZE

It has been assumed that a section of the polymer chain which occupies a volume equal to that of one solvent molecule is equally free to occupy any one of $\gamma-1$ cells, entirely independent of the configuration of preceding segments of the chain. If the solvent molecule is very small, or if there are limitations, perhaps steric in nature, on the tortuosity which the chain may comfortably assume, then the size of the section of the chain which is free to orient itself at random, irrespective of the orientation of the preceding sections, may be equivalent to the volume occupied by several solvent molecules. In this situation, we may construct a new lattice in which one cell will accommodate either $\beta$ solvent molecules or one segment of the polymer chain.

The entropy of mixing according to this revised model will be given by either of the Eqs. (7) or (10), provided that $n$ is replaced by $n' = n/\beta$; $x$ likewise has been decreased by the same factor, but a modified symbol is unnecessary. Differentiating the resulting expression with respect to $n$ (not $n'$)[11]

$$\Delta\bar{S}_1 = -(R/\beta)[\ln (1-v_2) + (1-1/x)v_2] \quad (18)$$

$$= (Rv_2/\beta)(1/x + v_2/2 + v_2^2/3 + \cdots), \quad (18.1)$$

and

$$\Delta\bar{F}_1 = (RT/\beta)[\ln (1-v_2) + (1-1/x)v_2 + Kv_2^2/2] \quad (19)$$

$$= -(RTv_2/\beta)[1/x + (1-K)v_2/2 + v_2^2/3 + \cdots)], \quad (19.1)$$

where $K$ is re-defined as $2\beta BV_1/RT$. Equation (19.1) reduces to $\Delta\bar{F}_1 = -RTX_2$ at infinite dilution, as is required. Equation (12) for the partial molal entropy of the solute can be applied intact when $\beta > 1$, except that $x$ must be taken equal to the number of re-defined segments per chain. Consequently, Eq. (17) can be written

$$\Delta\bar{F}_2 = RT[\ln (1-v_1) - (x-1)v_1 + Kxv_1^2/2]. \quad (17.1)$$

## COMPARISONS WITH EXPERIMENTAL DATA

Osmotic pressures of dilute polymer solutions have been investigated quite extensively,[15-19] as a

[15] H. Staudinger and G. V. Schulz, Ber. **68**, 2320, 2336 (1935); G. V. Schulz, Zeits. f. physik. Chemie **A176**, 317 (1936).

means for determination of molecular weight. Strong deviation from Van't Hoff's law, i.e., from "ideality," are invariably observed at low concentrations, necessitating a frequently precarious extrapolation to infinite dilution. Experimental results for a number of dilute polymer solutions[15,16,19,20] support the simple relationship between osmotic pressure $\pi$ and concentration $c$ of polymer (in grams per cc)

$$\pi = RTc/\bar{M}_n + bc^2, \tag{20}$$

where $\bar{M}_n$ is the number average molecular weight of the polymer and $b$ is a constant, independent of $\bar{M}_n$,[15,19] representing the degree of departure from ideality.

For dilute solutions Eq. (19.1) yields

$$\pi = -\Delta\bar{F}_1/V_1 \cong RTv_2/V_1\beta x + RT(1-K)v_2^2/2V_1\beta$$

which reduces at once to (20);[21] overlooking the difference between volume and weight concentration in the second term

$$b \cong RT(1-K)/2V_1\beta. \tag{21}$$

Huggins[9,10] has reported a similar deduction of (20) for the case $K=0$, $\beta=1$.

When various solvents or solvent mixtures are considered, according to (21) the greater the heat of mixing the smaller will be the value of $b$ at a given temperature, since $K$ depends directly on the heat of mixing constant $B$. As $K$ approaches unity $b$ approaches zero, and the solution approaches classical "ideality." When $K$ becomes but slightly greater than unity, ($x$ large), the region of partial miscibility is reached and the polymer will no longer dissolve to an appreciable concentration (cf. *seq.*). Thus, a dilute high polymer solution should be most nearly "ideal" when it is approximately on the verge of precipitation. Osmotic pressure measurements on rubber dissolved in benzene-alcohol mixtures[22] and on solutions of polyvinyl chloride in tetrahydrofurane, a good solvent, and in dioxane, a poor solvent,[23] confirm this deduction.[24] However, to conclude, as Gee[22] has done, that a better extrapolation to infinite dilution is obtained in the presence of alcohol is not necessarily correct; higher terms in the series expansion of (19) must be included if the extrapolation is to be improved.

Although the statistical theory presented above predicts the correct form for the osmotic pressure-concentration relationship (20), quantitative correlation with the observed "deviation term" (i.e., $bc^2$) requires a larger value of $\beta$ than would be expected from steric considerations regarding chain flexibility. Thus, from osmotic pressure measurements on dilute solutions of rubber in toluene, Meyer, Wolff and Boissonnas found $V_1 b = 56$ cal. at 298°K. The heat of mixing, deduced from the temperature coefficient of the osmotic pressure, was negligibly positive.[25] Taking $K=0$, according to (21) $bV_1 = 300/\beta$, or $\beta \cong 5.3$, which corresponds to about seven isoprene units, or 28 chain atoms, per segment. A similar value for $bV_1$ was obtained by Wolff[17] for gutta-percha in toluene.

For the system toluene-polystyrene, according to osmotic pressure measurements by Schulz,[15] $bV_1 = 39$ cal. at ordinary temperature. Although reliable data concerning the heat of mixing do not appear to have been obtained,[26] certainly the heat effect accompanying mixing of two such chemically similar materials is negligible, and it may be assumed that $K=0$. A value of $\beta=8$ is

[16] K. H. Meyer, E. Wolff and Ch. G. Boissonnas, Helv. Chim. Acta **23**, 430 (1940).

[17] E. Wolff, Helv. Chim. Acta, **23**, 439 (1940).

[18] O. Hagger and A. J. A. Van der Wijk, Helv. Chim. Acta, **23**, 484 (1940).

[19] See also, H. Mark, *Physical Chemistry of High Polymeric Systems* (Interscience Publishers, Inc., New York, 1940), pp. 228-245.

[20] G. Gee, Trans. Faraday Soc. **36**, 1161 (1940).

[21] Actually, the partial molal volume $\bar{V}_1$ should be used in place of $V_1$, but since the difference between them is so small in dilute solutions (see ref. (16)) they need not be distinguished here.

[22] G. Gee, Trans. Faraday Soc. **36**, 1171 (1940).

[23] H. Staudinger and J. Schneiders, Ann. d. Chemie **541**, 151 (1939).

[24] R. E. Powell, C. R. Clark and H. Eyring, in a paper presented at the Conference on Viscosity sponsored by the New York Academy of Sciences, February 14, 1941, have reached the fantastic conclusion from Gee's results that a benzene-methanol mixture is a better solvent for rubber hydrocarbon than benzene alone. Apparently they have confused the literal meaning of the term "ideal" with its conventional meaning with reference to the so-called "ideal" solution laws. Addition of methanol to the benzene solution of rubber *decreases* $-\Delta\bar{F}_1$, the free energy of dilution, thus decreasing the thermodynamic solvent power. Since $-\Delta\bar{F}_1$ is greater for pure benzene solutions than $-\Delta\bar{F}_1$ for an "ideal" solution, addition of methanol decreases the discrepancy between observed and "ideal" values, but this is another matter.

[25] L. Hock and H. Schmidt, Kautschuk **10**, 33 (1934), have shown by direct calorimetric measurements that the heat of mixing of benzene and rubber is positive, but very small.

[26] See Ch. G. Boissonnas and K. H. Meyer, Zeits. f. physik. Chemie **B44**, 392 (1939).

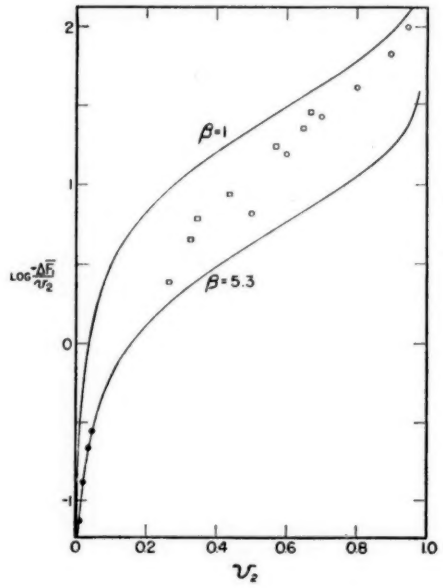


FIG. 1. Partial molal free energy as a function of the volume fraction of polymer for $\beta = 1$ and $\beta = 5.3$. ●—Osmotic pressure results for toluene-rubber, reference 16; ○—results from vapor pressures of toluene-rubber mixtures, reference 16; □—results from vapor pressures of benzene-rubber mixtures, reference 28.

required in order to bring the theoretically derived relationship into agreement with experiment; the corresponding segment contains about 16 chain atoms.

If rotation about each single bond in the chain were completely free, one or two single bonds should be sufficient to allow a new choice of direction of the chain independent of its preceding portions. Allowances for the limitations on the effective available configurations due to the potential restricting rotation about single carbon-carbon bonds and to the steric interferences of side chain substituents, presumably would raise the segment size somewhat. But it is difficult to account for segments of the size indicated by the above analysis on these grounds alone. Over-simplifications inherent in the model which has been postulated, and in particular assumption 4, probably are responsible for a considerable part of the discrepancy. The latter assumption allows too many configurations to be included, thus giving a configurational entropy which is too large.

The segment sizes calculated above are similar to those deduced from the temperature coefficients of polymer viscosities,[27] but the writer is not inclined to consider this as more than a coincidence. Vicsous flow is a kinetic phenomenon, whereas the thermodynamic properties of polymer solutions (taking the pure liquids as reference states) depend primarily upon configurational characteristics, according to the premises of this paper. Unless it can be shown that kinetic and configurational segments should be the same, correlation[7] of these independently estimated segment sizes is likely to be illusory.

In Fig. 1 partial molal free energies calculated from Eq. (19) are compared with experimental values for solutions of rubber in toluene (Meyer, Wolff and Boissonnas[16]) and in benzene (Stamberger[28]). The dilute solution data, which are from those discussed previously, were obtained osmotically. Data at higher concentrations ($v_2 > 0.20$) are based on vapor pressure measurements.[29] Stamberger[28] found no perceptible differences in the vapor pressure lowering for samples of rubber varying considerably in molecular weight. This is in agreement with Eq. (19) which predicts virtual independence of $\Delta \bar{F}_1$ on $x$ when $x$ is large and the solution is not too dilute.

The upper curve in the figure has been calculated from (19) taking $K = 0$, $\beta = 1$ and $x = 2900$, which corresponds to the average molecular weight, 270,000, obtained by Meyer and co-workers[16] from the limiting value of $\pi/c$. For the lower curve a value of $\beta = 5.3$ has been chosen in order to obtain agreement with experiment at low concentrations (see above). The value of $x$ has been lowered correspondingly to 550 in order to preserve consistency with the observed molecular weight. With increasing concentration the experimental points depart from the $\beta = 5.3$ curve, approaching the $\beta = 1$ curve at high concentrations. The comparison of observed and calculated values at high concentrations of polymer is shown more effectively in Table I by a tabulation of observed activities $a_1 = p_1/p_1^0$ and those calculated from (19) and the relationship $\ln a_1 = \Delta \bar{F}_1/RT$, taking $\beta = 1$.

[27] P. J. Flory, J. Am. Chem. Soc. **62**, 1057 (1940); W. Kauzman and H. Eyring, *ibid.* **62**, 3113 (1940).

[28] P. Stamberger, J. Chem. Soc. 2318 (1929).

[29] Concentrations for the experimental data actually are in weight fractions, although volume fractions are indicated. The difference is unimportant, however, since the densities of the two components are similar.

The measure of agreement in this range is all that should be expected considering the crudity of the original assumptions.

It would be possible, of course, to improve the agreement between theory and experiment by assuming an appropriate dependence of $\beta$ on $v_2$. However, this apparent variation of $\beta$ may reflect imperfections in the theory, rather than an actual variation in segment size with concentration.

## PHASE EQUILIBRIA

When there is a large heat effect accompanying the mixing of two liquids composed of molecules of ordinary size, the observed entropy of mixing usually deviates considerably from the ideal entropy given by (1), i.e., the solution is not "regular."[30] Due to differences in the energies of interaction between neighboring pairs of like and unlike molecules, distribution of the two species is not random, as is assumed in the derivation of (1). Furthermore, if $\Delta H<0$ the comparatively large solvent solute interactions in the solution are likely to lead to a higher degree of local orientation of neighboring pairs than is found in the pure components, thus decreasing the entropy of mixing; if $\Delta H>0$, the opposite is likely to be true.

Similarly, in the case of polymer solutions for which $\Delta H$ is large in magnitude the entropy of mixing should not be expected to agree with that calculated assuming random distribution of the two species, random configurations for the polymer molecules, and packing and local orientations equivalent to the pure liquid components.[18] "Deviations" should be expected to arise from the same sources discussed above for simple molecules. When $\Delta H>0$, moreover, compact configurations of the polymer chains should be preferred, thus decreasing the configurational entropy (cf. *seq.*).

In spite of these additional limitations imposed on the partial molal entropy and free energy Eqs. (18) and (19) when $\Delta H\gg 0$, it is of interest to examine the character of the phase-composition diagram which they predict when $\Delta H$ is sufficiently large to cause separation into two phases.

Equilibrium between two phases in a binary system requires that their compositions $v_2$ and $v'_2$ shall be such that

$$\Delta\bar{F}_1(v_2)=\Delta\bar{F}_1(v'_2),\quad \Delta\bar{F}_2(v_2)=\Delta\bar{F}_2(v'_2). \tag{22}$$

When $\Delta\bar{H}_1=0$, i.e., when $K=2\beta BV_1/RT=0$, $\Delta\bar{F}_1$ decreases continuously as $v_2$ increases from zero to unity. But when $K$ is sufficiently positive, according to (19) the curve for $\Delta\bar{F}_1$ will possess a maximum and a minimum in this range. Differentiating (19) with respect to $v_2$ and equating to zero

$$Kxv_2^2-(Kx-x+1)v_2+1=0,$$

the solution of which is

$$v_2=\frac{Kx-(x-1)\pm[(Kx-x+1)^2-4Kx]^{\frac{1}{2}}}{2Kx}. \tag{23}$$

The critical condition for incipient separation into two phases requires that the maximum and minimum in $\Delta\bar{F}_1$ coincide, i.e., that the two roots of (23) shall be equal. This occurs when[11]

$$K\text{ (critical)}=(1+\sqrt{x})^2/x. \tag{24}$$

Substituting (24) in (23)

$$v_2\text{ (critical)}=1/(1+\sqrt{x}). \tag{25}$$[11]

When $x$ is large the critical value of $K$ is slightly greater than unity, and it approaches unity as $x$ approaches infinity; at larger values of $K$ two phases will co-exist in equilibrium. The critical composition, at which the two phases become identical, according to (25), occurs at a low concentration when $x$ is large. The same relationships could have been derived by setting $\partial\Delta\bar{F}_2/\partial v_2$ equal to zero, since

$$\partial\Delta\bar{F}_2/\partial v_2=-\left(\frac{\beta x v_1}{v_2}\right)\partial\Delta\bar{F}_1/\partial v_2. \tag{26}$$

In Fig. 2, $-\beta\Delta\bar{F}_1/RT$ calculated from (19) when $x=1000$ is plotted against $v_2$ for several

TABLE I.

| $v_2$ | $a_1$ (obs.)[16] | $a_1$ (calc.) |
|---|---|---|
| 0.95 | 0.20 | 0.13 |
| 0.90 | 0.36 | 0.25 |
| 0.80 | 0.57 | 0.45 |
| 0.70 | 0.73 | 0.60 |
| 0.60 | 0.86 | 0.73 |

[30] J. H. Hildebrand, *Solubility of Non-Electrolytes* (Chemical Catalog Company, New York, 1936), second edition, p. 65.

values of $K$ in the neighborhood of $K$ (critical) $=1.0644$. Two scales have been used in order to cover in a single graph a broader concentration range. The character of the curves changes very rapidly with $K$. Since $K$ depends inversely on the absolute temperature, these curves may be regarded as representative of a series of temperatures in the vicinity of the critical temperature for total miscibility. The corresponding curves for $-\Delta\bar{F}_2/RT$ show related characteristics, as is required by (26); the occurrence of a maximum in $\Delta\bar{F}_1$ is accompanied by a minimum in $\Delta\bar{F}_2$, and vice versa.

When $K$ exceeds the critical value, there exists a pair of values $v_2$ and $v'_2$ which satisfies the equilibrium conditions (22). The smaller of these ($v_2$) will lie between zero and the maximum in $-\Delta\bar{F}_1$ plotted against $v_2$, as in Fig. 2; the larger ($v'_2$) will lie at a concentration greater than that at the minimum in $-\Delta\bar{F}_1$. The value of $\Delta\bar{F}_1(v_2) = \Delta\bar{F}_1(v'_2)$ must necessarily be small, since $\Delta\bar{F}_1$ at the maximum in the curve is small. In fact, except when $K$ is very near $K$(critical), it is permissible to set $\Delta\bar{F}_1(v'_2)=0$ and to compute $v'_2$ from $K$ using Eq. (19); $-\partial\Delta\bar{F}_1/\partial v_2$ is so large at $v'_2$ that the error so introduced is insignificant.

Since (19) can be solved explicitly for $K$ but not for $v'_2$, it is more convenient, having set $\Delta\bar{F}_1=0$ to compute $K$ for a given value of $v'_2$. That is, we may take

$$K=-2[\ln(1-v'_2)+(1-1/x)v'_2]/(v'_2)^2. \quad (27)$$

Substituting (17.1) in the second part of (22)

$$(\ln v_2)/x-(1-1/x)(1-v_2)+K(1-v_2)^2/2 = (\ln v'_2)/x-(1-1/x)(1-v'_2) +K(1-v'_2)^2/2, \quad (28)$$

which can be solved by trial for $v_2$ using the above values of $v'_2$ and $K$. If necessary, a second approximation can be computed by substituting the first approximation values of $K$ and $v_2$ into (19) to obtain $\Delta\bar{F}_1$, which in combination with $v'_2$ will yield a second approximation value for $K$. The second approximation value of $v_2$ can then be obtained from (28).

In the range where this procedure is applicable $v_2$ is quite small (assuming a large value of $x$). Replacing $(1-v_2)$ and $(1-v_2)^2$ by unity in (28), substitution therein of (27) for $K$, and expansion

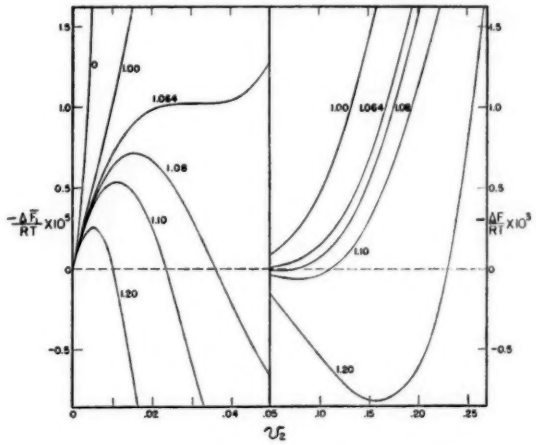


FIG. 2. Partial molal free energies as functions of the volume fraction of polymer for various values of $K$ in the critical region for partial miscibility.

in series gives as an approximate relationship between $v_2$ and $v'_2$

$$(1/x)\ln(v'_2/v_2)=2/x+(v'_2)^2/2\cdot3 +(v'_2)^3\cdot2/3\cdot4+(v'_2)^4\cdot3/4\cdot5+\cdots. \quad (29)$$

These procedures are unsatisfactory very near the critical point, e.g., for $K<1.10$ when $x=1000$. Here it is necessary to solve for $K$ and $v_2$ by trial.

The curve in Fig. 3, showing $v_2$ and $v'_2$ as a function of $1/K$ when $x=1000$, has been calculated as described above. Since the ordinate is proportional to the absolute temperature, the curve represents the calculated temperature-composition diagram. The concentration ($v_2$) of polymer in the solvent phase rapidly approaches a negligible value as $1/K$ decreases. This is amplified by the following calculated compositions which extend beyond the range of Fig. 3. See Table II.

Thus, the theory predicts an extremely unsymmetrical phase composition relationship. The solvent is readily soluble in the polymer even at large values of $K$ (e.g., far below the critical temperature for complete miscibility), but the polymer will dissolve perceptibly in the solvent only very near the critical point, and then only to a small extent.[11]

These deductions are confirmed by the work of Brönsted and Volqvartz[31] on mixtures of various lauric acid esters with high molecular weight

[31] J. N. Brönsted and K. Volqvartz, Trans. Faraday Soc. **35**, 576 (1939); *ibid.* **36**, 619 (1940).

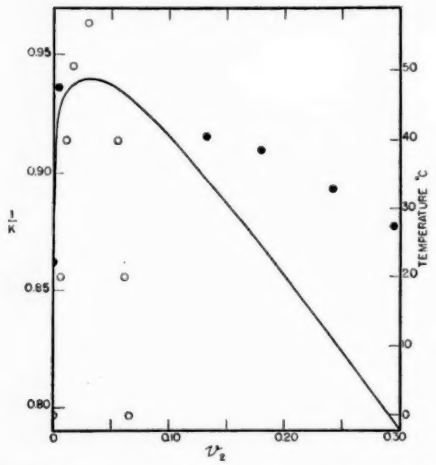


FIG. 3. Phase composition curve calculated for a solution of a polymer composed of 1000 segments. ●—*n*-propyl laurate-polystyrene, reference 31; ○—chloroform-cellulose acetate, reference 32.

(average ca. 300,000) polystyrene, which had been fractionated to remove low molecular weight constituents. Below the critical temperature for complete miscibility, none of these were observed to dissolve the polymer to an appreciable extent, although the polymer imbibed as much as several times its volume of solvent. Brönsted and Volqvartz concluded that their results were "compatible with the existence of a critical point at which the solubility of solvent in the swelled phase is infinite." Their results are also consistent with a critical value of $v_2$ slightly greater than zero, which would be in accord with theoretical predictions.

Brönsted and Volqvartz's data for the *n*-propyl laurate-polystyrene system are shown in Fig. 3. The temperature scale, shown on the right, has been related to $1/K$ by an arbitrary proportionality factor (340) so that the absolute temperature is proportional to $1/K$, as the definition of $K$ requires. Results of Papkov, Rogovin, and Kargin[32] on the chloroform-cellulose acetate (average molecular weight about 175,000)[33] system are also shown using the same temperature scale.

Quantitative agreement between theory and experiment cannot be expected in view of the various approximations which have been introduced. But the ability of the theory to predict the two outstanding characteristics of such binary systems, namely, a very low critical composition, and a high swelling capacity accompanied by negligible solubility, is a most gratifying confirmation of the validity of Meyer's model and the statistical treatment of it which has been presented here. Many of the so-called gels composed of polymers saturated with solvent doubtless owe their existence merely to this peculiarity of the temperature-composition curve, rather than to any peculiar colloidal structure, as generally has been assumed.

[32] S. Papkov, S. Rogovin, and V. Kargin, Acta Physicochim. U.R.S.S. **8**, 647 (1938).

[33] This estimated molecular weight is based on a specific viscosity given by the above authors, and the intrinsic viscosity-molecular weight data of E. O. Kraemer, Ind. Eng. Chem. **30**, 1200 (1938).

## MOLECULAR CONFIGURATION IN POOR SOLVENTS

Staudinger and Heuer[34] observed that the relative viscosity of a dilute solution of polystyrene was less in a poor solvent than in a good one at the same concentration. They also found that the addition of a precipitant, e.g., ethanol, to a solution of polystyrene in a solvent such as toluene reduced the relative viscosity continuously to the point of precipitation. Staudinger and Schneiders[23] found lower viscosities for solutions of polyvinyl chloride in dioxane than in tetrahydrofurane, which their osmotic pressure results showed to be a better solvent. Similar results were obtained by Gee[22] on solutions of rubber in various solvents and solvent mixtures.

The diminution of viscosities in poor solvents frequently has been attributed to decreased solvation. If by "solvation" some specific interaction between solute and solvent is meant, it is difficult to conceive of solvation in a toluene solution of polystyrene, where the van der Waals forces between like and unlike components are both similar and small. Furthermore, if solvation does occur, how can it be so markedly decreased

TABLE II.

| $1/K$ | $v_2$ | $v'_2$ |
|---|---|---|
| 0.862 | $1.4\times10^{-5}$ | 0.1915 |
| 0.833 | $1.7\times10^{-7}$ | 0.2357 |
| 0.770 | $1.3\times10^{-13}$ | 0.3300 |
| 0.715 | $1\times10^{-21}$ | 0.407 |
| 0.625 | $5\times10^{-42}$ | 0.527 |
| 0.500 | $3\times10^{-95}$ | 0.683 |

[34] H. Staudinger and W. Heuer, Zeits. f. physik. Chemie **A171**, 129 (1934).

by the addition of a few cc of alcohol which has no particular affinity for either component?

When the heat of mixing of polymer and solvent is positive, i.e., in a poor solvent medium, the polymer molecules should tend to prefer more compact configurations where intramolecular contacts are more numerous. As is well known, globular or spherical polymer molecules enhance the viscosity of their solutions relatively little in contrast to the marked effects of uncoiled long polymer chains which assume more or less random configurations. Therefore, the low relative viscosities in poor solvents very probably reflect changes in average configuration of the polymer molecules, dependent upon the solvent medium. Intrinsic viscosities at incipient precipitation are of the order of one-half or less of the values for the same polymers in a good solvent medium.[22] This would lead to the conclusion that the polymer molecule at the critical point pervades about the same volume as another molecule of half its chain length in a good solvent.

## CONCLUSIONS

Quantitative statistical treatment of Meyer's model accounts for the following hitherto unexplained peculiar properties of high polymer solutions: (a) the shape of the partial molal free energy-composition diagram throughout the composition range (i.e., the large deviation from "ideal" entropies), (b) the virtual independence of partial pressure on molecular weight of the polymer except in dilute solutions, and (c) the extreme dissymmetry of the mutual solubility-temperature diagram and the limited high swelling capacity of linear polymers in certain media. These achievements confirm the correctness of the general point of view regarding these systems. On the other hand, quantitative agreement between calculations and observations is not particularly good, presumably due to imperfections of the model itself and to limitations of the present treatment imposed by assumption 4.

---

JANUARY, 1942 JOURNAL OF CHEMICAL PHYSICS VOLUME 10

# Statistical Mechanics of Nearest Neighbor Systems

## II. General Theory and Application to Two-Dimensional Ferromagnets

ELLIOTT W. MONTROLL*
*Sterling Chemistry Laboratory, Yale University, New Haven, Connecticut*
(Received October 2, 1941)

This is a continuation of an effort to reduce to the solution of a characteristic value problem the rigorous calculation of thermodynamic properties of systems in which the intermolecular forces are sufficiently short ranged so that practically the entire potential energy of the system results from interactions between nearest neighbors. The partition function of such a system can be expressed in terms of the largest characteristic value of a linear operator equation and finally as the ratio of partition functions of systems with relatively few particles whose potential energy functions differ somewhat from those in the original system. A method of evaluating grand partition functions and one of introducing interactions between more distant neighbors are discussed. The general theory is applied to the calculation of magnetization, internal energy, and specific heat of two-dimensional ferromagnets on the basis of the Ising model. There seems to exist a λ-point phase transition in the change from ferromagnetic to nonferromagnetic states.

## I. INTRODUCTION

THE intermolecular forces in many solids are sufficiently short ranged to permit the total potential energy of the solid to be represented by the sum of the interactions of each molecule with its nearest neighbors. With this approximation the evaluation of the potential energy contribution to the partition function and the thermodynamic properties of a solid can

* Sterling Research Fellow in Chemistry, Yale University. Present address, Cornell University, Ithaca, New York.

be reduced to the solution of a characteristic value problem.[1,2] Inasmuch as such problems have been much studied while the summation of highly multiple sums has been a rather neglected subject, the reduction is an advantageous one.

Suppose a system can be divided into $L\times M\times N$ cells so that there will be $L$ layers, each composed of $N\times M$ cells and each layer will have the same average behavior as any other layer. The molecules in each cell may have several or even a continuum of possible configurations. Since the same is true of each layer, let us define a set $\{\alpha_i\}$ of all those configurations available to a physical coordinate $\alpha$ of a layer. For example, in a binary substitutional alloy $\alpha_i$ might represent an $i$th arrangement of the two kinds of atoms in a layer.

If $v(\alpha_m)$ is the total potential energy with respect to a coordinate $\alpha$ between all neighboring cells of a layer in the $m$th configuration, and if $v(\alpha_m, \alpha_n)$ is the total potential of interaction between cells of one layer in the $m$th configuration with their nearest neighbors in the $n$th configuration, the potential energy factor of the partition function with respect to the coordinate $\alpha$ is[3]

$$Z=\sum_{\{\alpha_1\}}\cdots\sum_{\{\alpha_L\}}\exp-\theta[v(\alpha_1)+\cdots+v(\alpha_L)+v(\alpha_1,\alpha_2)+\cdots+v(\alpha_{L-1},\alpha_L)] \quad (1)$$

Making the substitutions

$$V(\alpha_i,\alpha_j)=v(\alpha_i)/2+v(\alpha_i,\alpha_j)+v(\alpha_j)/2);\qquad \theta=1/kT \quad (2)$$

(1) becomes

$$Z=\sum_{\{\alpha_1\}}\cdots\sum_{\{\alpha_L\}}\prod_{i=1}^{L-1}\exp-\theta V(\alpha_i,\alpha_{i+1}). \quad (3)$$

If $\{\psi_n\}$ is the set of orthonormal characteristic vectors and $\{\lambda_n\}$ the corresponding set of characteristic values of the matrix equation

$$\lambda\psi=\mathbf{exp}\,[\,-\theta\mathbf{V}]\cdot\psi \quad (4)$$

$$\lambda\begin{bmatrix}\psi(\alpha_1)\\ \psi(\alpha_2)\\ \cdot\\ \cdot\end{bmatrix}=\begin{bmatrix}\exp-\theta V(\alpha_1,\alpha_1) & \exp-\theta V(\alpha_1,\alpha_2) & \cdots\\ \exp-\theta V(\alpha_2,\alpha_1) & \exp-\theta V(\alpha_2,\alpha_2) & \cdots\\ \cdot & \cdot & \cdots\\ \cdot & \cdot & \cdots\end{bmatrix}\begin{bmatrix}\psi(\alpha_1)\\ \psi(\alpha_2)\\ \cdot\\ \cdot\end{bmatrix}$$

(when the $\mathbf{exp}\,-\theta\mathbf{V}$ matrix is symmetrical), by expanding $\exp-\theta V(\alpha_i,\alpha_j)$ as a bilinear combination of $\{\psi_n\}$ it can be shown that[1]

$$Z=\lambda_{\max}^{L-1}\Big[\sum_{\{\alpha_1\}}\psi_{\max}(\alpha_1)\Big]^2 \quad (5)$$

where $\lambda_{\max}$ is the largest characteristic value of (4).

## II. PARTITION FUNCTION BY METHOD OF SUCCESSIVE APPROXIMATIONS

The secular equation of the matrix in (4) corresponding to a real crystal is of too great an order to be solved directly, so it seems necessary to seek a somewhat indirect method of solution that will lead to correct results. In studying long, narrow (three and four atoms wide), two-dimensional ferromagnetic strips[1] it was found that the method of successive approximations leads to asymptotic expressions for $\lambda_{\max}$ which show excellent agreement with the exact values as calculated numerically. This suggests that the same approach might give good results when applied to real crystals.

In the method of successive approximations one first guesses a reasonable vector $\psi_0$ and calculates

$$\psi_1{}^u=(\mathbf{exp}\;\;-\mathbf{V}\theta)\cdot\psi_0,$$

i.e.,

$$\psi_1{}^u(\alpha_1)=\sum_{\alpha_2}\psi_0(\alpha_2)\exp-\theta V(\alpha_1,\alpha_2).$$

Then some value of $\alpha_1$, say $\alpha_1=0$, is chosen and one sets[4]

$$\psi_1(0)=\psi_0(0)=1,$$

$$\psi_1(\alpha_1)=\psi_1{}^u(\alpha_1)/\psi_1{}^u(0)=\sum_{\alpha_2}\psi_0(\alpha_2)\exp-\theta V(\alpha_1,\alpha_2)/\sum_{\alpha_2}\psi_0(\alpha_2)\exp-\theta V(0,\alpha_2).$$

[1] E. Montroll, J. Chem. Phys. **9**, 706 (1941). Henceforth this paper will be referred to as SM-I.

[2] H. Kramers and G. Wannier, Phys. Rev. **60**, 252 and 263 (1941). These papers will be designated by KW-I and KW-II.

[3] Note the implicit assumption of independence of the various kinds of coordinates. For example, in a ferromagnetic system this would be equivalent to the assumption that spin orientations are independent of lattice vibrations.

[4] The superscript $u$ is used to imply that $\psi_1{}^u(0)$ has not yet been normalized to unity. For a detailed mathematical discussion of the method of successive approximations see Frazier, Duncan, and Collar, *Elementary Matrices* (Cambridge University Press, 1938), p. 140.

$\psi_1(\alpha_1)$ is the second approximation of $\psi(\alpha_1)$, and to find the $(i+1)$st approximation one proceeds according to the general scheme

$$\psi_i{}^u(\alpha_1)=\sum_{\alpha_2}\psi_{i-1}(\alpha_2)\exp -\theta V(\alpha_1,\alpha_2),$$
$$\psi_i(\alpha_1)=\psi_i{}^u(\alpha_1)/\psi_i{}^u(0). \tag{6}$$

The corresponding characteristic value is

$$\lambda_i=\sum_{\alpha_1,\,\alpha_2}\psi_i(\alpha_1)\psi_i(\alpha_2)\exp -\theta V(\alpha_1,\alpha_2)/\sum_{\alpha_1,\,\alpha_2}\psi_i(\alpha_1)\psi_i(\alpha_2). \tag{7}$$

Using this procedure we shall now develop a power series in $\theta$ for $\lambda_{\max}$ and $\psi_{\max}(\alpha)$ of a real crystal. Since this development is the appropriate one for high temperatures, the logical first approximation $\psi_0$ of $\psi$ should be that which corresponds to a system in a state of complete disorder; that is, all configurations of a given layer should be chosen as being equally probable. Such a $\psi$ (unnormalized) is

$$\psi_0=(1,\,1,\,1,\,\cdots,\,1),$$
i.e., $$\psi_0(\alpha)=1 \text{ for all } \alpha.$$

Then if there are $\nu$ possible configurations per lattice point and $\nu^{MN}$ per layer

$$\psi_1{}^u(\alpha_1)=\sum_{\{\alpha_2\}}1\cdot[1-\theta V(\alpha_1,\alpha_2)+\theta^2V^2(\alpha_1,\alpha_2)/2-\cdots]$$
$$=\nu^{MN}-\theta\sum_{\{\alpha_2\}}V(\alpha_1,\alpha_2)+\theta^2\sum_{\{\alpha_2\}}V^2(\alpha_1,\alpha_2)/2-\cdots$$

and

$$\psi_1(\alpha_1)=\psi_1{}^u(\alpha_1)/\psi_1{}^u(0)$$
$$=1-\theta\nu^{-MN}\sum_{\{\alpha_2\}}[V(\alpha_1,\alpha_2)-V(0,\alpha_2)]+\theta^2\nu^{-MN}\sum_{\{\alpha_2\}}\{[V^2(\alpha_1,\alpha_2)-V^2(0,\alpha_2)]/2$$
$$-V(0,\alpha_3)[V(\alpha_1,\alpha_2)-V(0,\alpha_2)]\}+\cdots.$$

Note that

$$\psi_1(\alpha_1)-\psi_0(\alpha_1)=0(\theta).$$

Now

$$\psi_2(\alpha_1)=\psi_2{}^u(\alpha_1)/\psi_2{}^u(0)=\frac{\sum\psi_1(\alpha_2)\{1-\theta V(\alpha_1,\alpha_2)+\theta^2V^2(\alpha_1,\alpha_2)/2-\cdots\}}{\sum\psi_1(\alpha_2)\{1-\theta V(0,\alpha_2)+\theta^2V^2(0,\alpha_2)/2-\cdots\}}.$$

So

$$\psi(\alpha_1)\sim\psi_2(\alpha_1)=1-\theta\nu^{-MN}\sum_{\{\alpha_2\}}[V(\alpha_1,\alpha_2)-V(0,\alpha_2)]+\theta^2\nu^{-MN}\{\sum_{\{\alpha_2\}}[V^2(\alpha_1,\alpha_2)-V^2(0,\alpha_2)]/2$$
$$+\nu^{-2MN}\sum_{\{\alpha_2,\,\alpha_3,\,\alpha_4\}}[V(\alpha_1,\alpha_2)-V(0,\alpha_2)][V(\alpha_2,\alpha_3)-V(0,\alpha_3)-V(\alpha_3,\alpha_4)]\}-\cdots. \tag{8}$$

Here we see that

$$\psi_2(\alpha_1)-\psi_1(\alpha_1)=0(\theta^2).$$

The coefficients of higher powers of $\theta$ are rather long expressions so we will not record them here. However, by continuing the process started above one can show, using the same sort of reasoning as that used in the appendix, that

$$\psi_l(\alpha)-\psi_{l-1}(\alpha)=0(\theta^l). \tag{9}$$

Since by definition

$$\psi_l{}^u(\alpha_1)=\sum_{\alpha_2}\psi_{l-1}(\alpha_2)\exp -\theta V(\alpha_1,\alpha_2)$$
$$=\psi_l{}^u(0)\psi_l{}^u(\alpha_1)/\psi_l{}^u(0)=\psi_l(\alpha_1)\psi_l{}^u(0)$$

and $\psi_l(\alpha)$ is equal to $\psi_{l-1}(\alpha)$ to within terms of order $\theta^l$, $\psi_l{}^u(0)$ is equal to $\lambda_{l-1}$ (the $l$th approximation to $\lambda_{\max}$) to within terms of order $\theta^l$. Thus

$$\lambda_0=\nu^{MN},$$
$$\lambda_1=\nu^{MN}-\nu^{-MN}\theta\sum_{\{\alpha_1,\,\alpha_2\}}V(\alpha_1,\alpha_2),$$

$$\lambda_{\max}\sim\lambda_2=\nu^{MN}-\nu^{-MN}\theta\sum_{\{\alpha_1,\,\alpha_2\}}V(\alpha_1,\,\alpha_2)+\theta^2\nu^{-MN}\{\sum_{\{\alpha_1,\,\alpha_2\}}V^2(\alpha_1,\,\alpha_2)/2$$
$$+\nu^{-MN}\sum_{\{\alpha_1,\,\alpha_2,\,\alpha_3\}}\cdots\sum V(\alpha_1,\,\alpha_2)\,V(\alpha_2,\,\alpha_3)-\nu^{-2MN}[\sum_{\{\alpha_1,\,\alpha_2\}}V(\alpha_1,\,\alpha_2)]^2\}. \quad (10)$$

At this point let us search for a physical interpretation of the iteration process described above. If the successive approximations are made without bothering to expand in a power series in $\theta$,

$$\psi_0(\alpha)=1 \text{ for all } \alpha.$$

Then

$$\psi_1(\alpha_1)=\sum_{\alpha_2}\exp-\theta V(\alpha_1,\,\alpha_2)/\sum_{\alpha_2}\exp-\theta V(0,\,\alpha_2),$$

$$\psi_2(\alpha_1)=\sum_{\alpha_2}\psi_1(\alpha_2)\exp-\theta V(\alpha_1,\,\alpha_2)/\sum_{\alpha_2}\psi_1(\alpha_2)\exp-\theta V(0,\,\alpha_2)$$
$$=\sum_{\alpha_2,\,\alpha_3}\exp-\theta[V(\alpha_1,\,\alpha_2)+V(\alpha_2,\,\alpha_3)]/\sum_{\alpha_2,\,\alpha_3}\exp-\theta[V(0,\,\alpha_2)+V(\alpha_2,\,\alpha_3)].$$

In general

$$\psi_l(\alpha_1)=\frac{\sum\cdots\sum\exp-\theta[V(\alpha_1,\,\alpha_2)+V(\alpha_2,\,\alpha_3)+\cdots+V(\alpha_l,\,\alpha_{l+1})]}{\sum\cdots\sum\exp-\theta[V(\alpha_1,\,\alpha_2)+V(\alpha_2,\,\alpha_3)+\cdots+V(\alpha_{l-1},\,\alpha_l)]}, \quad (11)$$

$$\psi_{\max}(\alpha)-\psi_l(\alpha)=0(\theta^{l+1}). \quad (12)$$

The characteristic value corresponding to $\psi_l(\alpha)$ is

$$\lambda_l=\psi_l^*(\exp\ -\theta V)\psi_l/\psi_l^*\cdot\psi_l$$
$$=\frac{\sum\cdots\sum\exp-\theta[V(\alpha_1,\,\alpha_2)+\cdots+V(\alpha_{2l},\,\alpha_{2l+1})]}{\sum\cdots\sum\exp-\theta[V(\alpha_1,\,\alpha_2)+\cdots+V(\alpha_{2l-1},\,\alpha_{2l})]}=\frac{S_{2l+1}}{S_{2l}},$$

but in the appendix it is shown that

$$S_{2l+1}/S_{2l}=S_{l+1}/S_l+0(\theta^{l+1}).$$

Therefore, remembering the remarks made following Eq. (9),

$$\lambda_{\max}=S_{l+1}/S_l+0(\theta^{l+1}). \quad (13)$$

Now

$$S_l=\sum_{\alpha_1}\cdots\sum_{\alpha_l}\exp-\theta[V(\alpha_1,\,\alpha_2)+\cdots+V(\alpha_{l-1},\,\alpha_l)] \quad (14)$$

is the partition function of a system $l$ layers thick in which the interaction between lattice points in the first (and in the $l$th) layer is one-half that between those of other layers of the system. Thus as $L\to\infty$, the $(L-1)$st root of $Z$ (see Eq. (5)), the partition function of a system $L$ layers thick, is equal, to within terms of $0[(1/kT)]^{l+1}$, to the partition function of a system of $(l+1)$ layers divided by that of a system of $l$ layers:

$$Z^{1/(L-1)}=S_{l+1}/S_l+0(\theta^{l+1}). \quad (15)$$

Since $S_l$ is the partition function of a system $l\times M\times N$,

$$S_l=[\mu(l)_{\max}]^{M+1}[\textstyle\sum_\beta\varphi(l,\,\beta)_{\max}]^2, \quad (16)$$

where $\mu(l)_{\max}$ is the largest characteristic value of

$$\mu(l)\varphi(l,\,\beta_1)=\sum_{\beta_2}\varphi(l,\,\beta_2)\exp-W_l(\beta_1,\,\beta_2)\theta \quad (17a)$$

with

$$W_l(\beta_1,\,\beta_2)=w_l(\beta_1)/2+w_l(\beta_1,\,\beta_2)+w_l(\beta_2)/2, \quad (17b)$$

$w_l(\beta_i)$ = potential energy of interaction between neighboring elements in the $i$th $l\times N$ layer in configuration $\beta_i$,

and

$w_l(\beta_i, \beta_j)$ = potential energy of interaction between elements in the $i$th $l\times N$ layer in configuration $\beta_i$, and their nearest neighbors in the $j$th layer in configuration $\beta_j$.

In the energy term $W_l(\beta_i, \beta_j)$ the interaction between the $N$ elements in the first row of the $i$th layer and their nearest neighbors in the first row of the $j$th layer (likewise for interactions between $l$th rows of the two layers) is reduced by half.

If we let

$$T_{m,l}=\sum_{\beta_1}\cdots\sum_{\beta_m}\exp -\theta[W_l(\beta_1,\beta_2)+\cdots+W_l(\beta_{m-1},\beta_m)]=T_{l,m}, \tag{18a}$$

by the same arguments as those used in the derivation of (13):

$$\mu(l)_{\max}=T_{m+1,l}/T_{m,l}+0(\theta^{m+1}) \tag{18b}$$

and

$$\begin{aligned} Z^{1/(L-1)(M-1)}&=\frac{T_{l+1,l+1}/T_{l,l+1}+0(\theta^{l+1})}{T_{l+1,l}/T_{l,l}+0(\theta^{l+1})}\\ &=T_{l+1,l+1}/T_{l,l}+0(\theta^{l+1}). \end{aligned} \tag{19}$$

Now $T_{l,l}$ is exactly the partition function of a system of $l\times l\times N$ lattice points in which the potential energy of interaction between all pairs of lattice points is the same as that between pairs in the original system, except: (1) for pairs both of whose components lie on one of the four faces of width $l$ and length $N$—the interaction between such pairs in one-half that between normal pairs; (2) for pairs both of whose components lie on one of the four edges (formed by the intersection of two of the $l\times N$ planes) of length $N$—the interaction between such pairs is one-fourth that between normal pairs. This means that the $l\times l\times N$ system can be "compressed" in the $N$ direction by the characteristic value method, and if $\omega(l, l)_{\max}$ is the largest characteristic value of the operator equation

$$\omega(l,l)\chi(l,l;\gamma_1)=\sum_{\gamma_2}\chi(l,l;\gamma_2)\exp -\theta X_{l,l}(\gamma_1,\gamma_2), \tag{20}$$

$$T_{l,l}=[\omega(l,l)_{\max}]^{N-1}[\textstyle\sum_\gamma \chi(l,l;\gamma)_{\max}]^2. \tag{21}$$

Neglecting 1 as compared with $L$, $M$, $N$

$$Z^{1/LMN}=\omega(l+1,l+1)_{\max}/\omega(l,l)_{\max}+0(\theta^{l+1}). \tag{22}$$

In Eq. (20)

$$X_{l,l}(\gamma_1,\gamma_2)=x_{l,l}(\gamma_1)/2+x_{l,l}(\gamma_1,\gamma_2)+x_{l,l}(\gamma_2)/2.$$

$x_{l,l}(\gamma_i)$ = total potential energy of interaction between elements in the first layer while it is in configuration $\gamma_i$. The interaction between pairs of elements on the border of the $l\times l$ square is only one-half that between other pairs of elements.

$x_{l,l}(\gamma_1, \gamma_2)$ = total potential energy of interaction between elements in the first layer in configuration $\gamma_1$ and their nearest neighbors in the second in configuration $\gamma_2$. The interaction between the four elements on the corners of the $l\times l$ square in layer 1 and their nearest neighbors on the corners of layer 2 in one-fourth that between pairs of internal neighbors. The interaction between elements on the $l\times 2$ faces is one-half that between pairs of internal elements.

Thus we have shown that in order to calculate the partition function correct to terms of order $(1/kT)^l$ of a system of $L\times M\times N$ cells (as $L, M, N\to\infty$) it is sufficient to find the largest characteristic value of an operator equation whose kernel involves the potential energy of a system of $l\times l\times 2$ cells.

The low temperature calculation of $\lambda_{max}$ can also be effected by the use of the method of successive approximations. Suppose there are two possible ordered configurations for a given layer[5] and that these are represented by $0_1$ and $0_2$. As a first approximation to $\psi$ we choose a vector which defines a completely ordered state:

$$\psi_0(0_2)=\psi_0(0_1)=1;\quad \psi_0(\alpha)=0 \text{ if } 0_1\neq\alpha\neq 0_2;\quad \psi_1{}^{u}(\alpha_1)=\exp\left[-\theta V(0_1,\alpha_1)\right]+\exp\left[-\theta V(0_2,\alpha_1)\right].$$

Here we shall keep

$$\psi_0(0_1)=\psi_1(0_1)=\cdots=1.$$

Then

$$\psi_1(\alpha_1)=\frac{\exp\left[-\theta V(0_1,\alpha_1)\right]+\exp\left[-\theta V(0_2,\alpha_1)\right]}{\exp\left[-\theta V(0_1,0_1)\right]+\exp\left[-\theta V(0_1,0_2)\right]},$$

$$\psi_2(\alpha_1)=\frac{\sum\limits_{\alpha_2}\left[\exp-\theta V(\alpha_2,0_1)+\exp-\theta V(\alpha_2,0_2)\right]\left[\exp-\theta V(\alpha_1,\alpha_2)\right]}{\sum\limits_{\alpha_2}\left[\exp-\theta V(\alpha_2,0_1)+\exp-\theta V(\alpha_2,0_2)\right]\left[\exp-\theta V(0_1,\alpha_2)\right]}.$$

By continuing the approximation process we finally obtain

$$\psi_n(\alpha_1)=\frac{\sum\cdots\sum\left\{\exp-\theta V(\alpha_n,0_1)+\exp-\theta V(\alpha_n,0_2)\right\}\left\{\exp-\theta\left[V(\alpha_1,\alpha_2)+\cdots+V(\alpha_{n-1},\alpha_n)\right]\right\}}{\sum\cdots\sum\left\{\exp-\theta V(\alpha_n,0_1)+\exp-\theta V(\alpha_n,0_2)\right\}\left\{\exp-\theta\left[V(0_1,\alpha_2)+\cdots+V(\alpha_{n-1},\alpha_n)\right]\right\}} \tag{23a}$$

and

$$\lambda_n=\sum_{\alpha_1,\alpha_2}\psi_n(\alpha_1)\psi_n(\alpha_2)\exp-\theta V(\alpha_1,\alpha_2)\Big/\sum_{\alpha_1,\alpha_2}\psi_n(\alpha_1)\psi_n(\alpha_2). \tag{23b}$$

It is apparent from Eqs. (23a) and (23b) that the low temperature expression for $\lambda_{max}$ is the quotien t of the partition functions of two smaller systems. Proceeding in a manner analogous to that used for the high temperature expressions, one can finally evaluate $Z$ as the ratio of characteristic values of operator equations whose kernels are functions of the potential energy between two small layers of lattice points. The details of this calculation will not be carried out here, but they will be apparent from the discussion of the special case of two-dimensional ferromagnetism at the end of this paper.

### III. GRAND PARTITION FUNCTION AND THE CHARACTERISTIC VALUE METHOD

In systems of more than one component it is usually necessary or at least it is usually more convenient to use the grand partition function for the calculation of thermodynamic quantities. So, we shall now investigate the applicability of the characteristic value method to the evaluation of grand partition functions.

The grand partition function[6] of a $k$ component system is defined as the sum

$$P=\sum_{n_1,}\sum_{n_2,\cdots,}\cdots\sum_{n_k,\,m}\exp\left(\mu_1 n_1+\mu_2 n_2+\cdots\mu_k n_k-E_m\right)\theta \tag{24}$$

over-all compositions $n_1, n_2, \cdots, n_k$ and over-all energy states $E_m$. The terms $\mu_i$ are the chemical potentials of the various components and are so chosen that

$$N_i=\frac{1}{P}\sum_{i=1,2,\cdots,k}\cdots\sum n_i\exp\theta(\mu_1 n_1+\cdots+\mu_k n_k-E_m), \tag{25}$$

equals the number of particles of the $i$th component of the system.

[5] This would be the case if each lattice point could achieve either of two configurations. The method can without difficulty be extended to the case of more than two ordered configurations per layer.

[6] For discussions of grand partition functions and their uses cf. Tolman, *Principles of Statistical Mechanics* (Oxford University Press, 1938), p. 619; Gibbs, *Collected Works* (Longmans, Green and Company, 1931), p. 187.

In a nearest neighbor system of the type discussed in Part I, retaining the notation introduced there,

$$P=\sum_{\alpha_1}\cdots\sum_{\alpha_L}\exp\theta[\mu_1 n_1(\alpha_1)+\cdots+\mu_k n_k(\alpha_1)-v(\alpha_1)+\mu_1 n_1(\alpha_2)+\cdots+\mu_k n_k(\alpha_2)-v(\alpha_2)$$
$$\cdots\cdots\cdots\cdots\cdots\cdots\cdots\cdots$$
$$+\mu_1 n_1(\alpha_L)+\cdots+\mu_k n_k(\alpha_L)-v(\alpha_L)-v(\alpha_1,\alpha_2)-v(\alpha_2,\alpha_3)-\cdots-v(\alpha_{L-1},\alpha_L)]$$

with $n_i(\alpha_j)$ being defined as the number of particles of kind $i$ in the $j$th layer when it is in configuration $\alpha_j$.

If we make the substitution

$$V(\alpha_i,\alpha_j)=-[\mu_1 n_1(\alpha_i)+\cdots+\mu_k n_k(\alpha_i)-v(\alpha_i)]/2+v(\alpha_i,\alpha_j)-[\mu_1 n_1(\alpha_j)+\cdots+\mu_k n_k(\alpha_j)-v(\alpha_j)]/2, \tag{26}$$
$$P=\sum_{\alpha_1}\cdots\sum_{\alpha_L}\prod_{i=1}^{L-1}\exp-\theta v(\alpha_i\alpha_{i+1})$$

and if the $\mathbf{\exp -\theta V}$ matrix is symmetrical the problem is formally the same as that of the evaluation of $Z$

$$P=\lambda_{\max}^{L-1}[\textstyle\sum_\alpha \psi_{\max}(\alpha)]^2. \tag{27}$$

The calculating devices introduced in studying $Z$ are valid for studying $P$.

As an example let us consider the grand partition function of a one-dimensional binary substitutional alloy. Let there be $N_0$ particles of kind "0" and $N_1$ particles of kind "1," and further let $E_{ij}$ be the energy of interaction of a particle of kind "$i$" with a nearest neighbor of kind "$j$." Since any lattice point can be occupied by either kind of particle,

$$P=\lambda_{\max}^{N_0+N_1-1}[\textstyle\sum_\alpha \psi_{\max}(\alpha)]^2$$

and the $\mathbf{\exp -\theta V}$ matrix is

$$\mathbf{\exp -\theta V}=\begin{pmatrix}\exp-\theta V(0,0) & \exp-\theta V(0,1)\\ \exp-\theta V(1,0) & \exp-\theta V(1,1)\end{pmatrix}$$
$$=\begin{pmatrix}\exp\theta(\mu_0-E_{00}) & \exp\theta[(\mu_0+\mu_1)/2-E_{10}]\\ \exp\theta[(\mu_0+\mu_1)/2-E_{10}] & \exp\theta(\mu_1-E_{11})\end{pmatrix}.$$

By simple algebra the roots of the secular equation of $\mathbf{\exp -\theta V}$ are

$$\lambda_1=\tfrac{1}{2}\{\exp\theta(\mu_0-E_{00})+\exp\theta(\mu_1-E_{11})+([\exp\theta(\mu_0-E_{00})-\exp\theta(\mu_1-E_{11})]^2+4\exp\theta(\mu_1+\mu_0-2E_{12}))^{\frac{1}{2}}\},$$

$$\lambda_2=\tfrac{1}{2}\{\exp\theta(\mu_0-E_{00})+\exp\theta(\mu_1-E_{11})-([\exp\theta(\mu_0-E_{00})-\exp\theta(\mu_1-E_{11})]^2+4\exp\theta(\mu_1+\mu_0-2E_{12}))^{\frac{1}{2}}\}.$$

Thus

$$P^{1/(N_0+N_1-1)}=\lambda_1$$

and the chemical potentials $\mu_0$, $\mu_1$ must be chosen to make simultaneously

$$N_0=\partial\log\lambda_1/\partial(\mu_0\theta),$$
$$N_1=\partial\log\lambda_1/\partial(\mu_1\theta).$$

Inasmuch as this problem was introduced merely as an example, we shall carry it no further. It might be mentioned however that there is no phase transition in this linear system.

## IV. INTRODUCTION OF INTERACTIONS WITH MORE DISTANT NEIGHBORS AS APPLIED TO LINEAR FERROMAGNETS

The characteristic value theory of the partition function developed in SM–I and in further studies of the theory as reported so far in this paper are adapted to "systems in which the molecular forces are sufficiently short ranged to permit the total energy of the system to be represented by the sum of the interactions of each molecule with its nearest neighbors." One might now ask if it is possible to include direct interactions between more distant neighbors (as well as the correlation effects which are automatically taken into account in the present method) and still retain some remnants of the characteristic value theory. Formally it is made possible by placing more than one molecule in each of the cells mentioned in the introduction. The potential energy terms in (1) would then represent interactions between multiply populated cells. Of course the $\exp -\theta V$ matrices would be of a higher order than those of the corresponding nearest neighbor systems. A further difficulty arises in that the $\exp -\theta V$ matrix of the extended problem may not be symmetrical even though that of the original problem is, so we cannot blindly use (5).

In order to understand an approach that is satisfactory for evaluating some partition functions in which interactions between more distant neighbors have been introduced, and in order to see what effect the introduction has on thermodynamic properties let us consider in detail the statistics of a linear ferromagnetic chain.

The seat of the magnetic properties of a ferromagnetic element is in the unpaired electrons of the $d$ shell of the atoms at each lattice point. We shall let $-\epsilon$ be the energy of interaction of two neighboring atoms whose unpaired spins are parallel and $+\epsilon$ that when they are antiparallel. Furthermore, we shall let $-f$ be the energy of interaction of two "next nearest neighbors" with parallel excess spins, and $f$ that with antiparallel spins. Also, we write $J=\epsilon/kT$ and $K=f/kT$. A linear chain of $N$ lattice points can be divided into $N/2$ cells containing two lattice points per cell

$$\begin{array}{ccccccccccccc} 1 & & 2 & 3 & & 4 & 5 & & 6 & & & N-1 & N \\ | & \times & | & \times & \times & | & \times & \times & | & \cdots & | & \times & \times & | . \\ & \mathrm{I} & & & \mathrm{II} & & & \mathrm{III} & & & & N/2 & & \end{array}$$

By representing a lattice point with excess $+$spin by a "0" and one with excess $-$spin by a "1," there exists a unique two digit number, $\alpha$, in the binary system which represents a given cell configuration. If we define $v(\sigma_i, \sigma_j)$ as the spin interaction between the $i$th lattice point in the configuration $\sigma_i$ and the $j$th lattice point in configuration $\sigma_j$, the partition function of our linear system is

$$Z=\sum_{\sigma_1}\cdots\sum_{\sigma_N}\exp -\theta[v(\sigma_1,\sigma_2)+v(\sigma_1,\sigma_3)+v(\sigma_2,\sigma_3)+v(\sigma_2,\sigma_4)+\cdots+v(\sigma_N,\sigma_{N-1})].$$

Then substituting

$$V(\alpha_i,\alpha_{i+1})=v(\sigma_{2i-3},\sigma_{2i-2})/2+v(\sigma_{2i-3},\sigma_{2i-1})+v(\sigma_{2i-2},\sigma_{2i-1})+v(\sigma_{2i-1},\sigma_{2i})+v(\sigma_{2i-1},\sigma_{2i})/2,$$

$$Z=\sum_{\alpha_1}\cdots\sum_{\alpha_{N/2}}\prod_{i=2}^{N/2-1}\exp -\theta V(\alpha_i,\alpha_{i+1}).$$

Now let us examine the unsymmetrical matrix

$$\mathbf{exp}\ -\boldsymbol{\theta}\mathbf{V}=\begin{array}{c|cccc} \alpha_2\backslash\alpha_1 & 00 & 01 & 11 & 10 \\ 00 & e^{2J+2K} & e^{J} & e^{-2K} & e^{-J} \\ 01 & e^{-J} & e^{-2J+2K} & e^{J} & e^{-2K} \\ 11 & e^{-2K} & e^{-J} & e^{2J+2K} & e^{J} \\ 10 & e^{J} & e^{-2K} & e^{-J} & e^{-2J+2K} \end{array}.$$

To demonstrate the calculation of the matrix elements let us consider the element in the 01th row and the 11th column. This is the term $\exp -\theta V(01, 11)$ and corresponds to the configuration

$$\begin{array}{cccc} 0 & 1 & 1 & 1 \\ \hline 1 & 2 & 3 & 4 \end{array}.$$

Since

$$v(\sigma_1,\sigma_2)=\epsilon,\quad v(\sigma_1,\sigma_3)=f,\quad v(\sigma_2,\sigma_3)=-\epsilon,\quad v(\sigma_2,\sigma_4)=-f,\quad v(\sigma_3,\sigma_4)=-\epsilon,$$

$$V(01,11)=\epsilon/2+(f-\epsilon-f)-\epsilon/2=-\epsilon=-JkT$$

and

$$\exp -\theta V(01,11)=e^{J}.$$

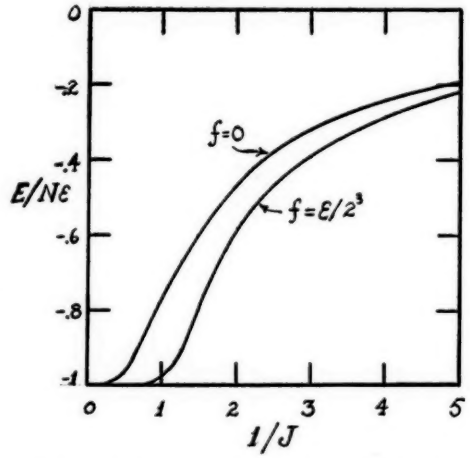


FIG. 1. Average internal energy of spin per lattice point (in units of $\epsilon$) for a nearest and next nearest neighbor system.

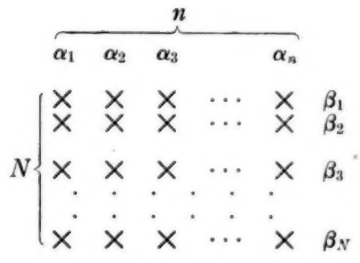


FIG. 2

The matrix

$$\mathbf{R}=2^{-\frac{1}{2}}\begin{bmatrix}1&0&1&0\\0&1&0&1\\1&0&-1&0\\0&1&0&-1\end{bmatrix}=\mathbf{R}^{-1}$$

transforms $\mathbf{exp}\ -\theta\mathbf{V}$ into

$$\mathbf{R}\ \mathbf{exp}\ (-\theta\mathbf{V})\mathbf{R}^{-1}=\begin{bmatrix}e^{2J+2K}+e^{-2K}&e^{J}+e^{-J}&0&0\\e^{J}+e^{-J}&e^{-2K}+e^{2K-2J}&0&0\\0&0&e^{2J+2K}-e^{-2K}&e^{J}-e^{-J}\\0&0&e^{-J}-e^{J}&e^{-2J+2K}-e^{-2K}\end{bmatrix}$$

and the roots of the symmetrical upper left factor of the secular equation of $\mathbf{R}\ \mathbf{exp}\ (-\theta\mathbf{V})\mathbf{R}^{-1}$ are

$$\lambda_1=e^{-2K}+e^{2K}\cosh 2J+2\cosh J(e^{4K}\sinh^2 J+1)^{\frac{1}{2}},$$

$$\lambda_2=e^{-2K}+e^{2K}\cosh 2J-2\cosh J(e^{4K}\sinh^2 J+1)^{\frac{1}{2}}.$$

The vectors

$$\phi_1^*=(A_1, B_1, 0, 0),\quad \phi_2^*=(A_2, B_2, 0, 0),$$

with

$$A_s=\frac{\lambda_s-e^{-2J+2K}-e^{-2K}}{[\lambda_s^2-2\lambda_s(e^{-2J+2K}+e^{-2K})+(e^{J}+e^{-J})^2+(e^{-2J+2K}+e^{-2K})^2]^{\frac{1}{2}}},$$

$$B_s=(1-A_s^2)^{\frac{1}{2}},$$

are the pair of orthonormal characteristic vectors of $\mathbf{R}\ \mathbf{exp}\ (-\theta\mathbf{V})\mathbf{R}^{-1}$, whose characteristic values are $\lambda_1$ and $\lambda_2$, respectively. The corresponding characteristic vectors of $\mathbf{exp}\ -\theta\mathbf{V}$ are

$$\psi_1^*=\phi_1^*R=(A_1, B_1, A_1, B_1)/\sqrt{2},\quad \psi_2^*=\phi_2^*R=(A_2, B_2, A_2, B_2)/\sqrt{2},$$

also with characteristic values $\lambda_1$ and $\lambda_2$.

At finite temperatures $>0$, the roots $\lambda_3$ and $\lambda_4$ of the secular equation of the lower right sub-matrix of $\mathbf{R}\ \mathbf{exp}\ (-\theta\mathbf{V})\mathbf{R}^{-1}$ have absolute values less than $\lambda_1$. Since their parent matrix is not symmetrical,

$$
\begin{array}{c} \\ N \end{array}
\begin{array}{c}
\begin{array}{ccccccc} \alpha_1 & \alpha_2 & \cdots & \alpha_n & & \end{array} \\
\left\{\begin{array}{ccccccc}
0 & \times & \times & \cdots & \times & 0 & \beta'_1 \\
0 & \times & \times & \cdots & \times & 0 & \beta'_2 \\
0 & \times & \times & \cdots & \times & 0 & \beta'_3 \\
\cdot & \cdot & \cdot & \cdot & \cdot & \cdot & \cdot \\
\cdot & \cdot & \cdot & \cdot & \cdot & \cdot & \cdot \\
0 & \times & \times & \cdots & \times & 0 & \beta'_{N-1} \\
0 & \times & \times & \cdots & \times & 0 & \beta'_N
\end{array}\right.
\end{array}
\qquad
\begin{array}{c} \\ N \end{array}
\begin{array}{c}
\begin{array}{ccccccc} \alpha_1 & \alpha_2 & \cdots & \alpha_n & & \end{array} \\
\left\{\begin{array}{ccccccc}
0 & \times & \times & \cdots & \times & 1 & \gamma'_1 \\
0 & \times & \times & \cdots & \times & 1 & \gamma'_2 \\
0 & \times & \times & \cdots & \times & 1 & \gamma'_3 \\
\cdot & \cdot & \cdot & \cdot & \cdot & \cdot & \cdot \\
\cdot & \cdot & \cdot & \cdot & \cdot & \cdot & \cdot \\
0 & \times & \times & \cdots & \times & 1 & \gamma'_{N-1} \\
0 & \times & \times & \cdots & \times & 1 & \gamma'_N
\end{array}\right.
\end{array}
$$

FIG. 3

the characteristic vectors differ fundamentally from $\phi_1$ and $\phi_2$. If $\phi_3{}^R=(0, 0, C_3, D_3)$ is a right characteristic vector with the property

$$[\mathbf{R}\ \exp -\theta\mathbf{V}\mathbf{R}^{-1}]\phi_3{}^R=\lambda_3\phi_3{}^R$$

it does not follow that $\phi_3{}^R[\ ]=\lambda_3\phi_3{}^R$; however, in our special case $\phi_3{}^L=(0, 0, C_3, -D_3)$ satisfies the equation $\phi_3{}^L[\ ]=\lambda_3\phi_3{}^L$. These vectors are biorthogonal to the other characteristic vectors (including $\phi_4{}^L$ and $\phi_4{}^R$ which correspond to $\lambda_4$) in the manner

$$\begin{aligned} &\phi_j{}^L\cdot\phi_i=0; \quad \phi_i{}^*\cdot\phi_j{}^R=0, \\ &\phi_4{}^L\cdot\phi_3{}^R=0; \quad \phi_3{}^L\cdot\phi_4{}^R=0, \end{aligned} \qquad (i=1, 2; j=3, 4)$$

and can be normalized so that

$$\phi_j{}^L\cdot\phi_j{}^R=1.$$

The corresponding characteristic vectors of $\exp -\theta V$ are

$$\psi_3{}^L=\phi_3{}^LR=(C_3, D_3, -C_3, -D_3)/\sqrt{2}; \quad \psi_3{}^R=(C_3, -D_3, -C_3, D_3)/\sqrt{2}$$

and

$$\psi_4{}^L=\phi_4{}^LR=(C_4, D_4, -C_4, -D_4)/\sqrt{2}; \quad \psi_3{}^R=(C_4, -D_4, -C_4, D_4)/\sqrt{2}.$$

By expanding

$$\exp -\theta V(\alpha_1, \alpha_2)=\textstyle\sum_i \lambda_i\psi_i{}^L(\alpha_1)\psi_i{}^R(\alpha_2)$$

$$(\text{with } \psi_1{}^L(\alpha)=\psi_1{}^R(\alpha)=\psi_1(\alpha) \quad \text{and} \quad \psi_2{}^L(\alpha)=\psi_2{}^R(\alpha)=\psi_2(\alpha))$$

and applying the orthonormality of the characteristic vectors,

$$Z=\lambda_1{}^{N/2-1}[\textstyle\sum_\alpha \psi_1(\alpha)]^2+\lambda_2{}^{N/2-1}[\sum_\alpha \psi_2(\alpha)]^2+\lambda_3{}^{N/2-1}[\sum \psi_3(\alpha)]^2+\lambda_4{}^{N/2-1}[\sum \psi_4(\alpha)]^2.$$

Since

$$\lambda_1>\lambda_2, \lambda_3, \lambda_4; \quad \lambda_1{}^{N/2-1}\gg\lambda_2{}^{N/2-1}, \lambda_3{}^{N/2-1}, \lambda_4{}^{N/2-1}$$

$$Z=\lambda_1{}^{N/2-1}[\textstyle\sum \psi_1(\alpha)]^2 \quad \text{and} \quad Z^{1/N}=\lambda_1{}^{\frac{1}{2}}$$

is the partition function per lattice point. Neglecting interactions between "next nearest" neighbors, $f=0$ and

$$\lambda_1=\lambda_{\max}=(e^J+e^{-J})^2,$$

yielding

$$Z^{1/N}=2\cosh J,$$

which agrees with the known partition function of nearest neighbor linear chains.[1,2]

Since the average internal energy of spin interaction is

$$E=\partial \log Z/\partial(-\theta),$$

it can be found from our expression for $Z$. $E/N\epsilon$ is plotted in Fig. 1 for $f=0$ and $f=\epsilon/2$[3].

## V. APPLICATION TO TWO-DIMENSIONAL FERROMAGNETS

As an application of Parts I and II, we shall calculate the high and low temperature partition function, internal energy, specific heat, and magnetization of two-dimensional $N\times M$ (as $N, M\to\infty$) ferromagnets. The definitions of interaction energies introduced in Part IV will be retained here. If our ferromagnet is inserted in a magnetic field $H$, the total energy of spin-field interaction is

$$-\mu(n_+-n_-)H=-\mu H\sum_{i=1}^{N}[n_+(\alpha_i)-n_-(\alpha_i)], \tag{28}$$

where

$\mu$ = magnetic moment of each spin,
$n_+(\alpha_i)$ = number of "+" spins in the $i$th row when it is in configuration $\alpha_i$,
$n_-(\alpha_i)$ = number of "−" spins in the $i$th row when it is in configuration $\alpha_i$,
$n_+=\sum n_+(\alpha_i)$ and $n_-=\sum n_-(\alpha_i)$.

We shall henceforth abbreviate $C=\mu H/kT$.

### 1. High Temperature Development

To derive a power series in $\theta=1/kT$ for $Z$ that is valid at high temperatures, the two-dimensional analogue of (13) will be used. This necessitates the calculation of

$$S_n=\sum\cdots\sum\exp-[V(\alpha_1,\alpha_2)+V(\alpha_2,\alpha_3)+\cdots+V(\alpha_{n-1},\alpha_n)]/kT \tag{29a}$$

and $S_{n+1}$ with the value of $n$ determined by the number of terms desired in the resulting power series.

These $S_n$'s correspond to partition functions of narrow strips of the sort exhibited in Fig. 2 in which the interactions between neighboring elements in chain $\alpha_1$ (and likewise those between neighboring elements of chain $\alpha_n$) are only one-half those between other adjacent elements in the lattice. Instead of expressing $S_n$ as a sum over configurations of the vertical chains (i.e., $\alpha$'s) in Fig. 3, one can equally well express it as a sum over configurations of horizontal chains (i.e., $\beta$'s)

$$S_n=\sum_{\beta_1}\cdots\sum_{\beta_N}\exp-\theta[W(\beta_1,\beta_2)+\cdots+W(\beta_{N-1},\beta_N)], \tag{29b}$$

$$W(\beta_i,\beta_j)=\tfrac{1}{2}\sum_{k=1}^{n-1}v(\sigma_{i,k},\sigma_{i,k+1})+\tfrac{1}{2}[v(\sigma_{i,1},\sigma_{j,1})+v(\sigma_{i,n},\sigma_{j,n})]+\sum_{k=1}^{n}v(\sigma_{i,k},\sigma_{j,k})$$
$$+\tfrac{1}{2}\sum_{k=1}^{n-1}v(\sigma_{j,k},\sigma_{j,k+1})-\frac{C}{2}\sum_{k=2}^{n-1}[n_+(\sigma_{i,k})+n_+(\sigma_{j,k})-n_-(\sigma_{i,k})-n_-(\sigma_{j,k})]$$
$$-\frac{C}{4}[n_+(\sigma_{i,1})+n_+(\sigma_{j,1})+n_+(\sigma_{i,n})+n_+(\sigma_{j,n})-n_-(\sigma_{i,1})-n(\sigma_{j,1})-n_-(\sigma_{i,n})-n_-(\sigma_{j,n})]$$

and $\sigma_{il}$ defines to the spin configuration of the $l$th element in the $i$th row.

$$\begin{aligned}
&n_+(\sigma)=1 \quad \text{if} \quad \sigma=0 \quad \text{(i.e., + spin)},\\
&n_+(\sigma)=0 \quad \text{if} \quad \sigma=1 \quad \text{(i.e., − spin)},\\
&n_-(\sigma)=0 \quad \text{if} \quad \sigma=0,\\
&n_-(\sigma)=1 \quad \text{if} \quad \sigma=1.
\end{aligned}$$

By expanding $\exp -W_n(\beta_i\beta_j)$ as a bilinear combination of the characteristic vectors of the equation[7]

$$\mu(n)\varphi(n,\beta_i)=\sum_{\beta_j}\exp-\theta W_n(\beta_i,\beta_j)\varphi(n,\beta_j), \tag{29c}$$

$$S_n=\mu(n)_{\max}^{N-1}[\textstyle\sum_\beta\varphi(n,\beta)]^2.$$

[7] $\mu(n)$ is a characteristic value corresponding to strips of width $n$.

If $n=2$, the exp $-\theta W$ matrix will be constructed so that the element in the $i$th row and $j$th column is the term

$$\exp -W(i-1, j-1)\theta.$$

The interaction energy in this term is that between a row in a configuration which corresponds to the two digit number $(i-1)$ in the binary system and a neighboring row in a configuration corresponding to the two digit number $(j-1)$. For example,

$$W(0, 1)=[v(0, 0)+v(0, 0)+v(0, 1)+v(0, 1)]/2-C[3n_+(0)-n_-(1)]/4$$

$$\begin{array}{ll} 0\text{—}0 & \beta_1=0 \\ \vert\ \square\ \vert & \\ 0\text{—}1 & \beta_2=1 \end{array}$$

but

$$v(0, 1)=\epsilon, \quad v(0, 0)=-\epsilon, \quad \epsilon=JkT.$$

Therefore $W(0, 1)=-C/2$. Similar calculations of the other matrix elements yield

$$\mathbf{exp}\ -\mathbf{W\theta}=\begin{bmatrix} e^{2J+C} & e^{C/2} & e^{C/2} & 1 \\ e^{C/2} & 1 & e^{-2J} & 1 \\ e^{C/2} & e^{-2J} & 1 & 1 \\ 1 & 1 & 1 & e^{2J-C} \end{bmatrix}.$$

Expanding each matrix element as a power series in $\theta$ (i.e., in powers of $J$ and $C$), choosing as a first approximation to the characteristic vector $\mathbf{exp}\ -\mathbf{W\theta}$ the unnormalized vector of complete disorder (1, 1, 1, 1) and finally proceeding by the method of successive approximations discussed in S.M.–I, Part–2, we obtain for the unnormalized characteristic vector $\boldsymbol{\phi}(2)_{\max}$ of $\mathbf{exp}\ -\mathbf{W\theta}$ and for its characteristic value $\mu(2)_{\max}$

$$\boldsymbol{\phi}(2)_{\max}=\begin{bmatrix} 1 \\ 1-J-C/2+C^2/8+J^2/2 \\ 1-J-C/2+C^2/8+J^2/2 \\ 1-C+C^2/2-CJ \end{bmatrix},$$

$$\mu(2)_{\max}=4+3J^2+C^2+0(\theta^3).$$

When $n=3$ the $\mathbf{exp}\ -\mathbf{W\theta}$ matrix is

$$\mathbf{exp}\ -\mathbf{W\theta}=\left[\begin{array}{cccc|cccc} e^{2C+4J} & e^{2J+3C/2} & e^{C} & e^{C/2} & e^{2J+3C/2} & e^{C} & e^{C/2} & 1 \\ e^{2J+3C/2} & e^{C+2J} & e^{-2J+C/2} & 1 & e^{C} & e^{C/2} & e^{-2J} & e^{-C/2} \\ e^{C} & e^{-2J+C/2} & 1 & e^{-C/2} & e^{-2J+C/2} & e^{-4J} & e^{-C/2} & e^{-C} \\ e^{C/2} & 1 & e^{-C/2} & e^{2J-C} & e^{-2J} & e^{-2J-C/2} & e^{-C} & e^{2J-3C/2} \\ \hline e^{2J+3C/2} & e^{C} & e^{-2J+C/2} & e^{-2J} & e^{2J+C} & e^{C/2} & 1 & e^{-C/2} \\ e^{C} & e^{C/2} & e^{-4J} & e^{-2J-C/2} & e^{C/2} & 1 & e^{-2J-C/2} & e^{-C} \\ e^{C/2} & e^{-2J} & e^{-C/2} & e^{-C} & 1 & e^{-2J-C/2} & e^{2J-C} & e^{2J-3C/2} \\ 1 & e^{-C/2} & e^{-C} & e^{2J-3C/2} & e^{-C/2} & e^{-C} & e^{2J-3C/2} & e^{4J-2C} \end{array}\right].$$

The characteristic vector $\boldsymbol{\phi}(3)_{\max}$ which corresponds to the largest characteristic value $\mu(3)_{\max}$

(unnormalized)

$$\phi(3)_{\max}=\begin{vmatrix} 1 & & \\ 1-C/2-J+C^2/8+J^2/2 & & \\ 1-2J-C+C^2/2+2J^2 & & \\ 1-3C/2-J+9C^2/8-CJ+J^2/2 & & \\ 1-C/2-J+C^2/8+J^2/2 & & \\ 1-2J-C+C^2/2+JC+2J^2 & & \\ 1-3J/2-J+9C^2/8-CJ+J^2/2 & & \\ 1-2C+2C^2-3CJ & & \end{vmatrix}$$

and

$$\mu(3)_{\max}=8+14J^2+6C^2+\cdots.$$

Then from Eqs. (13) and (29c) the first approximation to the partition function is (as $M$, $N\to\infty$ so that $M-1\to M$ and $N-1\to N$)

$$Z^{1/(N-1)}\sim S_3/S_2+0(\theta^3)$$

and

$$\begin{aligned} Z^{1/MN}&\sim\mu(3)_{\max}/\mu(2)_{\max}+0(\theta^3)\\ &\sim 2+2J^2+C^2+0(\theta^3). \end{aligned} \tag{30}$$

By the well-known relation between magnetization and the partition function

$$\mathfrak{M}/MN=\mu\partial\log Z/\partial C=\mu C+\cdots.$$

As the external field $C\to 0$, the magnetization per lattice point becomes zero and therefore in the temperature range where (30) is valid, a two-dimensional "ferromagnetic" system is not ferromagnetic.

In the absence of a magnetic field we have calculated by the above method

$$Z_0^{1/MN}\sim\mu(5)_{\max}/\mu(4)_{\max}+0(\theta^5)=2(1+J^2+4J^4/3+\cdots),$$

which agrees with the first three terms of the result of Kramers and Wannier[2,8] obtained by another method

$$Z_0^{1/MN}=2(1+J^2+4J^4/3+77J^6/45+\cdots). \tag{31}$$

Since

$$\bar{E}=\partial\log Z/\partial(-\theta)\quad\text{and}\quad J=\epsilon/kT=\epsilon\theta,$$

$$\bar{E}/MN\sim-\epsilon(2J+10J^3/3+64J^5/15+\cdots) \tag{32a}$$

and

$$C_v/kMN\sim J^2(2+10J^2+64J^4/3+\cdots). \tag{32b}$$

### 2. Low Temperature Development

To derive the low temperature exponential development for $Z$ we shall use Eq. (23) and therefore need

$$S_{0,n}=\sum_{\alpha_1}\cdots\sum_{\alpha_n}\exp-[V(0,\alpha_1)+V(\alpha_1,\alpha_2)+\cdots+V(\alpha_n,0)]/kT$$

and

$$S_{1,n}=\sum_{\alpha_1}\cdots\sum_{\alpha_n}\exp-[V(0,\alpha_1)+V(\alpha_1,\alpha_2)+\cdots+V(\alpha_n,1)]/kT.$$

These $S$'s correspond to partition functions of narrow strips as shown in Fig. 3, in which the interactions between neighboring elements in the chains of 0's and in the chain of 1's is only one-half that between other adjacent elements in the lattice. Instead of expressing the $S$'s as sums over configurations of vertical chains (i.e., in terms of $\alpha$'s) we shall express them as sums over horizontal (i.e., $\beta'$ and $\gamma'$) configurations. If we proceed in a manner analogous to that used in the low temper-

[8] See also W. Opechowski, Physica **4**, 181 (1937).

ature development

$$S_{0,n}+S_{1,n}={}_{n,0}\mu_{\max}^{N-1}[\sum \varphi_{\max}(\beta')]^2+{}_{n,1}\mu_{\max}^{N-1}[\sum \varphi_{\max}(\gamma')]^2,$$

where ${}_{n,0}\mu_{\max}$ and ${}_{n,1}\mu_{\max}$ are, respectively, the largest characteristic values of the matrices of interactions of two adjacent $\beta'$ rows and between two adjacent $\gamma'$ rows. Now

$${}_{n,0}\mu_{\max}=\exp[(2n+2)J+(n+1)C]+O(\exp[(2n-6)J+nC]),$$

$${}_{n,1}\mu_{\max}=\exp(2nJ+nC)+O(\exp[(2n-8)J+(n-1)C]).$$

So,

$$({}_{n,1}\mu_{\max}/{}_{n,0}\mu_{\max})^N=\exp-(2NJ+NC)+\cdots\rightarrow 0$$

as $N\rightarrow\infty$, and we can neglect $S_{1,n}$ as compared with $S_{0,n}$:

$$S_{0,n}+S_{1,n}=S_{0,n}[1+O(e^{-2NJ-NC})].$$

To find ${}_{1,0}\mu_{\max}$ we need the $\exp-\theta W(\beta'_1,\beta'_2)$ matrix of the configuration

| 1 | 2 | 3 | |
|---|---|---|---|
| 0 | $x_1$ | 0 | $\beta'_1$ |
| 0 | $x_2$ | 0 | $\beta'_2$ |

with

$$W(\beta_1,\beta_2)=v(0,x_1)/2+v(x_1,0)/2+v(0,x_2)/2+v(x_2,0)/2+v(0,0)/2+v(0,0)/2+v(x_1,x_2)-C$$
$$-[n_+(x_1)-n_-(x_1)+n_+(x_2)-n_-(x_2)]/2.$$

This matrix is

$$\exp-\mathbf{W}\theta=\begin{array}{c} x_2\backslash x_1 \\ 0 \\ 1 \end{array}\begin{array}{c} \begin{array}{cc} 0 & 1 \end{array} \\ \begin{pmatrix} e^{4J+2C} & e^{C} \\ e^{C} & 1 \end{pmatrix} \end{array}.$$

By the method of successive approximations (choosing the "ordered" vector (1, 0) as the first approximation)

$$\begin{pmatrix} e^{4J+2C} & e^{C} \\ e^{C} & 1 \end{pmatrix}\begin{pmatrix} 1 \\ 0 \end{pmatrix}=e^{4J+2C}\begin{pmatrix} 1 \\ e^{-4J-C} \end{pmatrix},$$

$$\begin{pmatrix} e^{4J+2C} & e^{C} \\ e^{C} & 1 \end{pmatrix}\begin{pmatrix} 1 \\ e^{-4J-C} \end{pmatrix}=(e^{4J+2C}+e^{-4J})\begin{pmatrix} 1 \\ e^{-4J-C}+e^{-8J-3C} \end{pmatrix},$$

until

$${}_{1,0}\mu_{\max}=e^{4J+2C}+e^{-4J}+e^{-8J-2C}+\cdots.$$

To continue further we must know ${}_{2,0}\mu_{\max}$ and therefore develop the $\exp-\theta W(\beta'_1,\beta'_2)$ matrix of the configuration

$$0\quad x_{11}\quad x_{12}\quad 0,$$
$$0\quad x_{21}\quad x_{22}\quad 0.$$

Again all interactions except those between $x$'s of adjacent rows are one-half their normal value. The matrix is

$$\begin{array}{c} x_{21}x_{22}\backslash x_{11}x_{12} \\ 00 \\ 01 \\ 10 \\ 11 \end{array}\begin{array}{c} \begin{array}{cccc} 00 & 01 & 10 & 11 \end{array} \\ \begin{pmatrix} e^{6J+3C} & e^{2J+2C} & e^{2J+2C} & e^{C} \\ e^{2J+2C} & e^{2J+C} & e^{C-2J} & 1 \\ e^{2J+2C} & e^{-2J+C} & e^{2J+C} & 1 \\ e^{C} & 1 & 1 & e^{2J-C} \end{pmatrix} \end{array}=\exp-\mathbf{V}\theta.$$

Starting with the "ordered" vector (1, 0, 0, 0) as a first approximation the method of successive approximations yields the unnormalized characteristic vector

$$\begin{bmatrix} 1 \\ e^{-4J-C}+e^{-8J-3C}+2e^{-12J-5C}-e^{-12J-3C}+\cdots \\ e^{-4J-C}+e^{-8J-3C}+2e^{-12J-5C}-e^{-12J-3C}+\cdots \\ e^{-6J-2C}+2e^{-10J-4C}+e^{-10J-6C}+\cdots \end{bmatrix}$$

and the corresponding characteristic value ${}_{2,0}\mu_{\max}$ is

$${}_{2,0}\mu_{\max}=e^{6J+3C}+2e^{-2J+C}+3e^{-6J-C}-2e^{-10J-C}+6e^{-10J-3C}+e^{-10J-5C}+\cdots.$$

From Eq. (23) it is apparent that

$$Z^{1/(M-1)}=S_{0,n+1}/S_{0,n}$$

and

$$Z^{1/(M-1)(N-1)}={}_{n+1,0}\mu_{\max}/{}_{n,0}\mu_{\max}$$

as $n\to\infty$.

Therefore as a first approximation

$$Z^{1/(M-1)(N-1)}\sim{}_{2,0}\mu_{\max}/{}_{1,0}\mu_{\max}=e^{2J+C}(1+e^{-8J-2C}+2e^{-12J-4C}+\cdots).$$

To find the next approximation we must calculate ${}_{3,0}\mu_{\max}$ from the matrix of the system

$$\begin{matrix} 0 & x_{11} & x_{12} & x_{13} & 0, \\ 0 & x_{21} & x_{22} & x_{23} & 0, \end{matrix}$$

with all interactions except those between $x$'s of adjacent rows having one-half their normal values. It turns out by method of successive approximations that

$${}_{3,0}\mu_{\max}=e^{8J+4C}+3e^{2C}+5e^{-4C}+e^{-8J}(-3+12e^{-2C}+3e^{-4C})+\cdots.$$

Thus as a second approximation (neglecting the "1" in the terms $N-1$ and $M-1$ since $N, M\to\infty$)

$$Z^{1/NM}\sim{}_{3,0}\mu_{\max}/{}_{2,0}\mu_{\max}=e^{2J+C}[1+e^{-8J-2C}+2e^{-12J-4C}+e^{-16J-4C}(-3+6e^{-2C}+2e^{-4C})+\cdots]. \quad (33a)$$

In the absence of an external magnetic field, $C=0$ and

$$Z_0^{1/MN}=e^{2J}(1+e^{-8J}+2e^{-12J}+5e^{-16J}+\cdots), \quad (33b)$$

which agrees with the results of Wannier and Kramers, KW–II.

For higher approximations it is necessary to find ${}_{4,0}\mu_{\max}$, ${}_{5,0}\mu_{\max}$, etc. by the same methods used for smaller values of $n$. In field free space ${}_{4,0}\mu_{\max}$ was of a value to make the next term in the $Z^{1/MN}$ series $14e^{-18J}$. The low temperature magnetization per lattice point is

$$\mathfrak{M}/MN=\mu\partial\log Z/\partial C$$
$$=\mu[1-2e^{-8J-2C}-8e^{-12J-4C}$$
$$+2e^{-16J-4C}(7-18e^{-2C}-8e^{-4C})+\cdots], \quad (34)$$

which shows that a two-dimensional "ferromagnet" is actually ferromagnetic in the temperature range for which (34) is valid, in the sense that its magnetization is greater than zero in the absence of an external magnetic field.

In zero external magnetic field and at low temperatures the average internal energy per lattice point is

$$\bar{E}/MN=-\epsilon(2-8e^{-8J}$$
$$-24e^{-12J}-72e^{-16J}-\cdots) \quad (35a)$$

and the specific heat per lattice point is

$$C/kMN=64J^2e^{-8J}(1+9e^{-4J}/2$$
$$+18e^{-8J}+\cdots). \quad (35b)$$

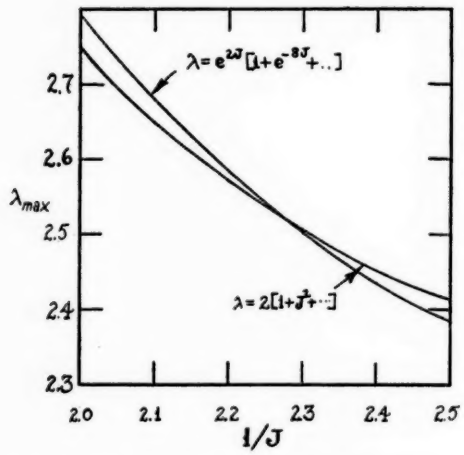


FIG. 4. $\lambda_{max}$ as a function of $1/J$ in the neighborhood of $J_c$.

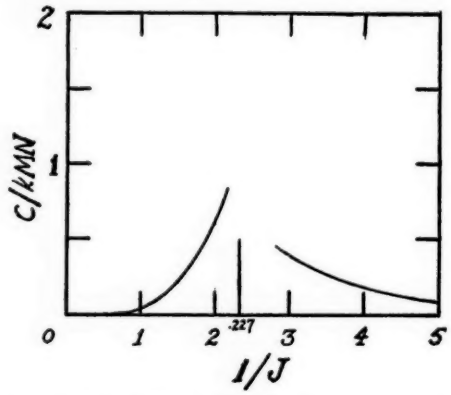


FIG. 5. Specific heat per lattice point in units of $k$.

### 3. Discussion

Equations (32) and (33) provide us with expressions for the average energy and specific heat due to spin interactions at high and low temperatures. A reasonable problem now is to find the temperature ranges in which each expression is valid and to locate the temperature of a phase transition if one exists. In SM–I, p. 710, it is pointed out that a necessary condition for the existence of a phase transition at a temperature $T_c$ is that the largest characteristic value of (4) be doubly degenerate. This condition of necessity results from supposing that the characteristic vector of (4) describing the most probable state of a layer of the system when $T>T_c$ is $\psi_2$ and when $T<T_c$ that it is $\psi_1$. Then if $\lambda_1$ is the characteristic value corresponding to $\psi_1$ and $\lambda_2$ is the characteristic value corresponding to $\psi_2$

$$\lambda_1=\lambda_{max}>\lambda_2 \text{ if } T<T_c,$$

$$\lambda_2=\lambda_{max}>\lambda_1 \text{ if } T>T_c.$$

Since at a transition point both phases (if there are two) are equally probable

$$\lambda_1=\lambda_2=\lambda_{max} \text{ if } T=T_c.$$

Applying this criterion to the two-dimensional ferromagnet problem, if there is a phase transition it must occur at the temperature at which the $Z_0^{1/MN}$ of Eq. (33b) is equal to the $Z_0^{1/MN}$ of Eq. (31). That is, at the temperature which makes

$$2(1+J^2+4J^4/3+77J^6/45+\cdots)$$
$$=e^{2J}(1+e^{-8J}+2e^{-12J}+5e^{-16J}+24e^{-20J}+\cdots).$$

From Fig. 4 where the functions on both sides of this equation are plotted separately, the point of intersection of the two curves, $J_c=0.44=\epsilon/kT_c$, gives the temperature of a phase transition if one exists. At this point $Z_0^{1/MN}=2.52$. Using a necessary condition that is a special property of a two-dimensional ferromagnet for the existence of a sharp phase transition, Kramers and Wannier KW–I, II have calculated $J_c=0.4407$ and $Z_0^{1/MN}=2.532$ which agrees closely with our results.

Unfortunately it is impossible from our equations to establish definitely the existence of a sharp phase transition at $J_c=0.44$. Since $Z_0^{1/MN}$ as defined by (31) is equal to $\lambda_{max}$ when $J>J_c$, (32) gives the correct asymptotic expression for the average internal energy and specific heat in this temperature range. When $J<J_c$ (35) is a valid asymptotic expression. If the specific heat is plotted as a function of $J$ (Fig. 5) the curves seem to be approaching a peak of the $\lambda$-point variety at $J=J_c$. Inasmuch as the series in (32) and (35) are probably asymptotic divergent series in the neighborhood of $J_c$ whose smallest terms (and therefore whose possible error[9]) are quite large, the calculated specific heat would probably be inaccurate around $J_c$. As has been mentioned before, the magnetization at zero external field is zero in the region of

[9] Knopp, *Theory and Applications of Infinite Series* (Blackie and Sons, 1928), p. 54.

validity of (30) while that in the region of validity of (34) is positive. Also, as $J \to J_c$, $\mathfrak{M}$, as defined by (34) decreases; but (34) does not have enough terms to decide whether or not it decreases continuously to zero at $J_c$. Approximate calculations of higher order terms indicate that the $\mathfrak{M}$ series is probably an asymptotic divergent one around $J_c$, so as in the case of the specific heat, this series gives there only a qualitative idea of the behavior of $\mathfrak{M}$. In spite of the inaccuracies near $J_c$, our results as do those of Kramers and Wannier seem to suggest the existence of a $\lambda$-point phase transition at $J_c$ that accompanies a change from a ferromagnetic state to an unferromagnetic state.

In conclusion, it seems apparent that the characteristic value method of treating nearest neighbor problems is adequate to give asymptotic formulae for physical properties at high and low temperatures and to locate the temperature of a phase transition if one exists, but at its present state of development the method cannot provide accurate values of physical quantities which are derivatives of the partition function, in the immediate neighborhood of a transition point.

The author wishes to thank Professor Lars Onsager for his enlightening discussions concerning this problem.

## APPENDIX[10]

### Proof that $\mathbf{S}_{2l+1}/\mathbf{S}_{2l} = \mathbf{S}_{l+1}/\mathbf{S}_l + \mathbf{O}(\boldsymbol{\theta}^{l+1})$

By definition

$$S_l = \sum_{\alpha_1} \cdots \sum_{\alpha_l} \prod_{i=1}^{l-1} \exp -\theta V(\alpha_i, \alpha_{i+1}).$$

Therefore, if $\{\lambda_i\}$ is the set of characteristic values corresponding to the set of characteristic vectors $\{\psi_j\}$ of the set of linear equations

$$\lambda\psi(\alpha_1) = \sum_{\alpha_2=1}^{\nu^{MN}} \psi(\alpha_2) \exp -\theta V(\alpha_1, \alpha_2)$$

and if there are $\nu$ configurations available to each lattice point

$$S_l = \sum_{j=1}^{\nu^{MN}} \lambda_j{}^{l-1} [\Sigma_\alpha \psi_j(\alpha)]^2,$$

$$S_{2l+1} S_l = \Sigma_i \lambda_i{}^{3l} [\Sigma_\alpha \psi_1(\alpha)]^2 + \sum_{i,j}{}' \lambda_i{}^{2l} \lambda_j{}^{l-1} [\Sigma_\alpha \psi_i(\alpha)]^2 [\Sigma_\alpha \psi_j(\alpha)]^2$$

(the prime on the $\Sigma$ is introduced to denote that the terms with $i=j$ are omitted). Using a similar expression for $S_{2l}S_{l+1}$

$$S_{2l+1}S_l - S_{2l}S_{l+1} = \sum_{i,j=1}{}' {}^{\nu^{MN}} [\lambda_i{}^{2l}\lambda_j{}^{l-1} - \lambda_i{}^{2l-1}\lambda_j{}^{l}] [\Sigma_\alpha \psi_i(\alpha)]^2 [\Sigma_\alpha \psi_j(\alpha)]^2. \quad (36)$$

Suppose $\lambda_i = \Sigma a_{ij}\theta^j$; $\lambda_1 = \lambda_{\max}$. Then as $\theta \to 0$ in the matrix $\mathbf{exp} - \boldsymbol{\theta}\mathbf{V}$, $\lambda_i \to a_{i0}$. Since as $\theta \to 0$ all the elements of $\mathbf{exp} - \boldsymbol{\theta}\mathbf{V}$ approach unity it is easily verified that $\lambda_1 = \lambda_{\max} \to \nu^{MN}$ and $\lambda_i \to 0$ if $i > 1$, or $\lambda_i = 0(\theta)$. Also, when $i > 1$, either $\psi_i(\alpha) = 0(\theta)$ or for every $\alpha$ which makes $\psi_i(\alpha) = c$ there exists a unique $\beta$ which makes $\psi_i(\beta) = -c$; for if a single $\alpha$ yielded $\psi_i(\alpha) = c$ and there existed no corresponding $\beta$ to make $\psi_i(\beta) = -c$,

$$\lambda_i = \sum_{\alpha_1 \alpha_2} \psi_i(\alpha_1)\psi_i(\alpha_2) \exp -\theta V(\alpha_1\alpha_2) = c^2 + 0(\theta)$$

contrary to our above conclusions. This implies

$$\Sigma_\alpha \psi_i(\alpha) = \begin{cases} 0(1) & \text{if } i = 1 \\ 0(\theta) & \text{if } i > 1. \end{cases}$$

Since all $\lambda_i = 0(\theta)$ except $\lambda_1$ which is $0(1)$, the dominant term in (36) as $\theta \to 0$ is

$$[\lambda_1{}^{2l}\lambda_j{}^{l-1} - \lambda_1{}^{2l}\lambda_j{}^{l}] [\Sigma_\alpha \psi_1(\alpha)]^2 [\Sigma_\alpha \psi_j(\alpha)]^2 \quad (j \neq 1)$$
$$= [0(1)0(\theta^{l-1}) - 0(1)0(\theta^l)] [0(1)]^2 [0(\theta)]^2$$
$$= 0(\theta^{l+1}) - 0(\theta^{l+2}) \to 0(\theta^{l+1}).$$

So we finally have

$$S_{2l+1}S_l - S_{2l}S_{l+1} = 0(\theta^{l+1})$$

or

$$S_{2l+1}/S_{2l} - S_{l+1}/S_l = 0(\theta^{l+1})/S_lS_{2l} = 0(\theta^{l+1}),$$

since $S_lS_{2l} \to 0(1)$ as $\theta \to 0$, and our theorem is proven.

[10] The notation $g(\theta) = 0[f(\theta)]$ as $\theta \to 0$ is used here in the usual sense that there exists some positive finite constant $A$ independent of $\theta$ such that as $\theta \to 0$, $|g(\theta)/f(\theta)|$ finally becomes and remains less than $A$.

# Letters to the Editor

*THIS section will accept reports of new work, provided these are terse and contain few figures, and especially few halftone cuts. The Editorial Board will not hold itself responsible for opinions expressed by the correspondents. Contributions to this section should not exceed 600 words in length and must reach the office of the Managing Editor not later than the 15th of the month preceding that of the issue in which the letter is to appear. No proof will be sent to the authors. The usual publication charge ($3.00 per page) will not be made and no reprints will be furnished free.*

## The Potential in a Solution Near a Charged Wall

W. G. EVERSOLE
*Division of Physical Chemistry, The State University of Iowa, Iowa City, Iowa*
December 1, 1941

IN recent papers in this Journal[1,2] an equation was derived relating the potential, ($\psi$), in a binary salt solution near a charged wall to the surface potential, ($\psi_0$), of the wall and the distance, ($X$), from the $\psi_0$ plane. The equation was derived without the usual simplifying assumption that $z\epsilon\psi \ll kT$ so it is valid for the relatively high potentials which may be encountered in electrokinetic measurements.

This equation with numerical values substituted for water solutions at 25° may be written

$$-\log \tanh (9.75z'\psi) = -\log \tanh (9.75z'\psi_0) + 0.142z'(\nu'C)^{\frac{1}{2}}X, \quad (1)$$

where $\psi$ and $\psi_0$ are in volts, $C$ in moles of salt per 1000 cc of solution, and $X$ in angstrom units.

In this form the equation is valid for binary salts and was shown to be a reasonable approximation for salts of other valence types if $z'$ and $\nu'$ are the valence and number of ions per salt molecule of the kind of ions having the opposite sign of charge to the solid wall. Equation (1) expresses $\psi$ as an explicit function of $X$ in which all of the quantities except $\psi_0$ are known.

Making the assumption that the electrokinetic potential, ($\xi$), is the potential at the distance, $t$, from the $\psi_0$ plane, Eq. (1) may be written

$$-\log \tanh (9.75z'\xi) = -\log \tanh (9.75z'\psi_0) + 0.142tz'(\nu'C)^{\frac{1}{2}}. \quad (1')$$

It is obvious that if $\psi_0$ and $t$ are independent of $C$, $-\log \tanh (9.75z'\xi)$ is a linear function of $C^{\frac{1}{2}}$. It is highly probable that the converse is also true since otherwise it would be necessary to assume that simultaneous changes in $\psi_0$ and $t$ would exactly compensate. Thus if the experimental curve is linear both $\psi_0$ and $t$ can be determined graphically.

Further attempts to derive analogous equations for salts of other valence types have been successful in two other special cases:

(1) $z'=2z$. This corresponds to a solution of a salt such as $BaCl_2$ or $Th(SO_4)_2$ in contact with a negative wall, or $K_2SO_4$ or $Ca_2Fe(CN)_6$ in contact with a positive wall. The equations analogous to Eqs. (1) and (1′) are

$$\log f_2(\psi) = \log f_2(\psi_0) + b_2z'C^{\frac{1}{2}}X \quad (2)$$

and

$$\log f_2(\xi) = \log f_2(\psi_0) + b_2z'C^{\frac{1}{2}}t, \quad (2')$$

where

$$f_2(y) = \frac{[\exp (z'\epsilon y/kT) + 2 \exp (z'\epsilon y/2kT)]^{\frac{1}{2}} + \sqrt{3}}{\exp (z'\epsilon y/2kT) - 1} + \frac{2}{\sqrt{3}},$$

$\epsilon/kT = 39$ at 25° and with $y$ in volts,

$$b_2 \equiv \frac{\sqrt{3}}{\ln 10}\left(\frac{\pi N\epsilon^2}{500DkT}\right)^{\frac{1}{2}} = 0.123 \text{ for water solutions at } 25°.$$

(2) $z'=\frac{1}{2}z$. This case corresponds to a salt such as $K_2SO_4$ with a negative wall or $BaCl_2$ with a positive wall. The corresponding equations are

$$\log f_3(\psi) = \log f_3(\psi_0) + b_3z'C^{\frac{1}{2}}X \quad (3)$$

and

$$\log f_3(\xi) = \log f_3(\psi_0) + b_3z'tC^{\frac{1}{2}}, \quad (3')$$

where

$$f_3(y) = \frac{[2 \exp (z'\epsilon y/kT) + 1]^{\frac{1}{2}} + \sqrt{3}}{[2 \exp (z'\epsilon y/kT) + 1]^{\frac{1}{2}} - \sqrt{3}}$$

and

$$b_3 = 2b_2 = 0.247 \text{ for water solutions at } 25°.$$

Using data of Kruyt and van der Willigen[3] for a negative glass wall, $\psi_0$ and $t$ were evaluated graphically by Eq. (2′) for $BaCl_2$ solutions, and by Eq. (3′) for $K_2SO_4$ solutions. Previously[2] these quantities were evaluated from the same data by Eq. (1′) which is an approximation for these salts. The results of the calculations were as follows:

For $BaCl_2$ Eq. (2′) gave $\psi_0 = 60$ mv and $t = 31.4$A, while Eq. (1′) gave $\psi_0 = 63$ mv and $t = 31$A.

For $K_2SO_4$ Eq. (3′) gave $\psi_0 = 77$ mv and $t = 29.4$A, while Eq. (1′) gave $\psi_0 = 77$ mv and $t = 30$A.

In view of the excellent agreement of these calculations, it is doubtful if the accuracy of existing electrokinetic potential data will justify the additional inconvenience involved in making calculations by means of the more exact equations.

[1] W. G. Eversole and P. H. Lahr, J. Chem. Phys. **9**, 530 (1941).
[2] W. G. Eversole and W. W. Boardman, J. Chem. Phys. **9**, 798 (1941).
[3] H. R. Kruyt and P. C. van der Willigen, Kolloid Zeits. **45**, 307 (1929).

## Ethylene-Ethane and Propylene-Propane Equilibria

GEORGE B. KISTIAKOWSKY
*Department of Chemistry, Harvard University, Cambridge, Massachusetts*
December 1, 1941

WE have determined the thermal equilibrium constants in the reactions $C_2H_6 = C_2H_4 + H_2$ and $C_3H_8 = C_3H_6 + H_2$ at two temperatures each and give the results in Table I.

The equilibrium was approached from both sides, using $Cr_2O_3$ as a catalyst.[1] It was found essential to have the catalyst aged, as otherwise less consistent data were obtained. The gases were recirculated over the catalyst and the position of equilibrium—once it was established—was

found to be independent of the number of passages over the catalyst and the initial gas composition.*

A special analytical procedure was developed which enabled us to measure accurately the quantity of hydrogen and total olefine in the gas mixture, and also to determine the amount of ethylene or propylene in the olefinic fraction.

Applying the van't Hoff isochore to the data of Table I, the heats of the two reactions are calculated to be $34.0\times10^3$ calories per mole at 415°C, and $30.8\times10^3$ calories per mole

TABLE I.

| Temp. | Initial excess of: | Number of experiments | Equilibrium constant, atmos. | Average, atmos. |
|---|---|---|---|---|
| 450°C | $C_2H_6$ | 4 | $5.12\pm0.09\times10^{-4}$ | $5.16\times10^{-4}$ |
| | $C_2H_4+H_2$ | 4 | $5.21\pm0.04\times10^{-4}$ | |
| 380°C | $C_2H_6$ | 3 | $3.94\pm0.04\times10^{-5}$ | $4.04\times10^{-5}$ |
| | $C_2H_6+H_2$ | 3 | $4.15\pm0.13\times10^{-5}$ | |
| 375°C | $C_3H_8$ | 3 | $5.25\pm0.08\times10^{-4}$ | $5.25\times10^{-4}$ |
| | $C_3H_6+H_2$ | 4 | $5.26\pm0.01\times10^{-4}$ | |
| 310°C | $C_3H_8$ | 1 | $3.69\times10^{-5}$ | $3.68\times10^{-5}$ |
| | $C_3H_6+H_2$ | 1 | $3.67\times10^{-5}$ | |

at 343°C. These values differ from those measured directly by Kistiakowsky *et al.*[2,3] at 82°C and extrapolated to the higher temperatures by means of the available heat capacity data ($33.9\times10^3$ and $31.1\times10^3$, respectively) by only a few hundred calories, which can be caused by errors in the equilibrium constants of less than 2 percent. Errors of this magnitude we consider inherent in our measurements.

We have calculated statistically equilibrium constants for the ethane-ethylene-hydrogen system, using the heat of reaction as given in the reference above, and molecular constants as given by Stitt;[4] Frost;[5] Burcik, Eyster, and Yost;[6] Smith;[7] Giauque;[8] and Davis and Johnston.[9] The result is $K_p=5.19\times10^{-4}$ at 450°C, for a potential barrier restricting internal rotation equal to 2750 calories per mole, as given by Kistiakowsky, Lacher, and Stitt.[10] The equilibrium constant for the propane-propylene-hydrogen system has also been calculated statistically, using the heat of reaction as given by Kistiakowsky *et al.*[3] The vibrational frequencies of propylene were taken from Wilson and Wells;[11] those of propane from Wu and Barker,[12] except that the four undetermined frequencies were taken as 2965, 1465, 1150, 1100. (This assignment gives heat capacities in satisfactory agreement with the experimental data reported by Kistiakowsky and Rice.[13]) Taking as the potential barriers restricting internal rotation 3300 calories for propane and 2100 for propylene, we obtain $K_p=5.6\times10^{-4}$ at 375°C, using Pitzer's tables[14] for the contributions from internal rotation.

The excellent agreement of calculated and experimental equilibrium constants for the ethane reaction shows how trustworthy can be the statistical calculations although merely the simple rigid rotator and harmonic oscillator molecular models are used, even at high temperatures, provided the molecular constants are accurately known, as is the case for this reaction.

The good agreement of calculated and experimental equilibrium constants for the propane reaction is an additional strong evidence, if such be needed, that propylene has a potential barrier of about 2100 calories and not, as Pitzer claims,[15] 800. Calculation of the equilibrium constant by Pitzer's assignment[16] gives the value $10.0\times10^{-4}$ at 375°C.

Detailed description of our work, as well as a discussion of the literature on the subject, will be published in this Journal with some delay because of pressure of national defense work.

[1] Frey and Huppke, Ind. Eng. Chem. **25**, 54 (1933).
* The slight effect of the initial gas composition on K evident from Table I is due to the inclusion in the averages of earlier runs made with an insufficiently aged catalyst.
[2] Kistiakowsky, Romeyn, Ruhoff, Smith, and Vaughan, J. Am. Chem. Soc. **57**, 65 (1935).
[3] Kistiakowsky, Ruhoff, Smith, and Vaughan, J. Am. Chem. Soc. **57**, 876 (1935).
[4] F. Stitt, J. Chem. Phys. **7**, 297 (1939).
[5] A. V. Frost, Comptes, rendus, U. S. S. R. 161 (1933).
[6] Burcik, Eyster, and Yost, J. Chem. Phys. **9**, 118 (1941).
[7] L. G. Smith, J. Chem. Phys. **8**, 798 (1940).
[8] W. F. Giauque, J. Am. Chem. Soc. **52**, 4816 (1930).
[9] Davis and Johnston, J. Am. Chem. Soc. **56**, 1045 (1934).
[10] Kistiakowsky, Lacher, and Stitt, J. Chem. Phys. **7**, 289 (1939).
[11] E. B. Wilson, Jr. and A. J. Wells, J. Chem. Phys. **9**, 319 (1941).
[12] V. L. Wu and E. F. Barker, J. Chem. Phys. **9**, 487 (1941).
[13] G. B. Kistiakowsky and W. A. Rice, J. Chem. Phys. **8**, 610 (1940).
[14] K. S. Pitzer, J. Chem. Phys. **5**, 469 (1937).
[15] K. S. Pitzer and W. D. Gwinn, J. Chem. Phys. **9**, 485 (1941).
[16] K. S. Pitzer, J. Chem. Phys. **5**, 473 (1937).

## Equilibrium in the Gas Reaction, $CHBr_3+Br_2\rightleftharpoons CBr_4+HBr$

JOHN W. STRONG AND ROBERT N. PEASE
*Frick Chemical Laboratory, Princeton University, Princeton, New Jersey*
December 11, 1941

RECENT calculations of partition functions for the bromomethanes[1] with other pertinent data indicate that such substitution reactions as

$$CH_2Br_2+Br_2\rightleftharpoons CHBr_3+HBr \quad (1)$$

and

$$CHBr_3+Br_2\rightleftharpoons CBr_4+HBr \quad (2)$$

should be incomplete in the gas phase. This has been confirmed by preliminary determinations of equilibrium in the latter reaction.

Samples of liquid bromoform and bromine were weighed out in glass ampoules. These were introduced into a Pyrex tube which was then evacuated, sealed, and heated in a vapor bath (either naphthalene b.p. 218°C, or α-bromonaphthalene, b.p. 281°C). Total pressures in the reaction tubes at the operating temperatures were about 1 atmos.

After heating, the tubes were quenched in a water spray, opened under potassium iodide solution, and the solution titrated with thiosulphate and with alkali. Data on hydrogen bromide formed were usually a littler lower (1–3 percent) than for bromine reacting, indicating possible side reactions other than substitution. No appreciable amounts of permanent gas were detected.

Principal sources of uncertainty follow from the facts that equilibrium was only approached from the one side, and that no allowance could be made for the formation of lower bromides (especially methylene dibromide). However, it was shown that variation of the heating time (0.5 to 4 hours) indicated a quite definite end-point short of complete reaction. Further, by increasing the ratio of bromine to bromoform up to as much as 5 to 1, the formation of lower bromides could be minimized.

Results calculated for the equilibrium constant, $[CBr_4][HBr]/[CHBr_3][Br_2]$, gave values of 0.30 to 0.32 at 218°C, and 0.26 to 0.30 at 283°C, (six experiments each) with no definite trends.

An equilibrium constant was calculated from the statistical data at 500°K (227°C) for purposes of comparison. For the function, $(E_0^0-F^0)/T$, Stevenson and Beach[1] find 73.56 and 78.43 at 500°K, for $CHBr_3$ and $CBr_4$, respectively. Gordon and Barnes[2] find corresponding values for $Br_2$ and HBr to be 55.01 and 44.14, respectively. Thus, at 500°K $(\Delta E_0^0-\Delta F^0)/T=-6.00$.

The value of $\Delta E_0^0$ is uncertain. Judging from heats of formation at 18°C, as estimated by Bichowsky and Rossini,[3] $\Delta E_{291}^0=-2650$ cal. Calculated heat capacities indicate that this should be increased to about $-3000$ cal. at 0°K.

Substituting this value for $\Delta E_0^0$, one obtains $\Delta F_{500}^0=0$, when $K_{500}=1$, which is in fair agreement with the experimental data in the corresponding temperature range. A value of $\Delta E_0^0$ nearer $-1800$ cal. would yield better agreement, and would be in better accord with the small observed temperature coefficient of the equilibrium constant.

To this extent, the calculations of Stevenson and Beach are confirmed.

[1] D. P. Stevenson and J. Y. Beach, J. Chem. Phys. **6**, 25, 341 (1938).
[2] Gordon and Barnes, J. Chem. Phys. **1**, 692 (1933).
[3] Bichowsky and Rossini, *Thermochemistry* (Reinhold Publishing Company, New York, 1936).

## Erratum: The Partition Function of Molecules with Internal Torsion

### I. Single Asymmetric Top Attached to Rigid Framework

[J. Chem. Phys. **9**, 807–815 (1941)]

DONNA PRICE
*Mallinckrodt Chemical Laboratory, Harvard University, Cambridge, Massachusetts*

| Page (subscript gives column) | Line | Corrected form |
|---|---|---|
| $810_1$ | Fine print, sixth equation. | $\eta^2=C^2+E^2-2\Sigma_\alpha a_{2\alpha}a_{3\alpha}EC=E^2+C^2$. |
| $810_1$ | Fine print, two lines above (14) | $\Sigma_\alpha\Delta_{\alpha+3}\gamma_\alpha^2\leq 0.058$; $\lambda^2M^{-1}=0.013$. |
| $810_2$ | 1 | (13) instead of (14). |
| $812_1$ | 4 and 6 | $h$ inserted before $\sqrt{2}$. |
| $812_1$ | 12 | $a_{2\alpha}C$ divided by $q\alpha$. |
| $812_1$ | Eqs. (29) and (30) | $\mathbf{R}^2$, $\mathbf{I}^2$, $\mathbf{S}^2$ instead of $R^2$, $I^2$, $S^2$. |
| $812_1$ | Eq. (29), last term | 3 instead of 5. |
| $812_1$ | Third line below (30) | $\mathbf{S}=C\Sigma_\alpha\Delta_{\alpha+3}a_{3\alpha}\mathbf{P}_\alpha$. |
| $812_2$ | Eq. (33), line 1 | $D_0$ instead of $D_1$. |
| $813_1$ | 2 | $D_0$ instead of $D_1$. |
| $813_2$ | 3 | $\sigma=AC^2\Sigma_\alpha\Delta_{\alpha+3}a_{3\alpha}{}^2$. |
| $814_2$ | 8 | + precedes sum. |

The last part of footnote 12, p. 814, should read: $M_{\pm 1}$ and $M_{\pm 2}$ are the same as above except for the factors of $\frac{1}{3}$ and $\frac{1}{12}$, respectively, instead of $\frac{1}{2}$.

$$N_{ij}=\delta_{ij}\square_i-A\Delta_i\Delta_jY_{ij},$$

$$Y_{ij}=\begin{cases}[g_ig_jY+\frac{1}{2}\beta^{-1}f_if_j], & i,j\leq 3\\ [q_{i'}q_{j'}Y+L(q_{i'}a_{3j'}+q_{j'}a_{3i'})+C^2a_{3i'}a_{3j'} & \\ \qquad +\frac{1}{2}\beta^{-1}l_{i'}l_{j'}], & i,j>3\\ [g_iq_{j'}Y+Lg_ia_{3j'}+\frac{1}{2}\beta^{-1}f_il_{j'}], & i\leq 3,j>3\end{cases}$$

where $Y=(1-\frac{1}{2}\beta^{-1}+\frac{3}{16}\beta^{-2})$, and $L=C(1-\frac{1}{4}\beta^{-1})$.

$$E_{ij}=-\Delta_i\Delta_jA\begin{cases}[g_ig_jE+\beta^{-1}f_if_j], & i,j\leq 3\\ [q_{i'}q_{j'}E-\frac{1}{2}\beta^{-1}(q_{i'}a_{3j'}+q_{j'}a_{3i'})C & \\ \qquad +\beta^{-1}l_{i'}l_{j'}], & i,j>3\\ [g_iq_{j'}E-\frac{1}{2}\beta^{-1}g_ia_{3j'}C+\beta^{-1}f_il_{j'}], & i\leq 3,j>3\end{cases}$$

where $E=(\frac{3}{8}\beta^{-2}-\beta^{-1})$. $F_{ij}$ should also include the factor $A$ as does $E_{ij}$.